

A CRYSTALLOGRAPHIC STUDY ON  
TOPOCHEMICAL PHOTOREACTION OF UNSYMMETRIC  
DIOLEFIN COMPOUNDS

(非対称ジオレフィン化合物のトポケミカル光反応挙動の  
結晶学的研究)

YASUNARI MAEKAWA

①

A CRYSTALLOGRAPHIC STUDY ON  
TOPOCHEMICAL PHOTOREACTION OF UNSYMMETRIC  
DIOLEFIN COMPOUNDS

(非対称ジオレフィン化合物のトポケミカル光反応挙動の結晶学的研究)

by  
YASUNARI MAEKAWA  
(前川康成)

Department of Synthetic Chemistry  
Faculty of Engineering  
The University of Tokyo

1991

## PREFACE

The studies presented in this thesis have been carried out under the direction of Professor Masaki Hasegawa at the University of Tokyo during 1986 - 1991. The thesis is concerned with the crystallographic study on the diversified topochemical reactions of unsymmetrically substituted diolefin compounds and their mixed crystals.

The author expresses his sincere gratitude to Professor Masaki Hasegawa for his valuable guidance and encouragement throughout the course of the study. The author wishes to thank Associate Professor Kazuhiko Saigo for significant suggestions and advice.

The author is grateful to Professor Yuji Ohashi of Tokyo Institute of Technology for his instruction of a crystal structure analysis. The author is also grateful to Dr. Kenji Takeda, Dr. Noriyuki Yonezawa, Dr. Yukihiro Hashimoto, and Mr. Masao Nohara for their useful suggestions.

The author would like to express his deep gratitude to Dr. Hiroki Kimoto for his useful guidance concerning a computer usage. Grateful acknowledgment is also made for the assistance and encouragement of Mr. Naotsugu Muro, Mr. Takehiro Tsutsumi, Mr. Makoto Sukegawa, Mr. Peng-Jin Lim, and Mr. Hisakazu Sakurai, and many members of Hasegawa Laboratory.

Finally, the author wishes to express his deep gratitude to his parents for their affectionate encouragement.

Yasunari Maekawa

Hasegawa Laboratory  
Department of Synthetic Chemistry  
Faculty of Engineering  
The University of Tokyo

January, 1991

## CONTENTS

PREFACE	1
CONTENTS	2
CHAPTER 1. General Introduction	
1. 1. Topochemical Reaction	4
1. 2. Topochemical Polymerization	7
1. 3. Crystal Engineering	10
1. 4. The Object of This Thesis	11
1. 5. References	11
CHAPTER 2. Crystallographic Interpretation of the Topochemical Behavior of Alkyl $\alpha$ -Cyano-4-[2-(4-pyridyl)ethenyl]cinnamates in the Crystalline State. Enhancement of Photopolymerizability by Complex Formation	
2. 1. Introduction	13
2. 2. Results and Discussion	
2. 2. 1. Diversified Photochemical Behavior on Varying the Ester Alkyl Group in the Monomers	13
2. 2. 2. Even-numbered Polymerization Mechanism	18
2. 2. 3. Strategies for Obtaining High Molecular Weight Polymer	21
2. 3. Conclusion	29
2. 4. Experimental	30
2. 5. References	41
CHAPTER 3. A Design for Photopolymerizable Molecular Arrangement of Diolenin Crystals	
3. 1. Introduction	42
3. 2. Results and Discussion	
3. 2. 1. Photoreaction of Monomers Having Pyrazyl Group	44
3. 2. 2. Photoreaction of Monomers Having Methylpyrazyl Group	45
3. 2. 3. Crystallographic Study	47
3. 3. Conclusion	55

3. 4. Experimental	55
3. 5. References	66
<b>CHAPTER 4. Quantitative Formation of a Highly Strained Tricyclic [2.2]Paracyclophane Derivative from a Mixed Crystal of Ethyl and Propyl <math>\alpha</math>-Cyano-4-[2-(4-pyridyl)ethenyl] cinnamates through a Topochemical Reaction</b>	
4. 1. Introduction	67
4. 2. Results and Discussion	
4. 2. 1. Preparation of the Mixed Crystals	68
4. 2. 2. Topochemical Photoreaction of the Mixed Crystal	69
4. 2. 3. Molecular Structure of the Tricyclic Dimer	73
4. 2. 4. Photochemical Properties of the Tricyclic Dimer	76
4. 2. 5. Crystallographic Interpretation of the Photoreaction of the Mixed Crystal	77
4. 3. Conclusion	79
4. 4. Experimental	80
4. 5. References	86
<b>CHAPTER 5. Preparation of a Crystalline Linear High Copolymer by Topochemical Photo-Polymerization of Diolefin Mixed Crystals.</b>	
5. 1. Introduction	88
5. 2. Results and Discussion	
5. 2. 1. Topochemical Behavior of a Mixed Crystal Prepared by Recrystallization from a Methanol Solution	89
5. 2. 2. Topochemical Behavior of a Mixed Crystal Prepared by Grinding of a Mixture of the Crystals	93
5. 3. Conclusion	94
5. 4. Experimental	95
5. 5. References	97
<b>LIST OF PUBLICATIONS</b>	99

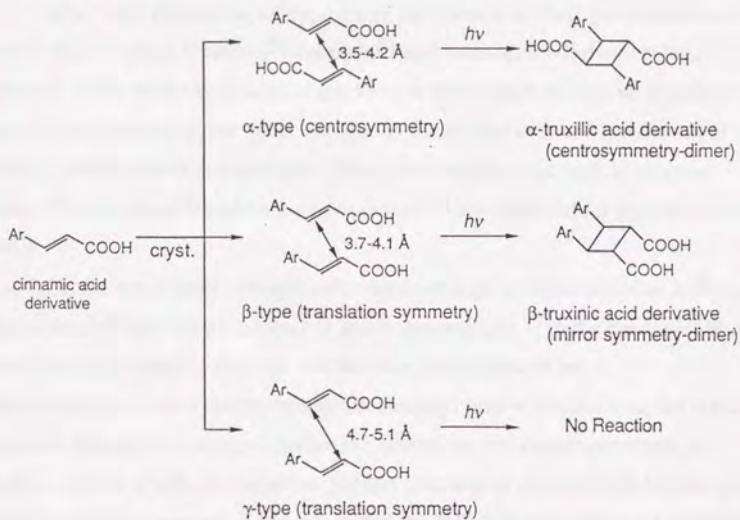
## CHAPTER 1

### General Introduction

#### 1. 1. A Topochemical Reaction

Intensive study concerning topochemical reactions has been carried out for recent three decades. The term of "topochemical reaction" is defined as the reaction in the crystalline state which proceeds under the crystal lattice control; thus, the possibility of the reaction and the structure of the resulting product are governed by the intermolecular geometry in the reactant crystal. Therefore, topochemical reaction is of interest in organic and polymer syntheses due to its regio- and/or stereo-selectivity arising from the periodic structure and constricting environment around molecules in a reactant crystal.

Scheme 1.1



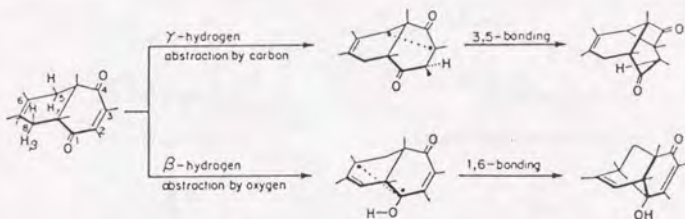
The feature of topochemical reaction was systematically exemplified by Schmidt and his co-workers for *trans*-cinnamic acid and its derivatives.<sup>1,2)</sup> On the basis of the shortest axis in a crystal, they classified these acids into three types;  $\beta$ -,  $\gamma$ -, and  $\alpha$ -types. The distance of the axis is  $3.9 \pm 0.2$ ,  $4.9 \pm 0.2$ , and  $>5.1$  Å for  $\alpha$ -,  $\beta$ -, and  $\gamma$ -types, respectively. In  $\alpha$ -type, the nearest neighboring double bonds, which are related by center of symmetry, are separated by a distance ranging from 3.5 to 4.2 Å and give a centrosymmetric dimer (an  $\alpha$ -truxillic acid derivative). In  $\beta$ -type, the nearest neighboring double bonds, which are related by translation symmetry, are separated by a distance ranging from 3.7 to 4.1 Å and give a mirror symmetric dimer (a  $\beta$ -truxinic acid derivative). In  $\gamma$ -type, the neighboring double bonds are separated by a distance ranging from 4.7 to 5.1 Å and are unable to react with each other. From these results Schmidt and his co-workers concluded that topochemical reaction proceeds with a minimum of atomic and molecular movement (topochemical principle).

After their pioneering study, a lot of topochemical [2+2] photoreactions of acrylic acid,<sup>3)</sup> diene,<sup>4)</sup> enone,<sup>5)</sup> thymine,<sup>6)</sup> and coumarin<sup>7)</sup> derivatives were reported. Most of the structures of products in these reactions can be explained by topochemical principle, but some exceptions for the distance and orientation of two reacting double bonds are emerged. Thus, new explanations such as reaction cavity,<sup>8)</sup> local stress,<sup>9)</sup> and lattice relaxability<sup>10)</sup> are proposed for the exceptional results.

On the other hand, unimolecular reactions such as intramolecular hydrogen abstraction,<sup>11)</sup> electrocyclization,<sup>12)</sup> and fragmentation<sup>13)</sup> in the crystalline state have been also studied. Scheffer and his co-workers studied the photorearrangement of tetrahydronaphthoquinones and its derivatives; the reaction proceeds through two steps; (i) hydrogen abstraction by carbonyl oxygen or olefinic carbon to afford a biradical, (ii) the coupling of the biradical to give a final rearrangement compound. They concluded the following topochemical principle for the unimolecular reaction: (1) The abstraction reaction is not governed by intermolecular arrangement but by intramolecular geometry (conformation of reactant molecule), namely, the distance and angle between the abstracted hydrogen

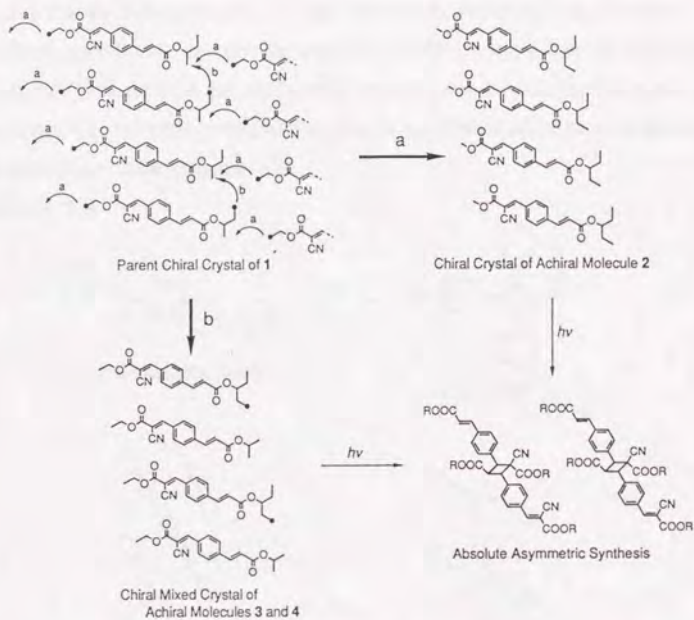
and the abstracting atom. (2) The reaction, in which the photoproduct has shape very similar to the conformation of a reactant molecule in the crystal, is allowed to proceed topochemically.<sup>11)</sup>

Scheme 1.2



In recent years there have been some successful reports concerning an absolute asymmetric synthesis in the crystalline state; the term of "absolute asymmetric synthesis" is defined as an asymmetric induction without any external chiral agent (chiral catalyst or chiral handle). Namely, the asymmetric environment of a chiral crystal is exploited for the asymmetric induction, and the chirality of the reactant crystal is transformed into the chirality of the product. First clear-cut example was substantiated by Lahav and his co-workers.<sup>14)</sup> In order to execute an absolute asymmetric synthesis, they exploited [2+2] photocycloaddition of unsymmetrically substituted diolefin compounds as a reactive chiral crystal. At first, they designed a chiral crystalline matrix (parent chiral crystal), in which an enantiometrically pure molecule **1** was arranged suitable for [2+2] photopolymerization, by using *sec*-butyl group as a chiral handle. In the next stage, they considered to modify the molecule into achiral ones with maintaining their crystalline structures being isomorphous to the parent crystal, and transferred one carbon in the ethyl group to the *sec*-butyl group of the interstack neighboring molecule (a in Scheme 1.3) or one carbon in the *sec*-butyl group to the *sec*-butyl group of the intrastacked neighboring molecule (b in Scheme 1.3), namely designed molecule **2** and a pair of **3** and **4**. Molecule **2** and an equimolar mixture of **3** and **4** take crystal structures isomorphous to crystal **1** and give chiral dimer, trimer, and oligomers with quantitative enantiomeric purities.

Scheme 1.3



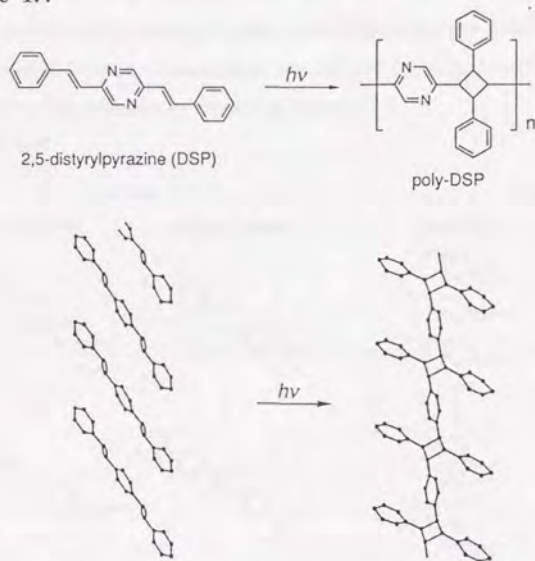
Furthermore, absolute asymmetric syntheses via unimolecular photorearrangements such as di- $\pi$ -methane<sup>15)</sup> and Norrish type II<sup>15,16)</sup> reactions were also reported.

## 1. 2. Topochemical Polymerization

Since the decade of 1950's, solid state polymerization had been studied for the chain reactions of vinyl and cyclic ether compounds initiated by  $\gamma$ -ray, uv light, catalysts, or heat. Among these reactions, the polymerization of trioxane (a cyclic ether compound) crystal afforded a highly crystalline polymer.<sup>17)</sup> However, no definite correlation had been demonstrated between the monomer and the polymer in the dimensions of the crystal unit cell. In 1967, Hasegawa substantiated the first example of topochemical photopolymerization by using 2,5-distyrylpyrazine (DSP) as a monomer.<sup>18)</sup> DSP crystal is topochemically converted into a crystalline linear

polymer by repeating [2+2] photocycloaddition. The crystallographic study has revealed that the polymerization of DSP follows the topochemical principle elucidated by Schmidt, and that the unit cell of DSP crystal is strictly induced to that of poly-DSP crystal with the retention of crystal symmetry during the reaction.<sup>19)</sup> Since then, a great number of diolefin crystals have been found to photopolymerize into crystalline linear polymers.<sup>20)</sup>

**Scheme 1.4**

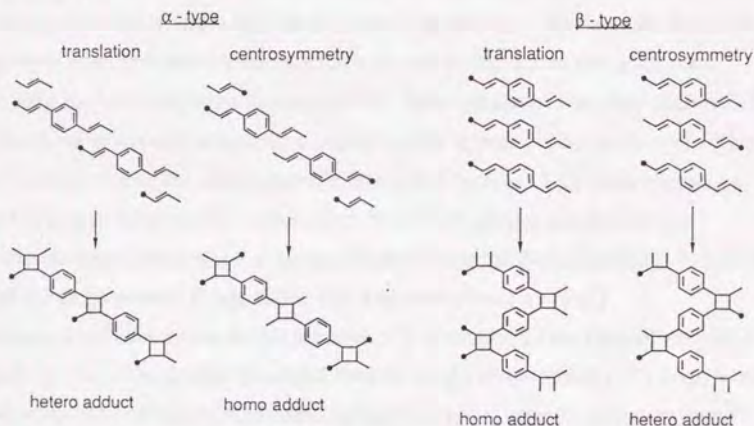


The polymerization of diacetylene derivative crystals has been revealed to proceed via topochemical chain reaction.<sup>21)</sup> Since the polymerization of diacetylene derivatives results in the conversion of the single crystals of the monomers to single crystals of polymers with long conjugation, the obtained polymers are expected to be useful as some optoelectronic materials.

In our laboratory, it has been recently found that, depending on molecular arrangement, unsymmetrically substituted diolefin crystals gave several types of dimers and/or polymers. The diversity of the photoproducts had not been achieved by topochemical polymerization of symmetric diolefin and diacetylene derivatives.

On the basis of the studies concerning the topochemical reactions carried out so far, the molecular arrangements of photoreactive, unsymmetrically substituted diethenylaromatic crystals are roughly classified into  $\alpha$ - and  $\beta$ -type packings, similar to those of monoolefin compounds. In  $\alpha$ -type packing, molecules are superimposed in the direction of long molecular axis displaced by about half a molecule. In  $\beta$ -type packing, molecules are superimposed without displacement in the direction of the long molecular axis. Each packing of the  $\alpha$ - and  $\beta$ -types is further classified into translation- and centrosymmetry-type packings. Therefore, four kinds of molecular arrangements are defined for unsymmetric diethenylaromatic crystals, as shown in Scheme 1.5.

Scheme 1.5



Corresponding to the molecular arrangements, the photoproducts are also classified into four types:  $\alpha$ - and  $\beta$ -type, and homo- and hetero-type adducts. The  $\alpha$ -type photoadduct is derived from an  $\alpha$ -type packing monomer and is characterized by a cyclobutane ring trans-1,3-substituted with arylene groups. The  $\beta$ -type photoadduct is derived from a  $\beta$ -type packing monomer and is characterized by a cyclobutane ring cis-1,2-substituted with the arylene groups. Each adduct of the  $\alpha$ - and  $\beta$ -types is further classified into homo- and hetero-type adducts. A homo-type adduct, which is derived either from the  $\alpha$ -centrosymmetry- or  $\beta$ -

translation-type packing, is formed from the same olefin groups. On the other hand, the hetero-type adduct, which is derived either from the  $\alpha$ -translation- or  $\beta$ -centrosymmetry-type packing, is formed from different olefin groups. As a result, four types of polymers having a linear or zigzag main chain structure can be assumed to be formed, depending on the molecular arrangement of the starting diethenylaromatic crystals.

### 1. 3. Crystal Engineering

The term of "crystal engineering", proposed by Schmidt,<sup>2)</sup> means the attempt to regulate the molecular arrangement of a crystal, which would result in the control of the chemical reaction course and the physical properties of a crystal. For crystal engineering, it may be the most important to understand the correlation between molecular and crystal structures as well as the factors that govern the packing mode of molecules in a crystal.<sup>22)</sup> Although there is no clear example of controlling molecular arrangement, some reports appear in literatures concerning crystal engineering by using a specific interaction such as Cl-Cl weak interaction and hydrogen bonding.<sup>23)</sup> It is realized that chloro groups that attached to aromatic rings tend to make a crystal structure being the  $\beta$ -type packing. Schmidt and Green prepared a  $\beta$ -type dimer and a tricyclic dimer by [2+2] photocycloaddition based on this principle.<sup>24)</sup> Recently, on the basis of statistic study by using Cambridge Structural Data Base of Crystallography, Desiraju found that other interactions, such as cyano-halogen<sup>25)</sup> and acetylenic proton-oxygen<sup>26)</sup> play a role in controlling molecular arrangement. Moreover, the design of molecular arrangement by hydrogen bonding is increasingly noted for crystal engineering. Hydrogen bonding is profitable for crystal engineering because hydrogen bonding is an interaction stronger than van der Waals force and has a directionality. Though one- or two-dimensionally oriented molecular array has been already achieved,<sup>27)</sup> the complete control of a molecular arrangement (three-dimensionally controlled molecular array) has not be realized yet.

#### 1. 4. The Object of This Thesis

From the viewpoint of synthetic chemistry, the following two points may be important for topochemical reactions: i) A study of reaction behavior of new compounds in order to discover a novel reaction, which can be achieved only in the crystalline state; ii) understanding of the correlation between molecular structure and molecular arrangement in order to control reaction in the crystalline state (crystal engineering).

As described above, unsymmetrically substituted diolefin compounds exhibit the diversity of photochemical behavior and give several types of photoproducts. Furthermore, there have been a few reports concerning topochemical polymerization of a mixed crystal. Thus, the author studied the topochemical behavior of newly synthesized diolefin compounds containing 4-pyridyl or 2-pyrazyl group and their mixed crystals and tried to interpret the diversity of the photochemical behavior on the basis of the X-ray crystal structure analysis.

#### 1. 5. References

- 1) Cohen, M. D.; Schmidt, G. M. J. *J. Chem. Soc.* **1964**, 1996.
- 2) Schmidt, G. M. J. *Pure Appl. Chem.* **1971**, 27, 647.
- 3) Lahav, M.; Schmidt, G. M. J. *J. Am. Chem. Soc.* **1962**, 84, 3970.
- 4) Green, B. S.; Lahav, M.; Schmidt, G. M. J. *J. Chem. Soc. B* **1971**, 1552.
- 5) Thomas, J. M. *Nature (London)* **1981**, 289, 633.
- 6) Frank, J. K.; Paul, I. C. *J. Am. Chem. Soc.* **1973**, 95, 2324.
- 7) Gnanaguru, K.; Ramasubbu, N.; Venkatesan, K.; Ramamurthy, V. *J. Org. Chem.* **1985**, 50, 2337.
- 8) Cohen, M. D. *Angew. Chem., Int. Ed. Engl.* **1975**, 14, 386. Ohashi, Y.; Yanagi, K.; Kurihara, T; Sasada, Y.; Ohgo, Y. *J. Am. Chem. Soc.* **1981**, 103, 5805.
- 9) MacBride, J. M. *Acc. Chem. Res.* **1983**, 16, 304.
- 10) Gavezzotti, A.; Simonetta, M. *Chem. Rev.* **1982**, 82, 1. Murthy, G. S.; Arjunan, P.; Venkatesan, K.; Ramamurthy, V. *Tetrahedron*, **1987**, 43, 1225.
- 11) Scheffer, J. R. *Acc. Chem. Res.* **1980**, 13, 283.

- 12) Quinkert, G.; Tabata, T.; Hickmann, E. A. J.; Dobrat, W. *Angew. Chem., Int. Ed. Engl.* **1971**, 10 199.
- 13) Santiago, A.; Becker, R. S. *J. Am. Chem. Soc.* **1968**, 90, 3654.
- 14) Addadi, L.; van Mil, J.; Lahav, M. *J. Am. Chem. Soc.* **1982**, 104, 3422.
- 15) Evans, S. V.; Garcia-Garibay, M.; Omkaram, N.; Scheffer, J. R.; Trotter, J.; Wireko, F. *J. Am. Chem. Soc.* **1986**, 108, 5648.
- 16) Sekine, A.; Hori, K.; Ohashi, Y.; Yagi, M.; Toda, F. *J. Am. Chem. Soc.* **1981**, 103, 5805.
- 17) Okamura, S.; Hayashi, K.; Nishii, M. *J. Polym. Sci., C-4* **1969**, 839.
- 18) Hasegawa, M.; Suzuki, Y. *J. Polym. Sci., B5* **1967**, 813.
- 19) Nakanishi, H.; Hasegawa, M.; Sasada, Y. *J. Polym. Sci., Polym. Phys. Ed.* **1977**, 15, 173.
- 20) Hasegawa, M. *Chem. Rev.* **1983**, 83, 507.
- 21) Wegner, G. *Makromol. Chem.* **1972**, 154, 35.
- 22) Kitaigorodsky, A. I. *Organic Crystals and Molecules*, Academic Press; New York, **1973**.
- 23) Mirsky, K.; Cohen, M. D. *Chem. Phys.* **1978**, 28, 193.
- 24) Elgavi, A.; Green, B. S.; Schmidt, G. M. J. *J. Am. Chem. Soc.* **1973**, 95, 2058.
- 25) Desiraju, G. R.; Harlow, R. L. *J. Am. Chem. Soc.* **1989**, 111, 6757.
- 26) Desiraju, G. R. *J. Chem. Soc., Chem. Commun.* **1990**, 454.
- 27) Etter, M. C.; Frankenbach, G. M. *Chem. Mater.* **1989**, 1, 10. Lehn, J.-M.; Mascal, M.; DeCian, A.; Fischer, J. *J. Chem. Soc., Chem. Commun.* **1990**, 479. Zhao, X.; Chang, Y.-L.; Fowler, F. W.; Lauher, J. W. *J. Am. Chem. Soc.* **1990**, 112, 6627.

## CHAPTER 2

### Crystallographic Interpretation of the Topochemical Behavior of Alkyl $\alpha$ -Cyano-4-[2-(4-pyridyl)ethenyl]cinnamates in the Crystalline State. Enhancement of Photopolymerizability by Complex Formation

#### 2. 1. Introduction

Intensive studies concerning topochemical [2+2] photopolymerization during the last decade have revealed the correlation between the molecular structure and the topochemical reactivity for a large number of diolefin crystals. In previous reports from our laboratory,<sup>1</sup> it was established that 1,4-diethenylaromatic derivatives, substituted by phenyl, 2- or 4-pyridyl, pyrazyl, alkoxycarbonyl, with or without cyano groups, were potent in forming photoreactive  $\alpha$ - or  $\beta$ -packing crystal. Recently, such an empirical rule concerning potent substituents was successfully applied to unsymmetrically substituted diolefin crystals. As a result, a variety of topochemical products were obtained by [2+2] photoreactions of these crystals.<sup>2</sup>

In this chapter, the author demonstrates the various photochemical behavior of methyl, ethyl, and propyl  $\alpha$ -cyano-4-[2-(4-pyridyl)ethenyl]cinnamate crystals (**1a**, **1b**, and **1c**) and the enhancement of polymerizability of the corresponding dimers by means of complex formation with a small molecule. Furthermore, the photochemical behavior of these unsymmetric diolefin crystals is interpreted in correlation to the crystal structures of the monomers, dimers, and the dimer complexes.

#### 2. 2. Results and Discussion

##### 2. 2. 1. Diversified Photochemical Behavior on Varying the Ester Alkyl Group in the Monomers

(a) Photochemical Behavior of Methyl, Ethyl, and Propyl  $\alpha$ -Cyano-4-[2-(4-pyridyl)ethenyl]cinnamates. Irradiation of **1a** for 26 h at room temperature gave amorphous oligomers ( $\eta_{inh} = 0.13$  dL/g) containing a

considerable amount of a dimer. The dimer (**2a**) was separated from the monomer and oligomers by preparative TLC. The cyclobutane in **2a** was confirmed by  $^1\text{H}$  NMR and MS spectroscopy to be of the  $\beta$ -homo-type structure, to which two pyridyl groups are attached; no other types of dimer was detected. Even though the dimerization proceeded with a morphological transformation from the crystalline to the amorphous phase, the  $\beta$ -homo-type dimer was exclusively obtained. The  $^1\text{H}$  NMR of the resulting oligomers showed signals in the region of a cyclobutane proton with indefinable broad signals. The spectral evidence implies that the dimerization proceeded under the lattice control of the monomer crystal, whereas a subsequent reaction occurred non-topochemically to give the amorphous oligomers.<sup>2e</sup>

Upon irradiation of **1b** for 7 h at room temperature, a homo-type linear polymer ( $\overline{M}_n = 3,100$ ) was produced with the accumulation of one type of the dimer at the intermediate stage.<sup>3</sup> Exclusive photoexcitation of the monomer with longer wavelengths than 410 nm resulted in a quantitative formation of the dimer (**2b**). The structure of **2b** was confirmed by  $^1\text{H}$  NMR and MS spectroscopy to have an  $\alpha$ -homo-type cyclobutane, on which two ester and two cyano groups are substituted. This cyclobutane structure was later substantiated by crystal structure analysis.

The GPC profile (Figure 2.1(a)) showed that the products consisted of molecular species only of even-numbered degree of polymerization during the early stage of the photoreaction (2 h). On further irradiation (7 h), the polymerization of **1b** proceeded along with a morphological transformation from the crystalline to the amorphous phase; the GPC profile (Figure 2.1(b)) became bimodal with polymerization. Its NMR spectrum showed two types of signals of cyclobutane protons: two proton signals appearing at  $\delta$  4.57 and 4.66 ppm (broad singlet) were assigned to be a cyclobutane ring substituted by two pyridyl groups, and proton signal appearing at  $\delta$  5.04 ppm (singlet) was assigned to be a cyclobutane ring substituted by two cyano and two ethoxycarbonyl groups. The GPC and  $^1\text{H}$  NMR analyses indicated that the final products comprised mainly an  $\alpha$ -homo-type polymer produced by a topochemically controlled process accompanied by a small amount of a non-topochemically produced polymer, which corresponded to a

region of higher molecular weight in the GPC profile.<sup>2e</sup>

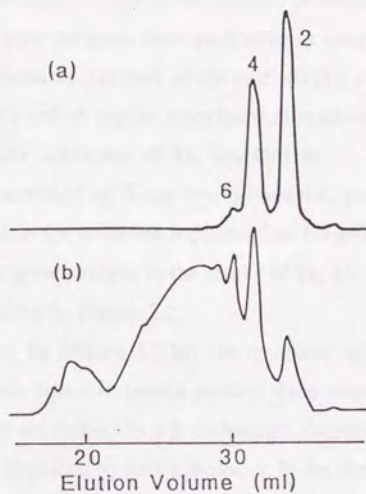
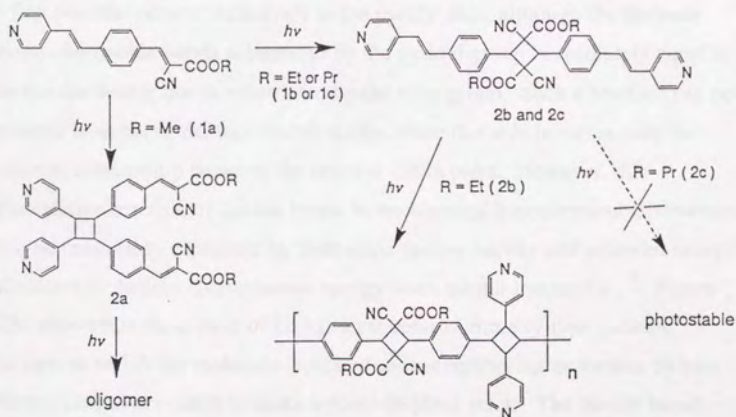


Figure 2.1. GPC profiles of the reaction products of **1b**: (a) irradiated for 2 h and (b) irradiated for 7 h.

Scheme 2.1



As previously reported,<sup>2c</sup> the irradiation of **1c** led quantitatively to a photostable dimer which had the same structure as **2b**.

As shown in Scheme 2.1, the photochemical behavior of the monomers in the crystalline state was quite different from each other in spite of the only slight modification in the chemical structure of the ester alkyl group in these monomers. The results doubtlessly reflect typical topochemical reaction behavior.

**(b) Crystal Structure Analyses of 1a, 1b, and 1c.** The crystal structures of **1a**, **1b**, and **1c**, determined by X-ray crystallography, were compared with each other in order to explain the observed topochemical behavior.

The molecular arrangements in the stacks of **1a**, **1b**, and **1c**, related to the photoreaction, are shown in Figure 2.2.

In the crystal of **1a** (Figure 2.2(a)), the monomer molecules are superimposed along the b-axis to form a parallel plane-to-plane stack; the nearest molecules in the stack are related by a  $\beta$ -translation. Namely, the molecules in the crystal of **1a** are not displaced by half a molecule in the direction of the molecular long axis, in contrast to photopolymerizable  $\alpha$ -type packing crystals.<sup>4</sup> The translationally related double bonds having the same substituents are the nearest (4.049 Å) and are within the photoreactive range accepted for the topochemical reaction in the crystalline state. This molecular arrangement results in the formation of a  $\beta$ -homo-type cyclobutane ring. Of further interest is the fact that the first reaction occurs exclusively at the pyridyl side, although the distance between the double bonds substituted by the pyridyl group is absolutely equal to that between the double bonds substituted by the ester group. Such a reaction can not be explained in terms of the topochemical rule, since this rule involves only the positional relationship between the reactive olefin pairs. However, this regioselective reaction of double bonds in the identical topochemical environment could be reasonably explained by both steric factors (cavity and potential energy) and electronic factors (perturbation energy from orbital interaction).<sup>5</sup> Figure 2.2(b) shows that the crystal of **1b** has an  $\alpha$ -centrosymmetry-type packing structure, in which the molecule is related to its neighboring molecules by two different inversion centers to make a plane-to-plane stack. The double bonds

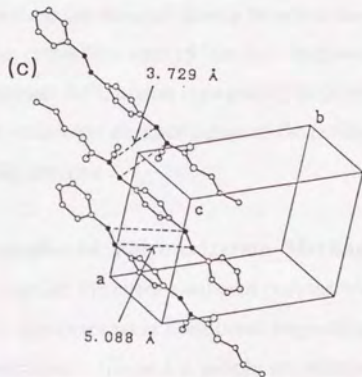
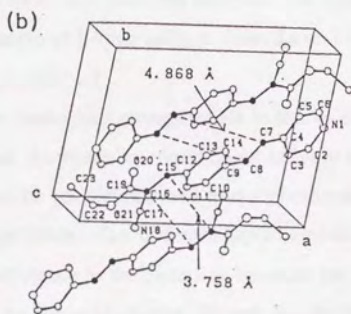
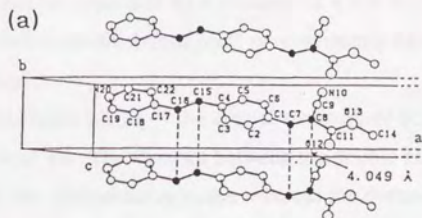


Figure 2.2. Crystal structures of **1a** (a), **1b** (b), and **1c** (c). The darkened atoms correspond to ethylenic carbons.

related by one inversion center are separated by a distance of 3.758 Å (C(15)=C(16)), whereas the double bonds on the other side of the molecule by the other inversion center are separated by a distance of 4.868 Å (C(7)=C(8)). Accordingly, the former double bonds react predominantly according to the topochemical principle.

As shown in Figure 2.2(c),<sup>2c</sup> the crystal structure of **1c** is nearly isomorphous to that of **1b**. The distance between the double bonds on the ester side (3.729 Å) is within the photoreactive range, whereas the distance between the double bonds on the pyridyl side (5.088 Å) is too far to react.

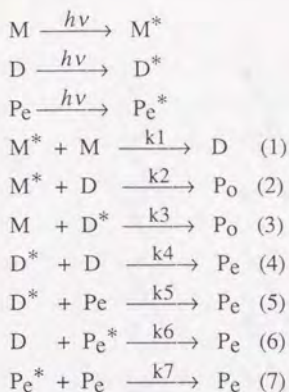
On the basis of crystal structure analyses, the experimental results concerning the exclusive formation of  $\beta$ -type adducts from **1a** and  $\alpha$ -type adducts from **1b** and **1c** could be clearly explained.

Although the molecular arrangements in stacks of **1b** and **1c** are quite similar to each other, **1c** photodimerized quantitatively into a photostable  $\alpha$ -type dimer (**2c**), whereas **1b** photodimerized into a photoreactive dimer (**2b**); further irradiation gave a polymer. The different topochemical behavior would be explained by the difference in the distances between the residual double bonds on the pyridyl side in as-prepared dimers, **2b** and **2c**. In the case of photostable dimer **2c**, the distance between the residual double bonds is longer than that accepted for a photoreaction in the crystalline state (5.066 Å). In contrast, although it has not yet yielded crystallographic information concerning as-prepared dimer **2b**, the dimerization of **1b** makes the distance between the residual double bonds in the dimer close to being reactive.

### 2. 2. 2. Even-numbered Polymerization Mechanism

In order to explain the even-numbered polymerization mechanism of **1b**, various elementary processes were considered regarding photoreaction. If photoadducts greater than a trimer are simply represented by P, all the elementary processes can be expressed in Eqs. (1)-(7), where M, D, P<sub>o</sub>, and P<sub>e</sub> represent the monomer, dimer, and polymers (greater than trimer) with odd- and even-numbered

degrees of polymerization;  $M^*$ ,  $D^*$ ,  $P_O^*$ , and  $P_e^*$  represent the corresponding excited species, respectively.



Upon irradiation with the longer wavelengths than 280 nm the monomer (**1b**) almost disappeared during the early stage of polymerization; the dimer and the tetramer were predominantly produced with a small amount of hexamer, as shown in Figure 2.1(a). The accumulation of the dimer and tetramer without the trimer indicates that not only the excited monomer is unable to react with the dimer, but also the excited dimer with the monomer: namely, Eqs. (2) and (3) do not occur. This means that the monomer in either ground or excited state cannot react with any species produced during photopolymerization. This selective reaction of the monomer is strongly supported by the fact that dimer **2b** was obtained in quantitative yield when monomer **1b** was exclusively photoexcited with the longer wavelength light than 410 nm. There is therefore no chance to yield photoproducts with an odd-numbered degree of polymerization ( $P_O$ ). As a result, the polymerization of **1b** should proceed by Eqs. (1) and (4)-(7), resulting in even-numbered polymerization. Moreover, since only the ester-side double bonds react in the dimerization, all of the growing species should have pyridylethenyl groups at both sides of the terminals during the entire course of polymerization.

It is obvious that the even-numbered polymerization mechanism can be interpreted in terms of the influence of the topochemical environment of the double bonds during the photopolymerization, as shown in Figure 2.3.

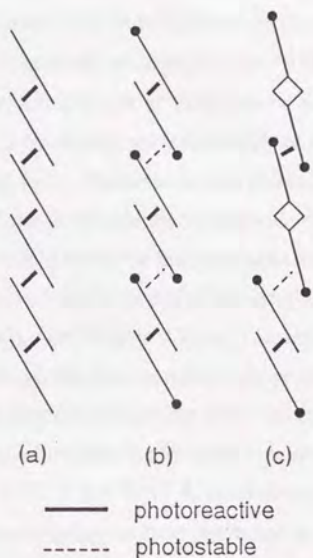


**Figure 2.3.** Schematic molecular arrangements: (a) in the monomer crystal of a symmetric diolefin, (b) in the monomer crystal of an unsymmetric diolefin, and (c) in the partially dimerized crystal of an unsymmetric diolefin.

Since the symmetric diolefin molecule in a crystal has a center of symmetry, the molecule is related to its two neighboring molecules by an equivalent inversion center (Figure 2.3(a)), resulting in the same topochemical environment around both double bonds. Thus, symmetric diolefin crystals do not have a definitive even-numbered polymerization mechanism with an accumulation of the dimer, which has been confirmed by GPC analysis of the oligomers obtained on the photoirradiation of diolefins with wavelengths longer than 280 nm.<sup>9</sup>

In contrast, as shown in Figure 2.3(b), the molecule of unsymmetric diolefins in an  $\alpha$ -centrosymmetry-type packing is related to its neighboring molecules by two different inversion centers, since the unsymmetric diolefin molecule has two double bonds substituted by different groups. This means that the topochemical environment around the double bonds is different (in the crystal of **1b**, the ester side and pyridyl side double bonds are separated by 3.758 Å and 4.868 Å, respectively). Therefore, a single type of dimer can be accumulated spontaneously during the intermediate stage of polymerization without any control of the wavelength of irradiating light. Furthermore, the distance between the residual double bond of the resulting dimer and the pyridyl side double bond of the neighboring monomers would be out of the photoreactive range, whereas the distance between the residual double bonds of two neighboring dimers would be suitable to react with each other (Figure 2.3(c)). Consequently, polymerization completely proceeds through the even-numbered polymerization mechanism.

Ethyl methyl 1,4-phenylenediacrylate (**1d**) is arranged according to the same  $\alpha$ -centrosymmetry-type packing (the methyl ester side and ethyl ester side double bonds are separated by 3.891 Å and 4.917 Å, respectively).<sup>2a</sup> The polymerization of **1d** mainly gave products having an even-numbered degree of polymerization with the accumulation of dimer. However, a small amount of the trimer was detected during the early stage of polymerization, indicating the occurrence of a reaction of the monomer with the dimer.<sup>2a,7</sup> Moreover, though monomer **1c** is also arranged in the  $\alpha$ -centrosymmetry-type packing, irradiation of **1c** with wavelengths longer than 280 nm gave a photostable dimer. The difference in the reaction behavior of **1b**, **1c**, and **1d** in the same  $\alpha$ -centrosymmetry-type packing depends on the distances between the monomer and the dimer and between the dimers, which are mainly governed by the topochemical environment of the initial monomer crystals.

**2. 2. 3. Strategies for Obtaining High Molecular Weight Polymer**  
**(a) Photochemical Behavior of Complexes of the Dimers with Small Molecules.** When **2b** was recrystallized from ethanol, 1-propanol, butyl

acetate, or p-xylene, 1:1 complexes of **2b** with the solvent molecule were obtained (**2b**•EtOH, **2b**•PrOH, **2b**•AcOBu, and **2b**•xylene). As shown in Figure 2.4(a), irradiation of **2b**•EtOH for 5 h gave an amorphous polymer with a molecular weight ( $\overline{M}_n$ ) of 5,000, higher than that of the polymer ( $\overline{M}_n = 3,100$ ) obtained directly from **1b**. Its GPC profile was nearly a unimodal molecular weight distribution, and its  $^1\text{H}$  NMR spectrum showed a predominant formation of two kinds of cyclobutane rings; two proton signals appearing at  $\delta$  4.57 and 4.66 ppm (broad singlet) were assigned to be a cyclobutane ring substituted by two pyridyl groups, and proton signal appearing at  $\delta$  5.04 ppm (singlet) was assigned to be a cyclobutane ring substituted by two cyano and two ethoxycarbonyl groups. These analyses indicate that polymerization proceeds strictly under the control of the crystal lattice of **2b**•EtOH to give an  $\alpha$ -homo-type polymer having the same structure as that obtained from **1b**.

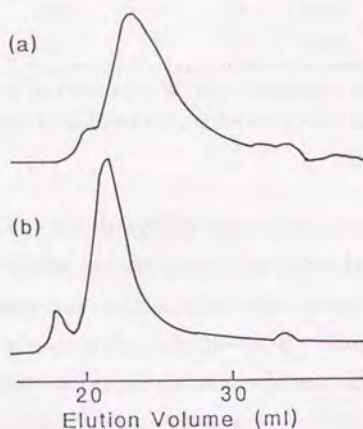


Figure 2.4. GPC profiles of the reaction products of **2b**•EtOH (a) and **2c**•EtOH (b).

Scheme 2.2

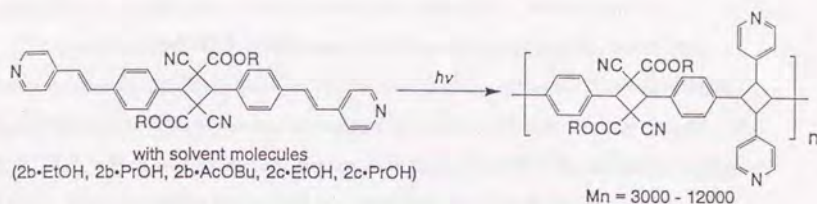


Table 2.1. Polymerization of the Dimer Complexes

compound	light source	dispersant	reaction time [h]	conv. [%]	$\overline{M}_n$	$\overline{M}_w/\overline{M}_n$	morphology of photoproducts
1b	100W	water	7	99	3,100	1.81	amorphous
2b•EtOH	500W	water	5	94	5,000	1.77	amorphous
2b•PrOH	500W	NO	5	99	5,200	1.72	amorphous
2b•AcOBu	500W	NO	5	96	3,600	1.91	amorphous
2b•xylene	500W	NO	5	0	—	—	crystal
1c	500W	water	2	100	(dimer)	—	crystal
2c•EtOH	100W	water	4	99	12,000	1.42	crystal
2c•PrOH	100W	water	4	99	3,000	1.78	crystal

a) A 100 W lamp set inside of the flask; a 500 W lamp set outside of the flask.

b) The reaction of the monomers and dimers was carried out at room temperature and  $-20\text{ }^\circ\text{C}$ , respectively.

Complexes **2b•PrOH** and **2b•AcOBu** showed the same type X-ray powder diffraction pattern as **2b•EtOH**, and also photopolymerized into amorphous polymers having an  $\alpha$ -homo-type structure with molecular weights ( $\overline{M}_n$ ) of 5,200 and 3,600, respectively, as well as that from **2b•EtOH**. However, **2b•xylene**, which showed a different X-ray powder diffraction pattern, was photostable.

The photopolymerization of the complex of a dimer with an alcohol molecule was also attempted to dimer **2c**, which was photostable in an as-prepared crystal. A complex of **2c** with an equimolar amount of 1-propanol (**2c•PrOH**), which was obtained by recrystallization of **2c** from 1-propanol, was converted into a

crystalline polymer ( $\overline{M}_n = 3,000$ ) upon irradiation for 1 h. The cyclobutane rings in the resulting polymer were the same type structure as those from **2b**.

Complex **2c•EtOH**, which was also formed by recrystallization from ethanol, showed an X-ray powder diffraction pattern different from **2c•PrOH**. Irradiation of **2c•EtOH** gave a crystalline polymer with a molecular weight ( $\overline{M}_n$ ) of 12,000, which was extremely higher than that of **2c•PrOH**, as shown in Figure 2.4(b). Polymerization proceeded by control of the crystal lattice, which was confirmed by its GPC profile and  $^1\text{H}$  NMR spectrum. The resulting polymer had cyclobutane rings of the same structures as those from **2b**, **2b•EtOH**, and **2c•PrOH**.

The  $\alpha$ -homo-type dimers generally crystallized as complexes with an appropriate small solvent molecule; these dimer complexes with an alcohol often enhanced the reactivity and polymerizability of the dimers. The relationship between the complexation and photopolymerizability of these crystals strongly suggests that complexation may be a useful method for a crystal design aimed at enhancing photopolymerizability.

**(b) Crystal Structure Analyses of 2b•EtOH and 2c•PrOH.** In order to elucidate the role of an alcohol molecule for the enhancement of the photoreactivity of the dimers, crystal structure analyses of as-prepared dimer crystals and the complexes of the dimers with the alcohol were performed. The crystal structure analyses were successful for **2b•EtOH** and **2c•PrOH**. However, the crystal structure analyses of **2b** and **2c•EtOH** could not be solved since recrystallized **2b** showed a different crystal packing from as-prepared **2b** (determined by X-ray powder diffraction analysis) and the standard reflections of **2c•EtOH** changed during data collection.

The molecular structures with the numbering of atoms of **2b•EtOH** and **2c•PrOH** are shown in Figures 2.5 (a) and (b), respectively. Though the molecular structures of the dimers in complexes **2b•EtOH** and **2c•PrOH** are almost identical to each other, they are different from that in the **2c** crystal. Since the dimer molecule in the crystal of **2c** occupies a crystallographic center of symmetry, as reported in previous paper,<sup>2c</sup> the cyclobutane ring is required to be

planar, and the phenylene groups are also required to be parallel to each other according to symmetry. On the other hand, since the dimer molecules in complexes **2b**•EtOH and **2c**•PrOH have no inversion center in the molecules, the cyclobutane rings are puckered and the two phenylene rings, attached to cyclobutane rings, are nearly perpendicular to each other, as is shown in Figure 2.5(a).<sup>8</sup>

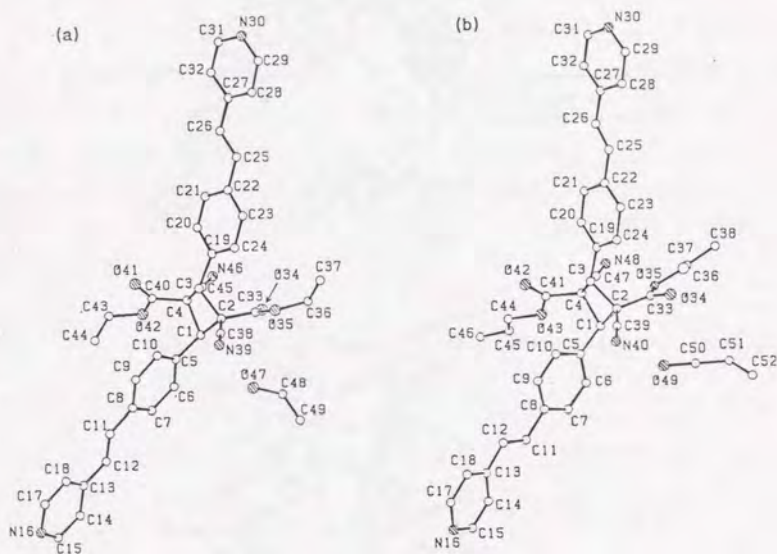


**Figure 2.5.** Molecular structures of **2b**•EtOH (a) and **2c**•PrOH (b) with numbering of atoms. The shaded atoms correspond to hetero atoms.

The crystal structures of complexes **2b**•EtOH and **2c**•PrOH are shown in Figures 2.6 (a) and (b), respectively. The dimer component in complex **2c**•PrOH is related to its neighboring molecules by two different inversion centers. Two pairs of residual double bonds are separated by distances of 3.835 Å (C(11)=C(12)) and 4.208 Å (C(25)=C(26)). Therefore, the photoreaction would proceed through the formation of  $\alpha$ -type cyclobutane rings.

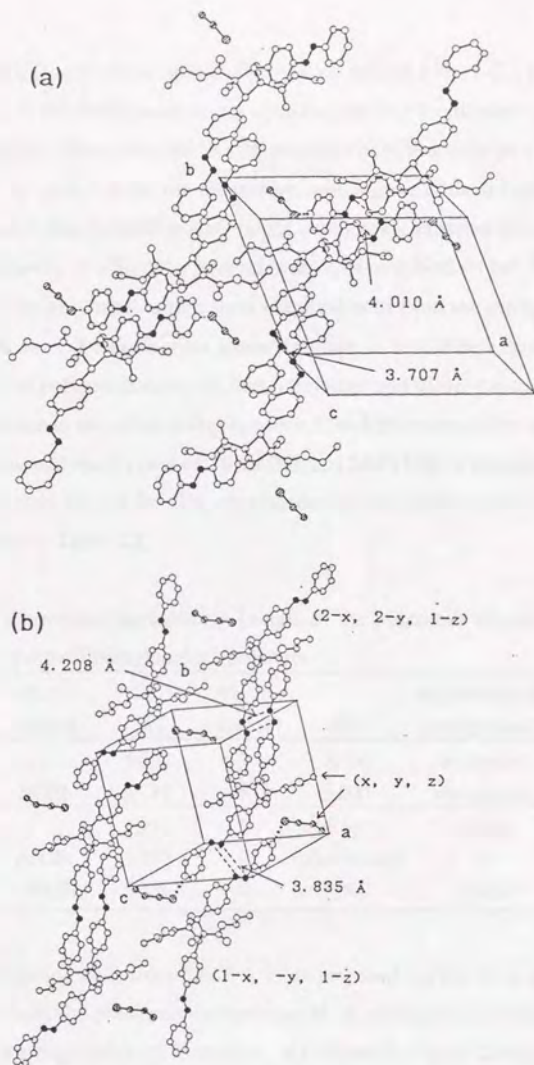


Figure 2.6. Crystal structures of **2b**•EtOH (a) and **2c**•PrOH (b). The darkened and shaded atoms correspond to ethylenic carbon groups and the atoms of ethanol or 1-propanol, respectively.

A suitable length of the monomer repeating unit in a stack ( $L$ ) is considered to be about 7.5 Å for the formation of a cyclobutane ring (confirmed by using CPK molecular models). Moreover, this length seems to be reasonable on the basis of the fact that  $L$  is 7.0-7.7 Å for the monomers, which gave a linear high polymer upon irradiation in the crystalline state (eight compounds satisfied this range among the nine compounds, of which the structures have been solved so far).<sup>2,3</sup> In addition, since the polymers, which were obtained both from the monomer and from the dimer, have the same main-chain structure,  $L$  would be a common parameter for the polymerizability of both monomer and dimer crystals. The author thus examined the relationship between  $L$  and photoreactivity in order to explain the enhanced reactivities of **2b**•EtOH and **2c**•PrOH in comparison with as-prepared crystals **2b** and **2c**. The dependence of the topochemical reactivity on  $L$  is summarized in Table 2.2.

**Table 2.2.** Correlation between the Length of the Monomer Repeating Unit ( $L$ ) and the Photochemical Behavior

compound	recryst. solvent	$L$ [Å]	reaction time [h]	$\bar{M}_n$	morphology of photoproducts	ref.
<b>1b</b>		5.792	7	3,100	amorphous	this work
<b>2b</b> •EtOH	EtOH	6.987	5	5,000	amorphous	this work
<b>1c</b>		5.753	2	(dimer)	crystal	(2c)
<b>2c</b>	AcOEt	5.800	2	(photostable)	—	(2c)
<b>2c</b> •PrOH	n-PrOH	6.736	4	3,000	crystal	this work

The elongation of  $L$  from 5.800 Å in as-prepared crystal **2c** to 6.736 Å in **2c**•PrOH enhances the photopolymerizability of **2c**, although the elongation is still not sufficient for high-polymer formation. As shown in Figure 2.6(b), the 1-propanol molecule ( $x,y,z$ ) in **2c**•PrOH is hydrogen-bonded with the pyridyl nitrogen atom of the dimer (1- $x,-y,1-z$ ) (O(49)⋯N(16): 2.780 Å) and also contacts with the carbonyl carbon of the dimer ( $x,y,z$ ) within the van der Waals distance (O(49)⋯C(33): 3.027 Å). Subsequently, the 1-propanol molecule causes two

reactant dimer molecules to separate from each other to a distance ( $2L$ ) from 11.600 to 13.472 Å (Figure 2.7).

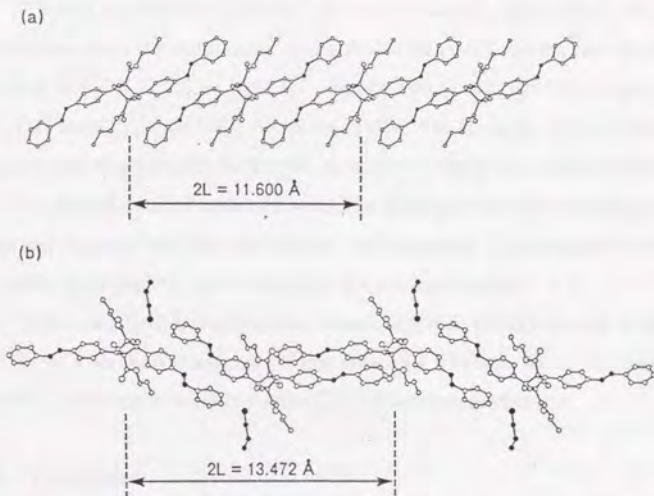


**Figure 2.7.** Molecular arrangements of **2c** (a) and **2c·PrOH** (b) viewed perpendicular to the direction of the polymer chain with the length of the repeating units of the dimer ( $2L$ ).

The crystal structure of complex **2b·EtOH** is similar to that of complex **2c·PrOH**. Two pairs of residual double bonds in **2b·EtOH** are arranged within the photoreactive distances (3.707 Å and 4.010 Å). The ethanol molecule doubtlessly plays the same role as does the 1-propanol molecule in complex **2c·PrOH**. Length  $L$  (6.987 Å) in complex **2b·EtOH** is also longer than that of monomer **1b** (5.792 Å).

Although no crystal structure analysis of **2c·EtOH** was successful, accurate cell dimensions were obtained by data collections during the early stage: monoclinic,  $a = 9.835(11)$ ,  $b = 21.210(8)$ ,  $c = 10.545(14)$  Å,  $\beta = 106.97(9)$ ,  $V = 2108(4)$  Å<sup>3</sup>. The crystal system of **2c·EtOH** (monoclinic) is different from those

of **2b**•EtOH and **2c**•PrOH (triclinic) and, therefore, the molecular arrangement of **2c**•EtOH would also be different from **2b**•EtOH and **2c**•PrOH.

Though the **2c**/EtOH ratio has not been accurately determined, the ratio can be estimated from the volume per dimer molecule ( $V/Z$ ). In the case of **2c**•EtOH, assuming that  $Z = 2$ ,  $V/Z$  is  $1054 \text{ \AA}^3$ . On the other hand, the  $V/Z$  values of **2c** and **2c**•PrOH are  $835 \text{ \AA}^3$  and  $949 \text{ \AA}^3$ , respectively. On the basis of these values, it can be concluded that complex **2c**•EtOH comprises a dimer and ethanol in the ratio of 1:2. The second ethanol molecule would be hydrogen-bonded with the pyridyl group and replaced between two dimers. Subsequently,  $L$  is elongated to make the molecular arrangement more favorable for polymerization.

These results demonstrate that complexation of the dimer with a solvent, such as alcohols, causes an elongation of the value of  $L$  to make the crystal structure of diolefinic compounds suitable for the [2+2] photopolymerization.

### 2. 3. Conclusion

Topochemical reactions of methyl, ethyl, and propyl  $\alpha$ -cyano-4-[2-(4-pyridyl)ethenyl]cinnamates (**1a**, **1b**, and **1c**) in the crystalline state afford homo-type dimers, oligomers, and polymers having either  $\alpha$ -type (from **1b** and **1c**) or  $\beta$ -type (from **1a**) cyclobutane ring. The diversified photoproducts, which are caused by difference in the ester alkyl moiety, have been elucidated on the basis of their crystal structure analyses.

The photoreaction of **1b** proceeds through an "even-numbered polymerization mechanism" during the entire course of photopolymerization.

Since an alcohol molecule is hydrogen-bonded with the pyridyl group of the dimer, it can be placed between two dimers, making  $L$  suitable for polymerization. Therefore, the complex formation of dimers with a solvent (especially alcohols) enhances the polymerizability. Complex formation is one of the promising crystal engineering techniques which can be used for the diolefin compounds in order to obtain polymers with high molecular weight.

## 2. 4. Experimental

**Measurements.** Infrared spectra were recorded on a Jasco IR-810 spectrophotometer, and  $^1\text{H}$  NMR spectra were measured by a Jeol PMX-60SI or Jeol GX-400 instrument. Ultraviolet absorption spectra were measured on a Shimadzu UV-260 spectrophotometer at a concentration of 0.01 g/L in  $\text{CH}_2\text{Cl}_2$  or 1,1,1,3,3,3-hexafluoro-2-propanol (HFIP). The melting points were measured by a Laboratory Devices MEL-TEMP and are uncorrected. Gel permeation chromatography (GPC) was performed at 40 °C by using Shodex GPC (AD 800/P + AD 805/S + AD 803/S + AD 802/S + AD 802/S) columns (DMF solution). Thermogravimetry (TG) and differential scanning calorimetry (DSC) were measured on a Rigaku Thermoflex TG-DSC instrument under a nitrogen stream with a heating rate of 5 °C/min for about 5 mg of the sample. X-ray powder diffraction analyses were carried out with a Rigaku Rotaflex RU-200 spectrometer ( $\lambda = 1.54184 \text{ \AA}$ ).

**Preparation of the Monomers.** 4-[2-(4-Pyridyl)ethenyl]benzaldehyde was prepared by the reaction of terephthalaldehyde and  $\gamma$ -picoline according to a method described in a literature.<sup>9</sup> A mixture of 4-[2-(4-pyridyl)ethenyl]benzaldehyde (0.012 mol) and methyl  $\alpha$ -cyanoacetate (0.018 mol) in methanol (60 ml) was stirred at room temperature for 7 h. The precipitated crystals were collected and dried. A pure crystal of **1a** was obtained by recrystallization from methanol.

A crystal of **1b** was prepared in a similar manner by a reaction with ethyl cyanoacetate in ethanol, followed by recrystallization from ethanol.

**1a:** 84% ; mp 195-196.5 °C; IR (KBr) 2230, 1720, 1600, 980, 830  $\text{cm}^{-1}$ ;  $^1\text{H}$  NMR ( $\text{CDCl}_3$ )  $\delta$  3.95 (s, 3H), 7.17 (d, 2H,  $J = 17 \text{ Hz}$ ), 7.32 (d, 2H,  $J = 17 \text{ Hz}$ ), 7.40 (m, 2H), 7.66 (d, 2H,  $J = 8 \text{ Hz}$ ), 8.03 (d, 2H,  $J = 8 \text{ Hz}$ ), 8.24 (s, 1H), 8.62 (m, 2H); UV ( $\epsilon$  in  $\text{CH}_2\text{Cl}_2$ ) 360 nm (45,300). Anal. Calcd for  $\text{C}_{18}\text{H}_{14}\text{O}_2\text{N}_2$  (%): C, 74.47, H, 4.87, N, 9.65. Found (%): C, 74.17, H, 4.70, N, 9.53.

**1b:** 89%; mp 172-173.5 °C; IR (KBr) 2230, 1720, 1600, 980, 840  $\text{cm}^{-1}$ ;  $^1\text{H}$  NMR ( $\text{CDCl}_3$ )  $\delta$  1.41 (t, 3H,  $J = 7 \text{ Hz}$ ), 4.40 (q, 2H,  $J = 4 \text{ Hz}$ ), 7.16 (d, 2H,  $J = 16 \text{ Hz}$ ), 7.32 (d, 2H,  $J = 16 \text{ Hz}$ ), 7.40 (m, 2H), 7.66 (d, 2H,  $J = 9 \text{ Hz}$ ), 8.03 (d, 2H,  $J = 9 \text{ Hz}$ ), 8.24 (s, 1H), 8.62 (m, 2H); UV ( $\epsilon$  in  $\text{CH}_2\text{Cl}_2$ ) 360 nm (43,900). Anal. Calcd

for C<sub>19</sub>H<sub>16</sub>O<sub>2</sub>N<sub>2</sub> (%): C, 74.98; H, 5.18; N, 9.20. Found (%): C, 74.94, H, 5.13; N, 9.25.

**Preparation of the Dimers.** Finely powdered crystals of **1a** (200 mg) were dispersed in 90 ml of a mixture of water and methanol (90/10 v/v) and irradiated by a 500-W high-pressure mercury lamp (Ushio USH-500D), set outside of the flask, through a Kenko L42 filter (cut off < 410 nm) for 45 h at room temperature with vigorous stirring. Monomer **1a** was mainly converted into dimer **2a** at the stage of ca. 50 % conversion. Dimer **2a** was separated from the monomer and oligomers by preparative TLC (silica gel, ethyl acetate). **2a**: 48 %; IR (KBr) 2230, 1720, 1600, 980, 840 cm<sup>-1</sup>; <sup>1</sup>H NMR (CDCl<sub>3</sub>) δ 3.91 (s, 6H), 4.51 (d, 2H, J = 8 Hz), 4.58 (d, 2H, J = 8 Hz), 7.01 (m, 2H), 7.22 (d, 2H, J = 9 Hz), 7.83 (d, 2H, J = 9 Hz), 7.83 (d, 2H, J = 9 Hz), 8.43 (m, 2H); UV (ε in CH<sub>2</sub>Cl<sub>2</sub>): 306 nm (53,300); MS m/e 398, 182 (unsymmetric cleavage of the cyclobutane ring).

The photoreaction was carried out for **1b** in the same manner for 6 h. Monomer **1b** was quantitatively converted into dimer **2b**. **2b**: mp 191.5-193 °C (decomposition); IR (KBr) 2250, 1745, 1600, 1000, 990, 975, 850, 830 cm<sup>-1</sup>; <sup>1</sup>H NMR (CDCl<sub>3</sub>) δ 0.96 (t, 6H, J = 7 Hz), 4.04 (dq, 2H, J<sub>1</sub> = 11 Hz, J<sub>2</sub> = 7 Hz), 4.09 (dq, 2H, J<sub>1</sub> = 11 Hz, J<sub>2</sub> = 7 Hz), 5.17 (s, 2H), 7.07 (d, 2H, J = 16 Hz), 7.29 (d, 2H, J = 16 Hz), 7.39 (m, 4H), 7.52 (d, 4H, J = 8 Hz), 7.61 (d, 4H, J = 8 Hz), 8.56 (m, 4H); UV (ε in CH<sub>2</sub>Cl<sub>2</sub>) 315 nm (66,500).

**Preparation of the Complexes.** Dimer **2b** was recrystallized from ethanol to form complex **2b**•EtOH in a molar ratio of 1:1. The stoichiometry was confirmed by its <sup>1</sup>H NMR spectrum. Moreover, TG-DSC analysis showed a broad endothermic peak at 78-164 °C with 8.1 % weight loss (in agreement with the theoretical value (7.0 %) for the evaporation of ethanol from complex **2b**•EtOH) and an exothermic peak corresponding to the decomposition at 199 °C.

Complexes **2b**•PrOH, **2b**•AcOBu, and **2b**•xylene were formed by recrystallization of **2b** with the corresponding solvent. The stoichiometries were confirmed by their <sup>1</sup>H NMR spectra and TG-DSC analyses.

Complexes **2c•EtOH** and **2c•PrOH** were formed by the recrystallization of **2c** with the corresponding solvent. The stoichiometries were confirmed by their  $^1\text{H}$  NMR spectra and TG-DSC analyses.

**Photoirradiation.** Photopolymerization was carried out as follows. Method 1): Finely powdered crystals (**1a**, **1b**, **2b•EtOH**, **2c•EtOH**, or **2c•PrOH**) were dispersed in 300 ml of water containing a few drops of a surfactant (Nikkol TL-10FF) and irradiated with a 100-W high-pressure mercury lamp (Eikousha EHB WF-100), set inside of the flask, through a Pyrex glass filter with vigorous stirring under a nitrogen atmosphere. Method 2): Finely powdered crystals (**2b•EtOH**, **2b•PrOH**, **2b•AcOBu**, or **2b•xylene**) were mixed with quartz particles and irradiated with a 500-W super-high-pressure mercury lamp (Eikousha EHB WF-500), set outside of the flask, through a UV 30 filter (cut off < 280 nm) with vigorous stirring under a nitrogen atmosphere. The photopolymerization of the dimers are carried out at  $-20\text{ }^\circ\text{C}$  to suppress a non-topochemical reaction.

**Photoproduct of 2b:** IR (KBr): 1740, 1600, 1240  $\text{cm}^{-1}$ .  $^1\text{H}$  NMR ( $\text{CDCl}_3$ )  $\delta$  0.7-0.9 (m, 6H), 3.60 (bs, 2H), 3.82 (bs, 2H), 4.57 (bs, 2H), 4.66 (bs, 2H), 5.04 (s, 2H), 7.2-7.4 (m, 12H), 8.2 - 8.5 (m, 4H); UV ( $\epsilon$  in  $\text{CH}_2\text{Cl}_2$ ): 234.4 nm (10,500).

**Photoproduct of 2b•EtOH:** IR (KBr) 1740, 1600, 1240  $\text{cm}^{-1}$ ;  $^1\text{H}$  NMR ( $\text{CDCl}_3$ )  $\delta$  0.7-0.9 (m, 6H), 3.60 (bs, 2H), 3.82 (bs, 2H), 4.57 (bs, 2H), 4.66 (bs, 2H), 5.04 (s, 2H), 7.2-7.4 (m, 12H), 8.2-8.5 (m, 4H); UV ( $\epsilon$  in  $\text{CH}_2\text{Cl}_2$ ) 234 nm (9,650).

Photoproducts of **2b•PrOH** and **2b•AcOBu** showed the same NMR spectrum as that of **2b•EtOH**.

**Photoproduct of 2c•EtOH:** IR (KBr) 1740, 1600, 1240  $\text{cm}^{-1}$ ;  $^1\text{H}$  NMR ( $\text{CDCl}_3$ )  $\delta$  0.5-0.7 (m, 6H), 1.2-1.4 (m, 4H), 3.50 (bs, 2H), 3.80 (bs, 2H), 4.57 (bs, 2H), 4.66 (bs, 2H), 5.04 (s, 2H), 7.0-7.4 (m, 12H), 8.31 (bs, 4H); UV ( $\epsilon$  in  $\text{CH}_2\text{Cl}_2$ ): 234 nm (9500).

The photoproduct of **2c•PrOH** showed the same NMR spectrum as that of **2c•EtOH**.

**X-ray Measurement.** Intensity data were measured on a Rigaku four-circle diffractometer with graphite monochromated Cu-K $\alpha$  radiation. Accurate cell dimensions were obtained by least-squares refinement of 15 reflections for **1a** and **1b** and 20 reflections for **2b•EtOH** and **2c•PrOH** accurately centered reflections in the range  $40^\circ < 2\theta < 60^\circ$ . Data were collected with three check reflections. The observed reflections ( $|F_0| > 3\sigma(|F_0|)$ ) were used in the solutions and refinements; no absorption correction was made. The structures were solved by a direct method with the MULTAN 78 program and refined by a full-matrix least-squares method with SHELXS 76. The intensity data collection, refinement details, and crystal data are summarized in Table 2.3. The positions of hydrogen atoms were obtained from a difference map. Final refinements were performed with the anisotropic thermal parameters for the non-hydrogen atoms and with isotropic ones for the hydrogen atoms. Isotropic thermal parameters of hydrogen atoms attached to sp<sup>3</sup> carbons are constructed to 1.2 times the B<sub>eq</sub> of parent carbons for **2b•EtOH** and **2c•PrOH**.

The intensity data collection, refinement details, and crystal data are summarized in Table 2.3. The final molecular coordinates and thermal parameters are listed in Tables 2.4, 2.5, 2.6, and 2.7.

**Table 2.3.** Summary of Crystal Data, Intensity Collection Parameters, and Refinement Details

compounds	1a	1b	2b•EtOH	2c•PrOH
formula	C <sub>18</sub> H <sub>14</sub> N <sub>2</sub> O <sub>2</sub>	C <sub>19</sub> H <sub>16</sub> N <sub>2</sub> O <sub>2</sub>	C <sub>38</sub> H <sub>32</sub> N <sub>4</sub> O <sub>4</sub> •C <sub>2</sub> H <sub>6</sub> O	C <sub>40</sub> H <sub>36</sub> N <sub>4</sub> O <sub>4</sub> •C <sub>3</sub> H <sub>8</sub> O
crystal system	monoclinic	triclinic	triclinic	triclinic
space group	P2 <sub>1</sub> /a	PI	PI	PI
a, Å	30.965(2)	11.651(1)	14.114(3)	13.706(2)
b, Å	4.049(0)	9.151(1)	12.763(3)	13.508(2)
c, Å	11.795(0)	7.814(1)	11.055(3)	12.110(2)
α, deg	85.84(1)	110.86(2)	110.75(1)	
β, deg	97.10(0)	104.44(1)	81.01(2)	102.88(1)
γ, deg	80.05(1)	110.66(3)	105.00(1)	
V, Å <sup>3</sup>	1467.5(1)	787.1(1)	1740(1)	1898(1)
Z	4	2	2	2
cryst. solv.	methanol	ethanol	ethanol	propanol
crystal size, mm <sup>3</sup>	0.35x0.2x0.04	0.5x0.4x0.05	0.7x0.5x0.1	0.3x0.2x0.05
Dcal	1.31	1.28	1.26	1.22
μ, cm <sup>-1</sup>	6.19	5.97	5.90	6.09
scan mode	2θ-ω	2θ-ω	2θ-ω	2θ-ω
2θmax, deg	125	125	125	125
unique reflcns	2480	2510	4941	5850
obsd reflcns	2092	2212	4041	3770
( F <sub>0</sub>   > 3σ( F <sub>0</sub>  ))				
R factor	0.067	0.055	0.098	0.088
Rw factor	0.067	0.074	0.115	0.091
largest shift/esd	0.42	0.22	0.49	0.47
largest peak, e/Å <sup>3</sup>	0.26	0.24	0.31	0.22

Table 2.4. Final Atomic Coordinates ( $\times 10^4$  for C, N, and O;  $\times 10^3$  for H) with Equivalent Isotropic Thermal Parameters,  $B_{eq}$  ( $\text{\AA}^2$ ), for Non-Hydrogen Atoms and Isotropic Thermal Parameters,  $B$  ( $\text{\AA}^2$ ), for Hydrogen Atoms for **1a**

$$B_{eq} = (1/3) \sum_i \sum_j B_{ij} a_i^* a_j^* a_{ij}$$

Atom	x	y	z	B or $B_{eq}$
C 1	-259( 1)	-1295( 8)	1347( 3)	3.9( 1)
C 2	-597( 1)	-1931( 8)	514( 3)	4.3( 1)
C 3	-1016( 1)	-904( 7)	608( 3)	3.9( 1)
C 4	-1085( 1)	775( 8)	1603( 3)	4.4( 1)
C 5	-750( 1)	1438( 8)	2459( 3)	3.9( 1)
C 6	-327( 1)	362( 7)	2347( 2)	3.2( 1)
C 7	10( 1)	1243( 7)	3274( 2)	3.3( 1)
C 8	437( 1)	522( 7)	3432( 2)	3.0( 1)
C 9	658( 1)	-1504( 7)	2698( 2)	3.3( 1)
N 10	842( 1)	-3173( 7)	2136( 2)	5.0( 1)
C 11	712( 1)	1977( 7)	4430( 2)	3.4( 1)
O 12	580( 1)	3833( 6)	5106( 2)	4.8( 1)
O 13	1123( 1)	1016( 5)	4470( 2)	4.1( 1)
C 14	1427( 1)	2463(12)	5371( 4)	5.1( 1)
C 15	-1353( 1)	-1561( 8)	-357( 3)	4.2( 1)
C 16	-1752( 1)	-393( 9)	-483( 3)	4.5( 1)
C 17	-2074( 1)	-1001( 8)	-1480( 3)	4.2( 1)
C 18	-1996( 1)	-2617(10)	-2470( 3)	5.1( 1)
C 19	-2334( 1)	-2995(11)	-3370( 3)	5.8( 1)
N 20	-2730( 1)	-1812( 8)	-3357( 3)	5.8( 1)
C 21	-2800( 1)	-252(11)	-2394( 3)	5.6( 1)
C 22	-2492( 1)	188(10)	-1470( 3)	4.9( 1)
H 1	6( 1)	-194( 9)	122( 3)	5.3( 8)
H 2	-56( 1)	-290(10)	-14( 4)	5.8( 9)
H 4	-134( 1)	142(10)	178( 3)	6.0( 9)
H 5	-80( 1)	247( 9)	320( 3)	4.5( 7)
H 7	-9( 1)	259( 9)	381( 3)	4.4( 7)
H141	168( 2)	128(11)	537( 4)	7.0(11)
H142	124( 2)	251(15)	601( 5)	10.7(16)
H143	147( 2)	474(14)	517( 4)	7.5(11)
H 15	-126( 1)	-317(11)	-100( 4)	7.5(11)
H 16	-183( 2)	99(13)	33( 4)	7.9(11)
H 18	-173( 1)	-350(10)	-254( 4)	6.3( 9)
H 19	-228( 1)	-412(10)	-405( 3)	5.6( 8)
H 21	-313( 1)	65(11)	-244( 4)	7.2(10)
H 22	-256( 1)	128( 9)	-75( 3)	5.3( 8)

Table 2.5. Final Atomic Coordinates ( $\times 10^4$  for C, N, and O;  $\times 10^3$  for H) with Equivalent Isotropic Thermal Parameters,  $B_{eq}$  ( $\text{\AA}^2$ ), for Non-Hydrogen Atoms and Isotropic Thermal Parameters,  $B$  ( $\text{\AA}^2$ ), for hydrogen Atoms for **1b**

$$B_{eq} = (1/3) \sum_i \sum_j B_{ij} a_i^* a_j^*$$

Atom	x	y	z	B or $B_{eq}$
N 1	9469 (2)	6264 (3)	-3338 (3)	5.2 (1)
C 2	8945 (2)	5081 (3)	-3636 (4)	4.9 (1)
C 3	8265 (2)	4559 (3)	-2587 (3)	4.1 (1)
C 4	8109 (2)	5283 (2)	-1139 (3)	3.4 (1)
C 5	8647 (2)	6513 (3)	-829 (3)	4.2 (1)
C 6	9312 (2)	6948 (3)	-1934 (4)	5.0 (1)
C 7	7426 (2)	4834 (2)	90 (3)	3.7 (1)
C 8	6789 (2)	3767 (2)	-75 (3)	3.7 (1)
C 9	6112 (2)	3340 (2)	1169 (3)	3.3 (1)
C 10	5330 (2)	2344 (2)	694 (3)	3.7 (1)
C 11	4660 (2)	1923 (2)	1809 (3)	3.7 (1)
C 12	4760 (2)	2450 (2)	3468 (3)	3.3 (1)
C 13	5569 (2)	3420 (2)	3947 (3)	3.9 (1)
C 14	6218 (2)	3856 (3)	2824 (3)	4.0 (1)
C 15	4098 (2)	2108 (2)	4734 (3)	3.3 (1)
C 16	3336 (2)	1150 (2)	4767 (3)	3.2 (1)
C 17	3048 (2)	167 (2)	3457 (3)	3.5 (1)
N 18	2814 (2)	-636 (2)	2414 (3)	5.1 (1)
C 19	2778 (2)	1081 (2)	6285 (3)	3.5 (1)
O 20	2950 (2)	1849 (2)	7480 (2)	5.3 (1)
O 21	2086 (1)	65 (2)	6155 (2)	4.0 (0)
C 22	1500 (2)	-132 (3)	7582 (4)	4.7 (1)
C 23	337 (2)	953 (3)	7239 (4)	5.3 (1)
H 2	910 (2)	453 (3)	-462 (4)	5.6 (6)
H 3	795 (2)	361 (3)	-288 (3)	3.9 (4)
H 5	850 (2)	707 (3)	16 (3)	4.4 (5)
H 6	966 (2)	787 (3)	-174 (3)	4.9 (6)
H 7	736 (2)	547 (3)	126 (4)	5.3 (6)
H 8	676 (3)	313 (4)	-116 (4)	6.5 (7)
H 10	521 (2)	187 (3)	-53 (4)	4.6 (5)
H 11	417 (3)	122 (4)	130 (4)	6.4 (7)
H 13	568 (2)	377 (3)	504 (4)	4.6 (5)
H 14	683 (2)	452 (3)	335 (4)	5.1 (6)
H 15	418 (2)	266 (2)	573 (3)	3.4 (4)
H221	138 (2)	-113 (3)	768 (4)	4.5 (5)
H222	205 (3)	-5 (3)	872 (4)	6.5 (7)
H231	50 (2)	204 (3)	702 (4)	5.6 (6)
H232	-33 (3)	74 (5)	596 (6)	9.4 (10)
H233	-5 (3)	88 (4)	825 (5)	7.3 (8)

Table 2.6. Final Atomic Coordinates ( $\times 10^4$  for C, N, and O;  $\times 10^3$  for H) with Equivalent Isotropic Thermal Parameters,  $B_{eq}$  ( $\text{\AA}^2$ ), for Non-Hydrogen Atoms and Isotropic Thermal Parameters,  $B$  ( $\text{\AA}^2$ ), for Hydrogen Atoms for **2b**•EtOH

$$B_{eq} = (1/3) \sum_i \sum_j B_{ij} a_i^* a_j^* a_{ij}$$

Atom	x	y	z	B or $B_{eq}$
C1	2460 (3)	5129 (3)	2563 (4)	4.3 (1)
C2	3556 (3)	5907 (3)	2298 (4)	4.7 (1)
C3	3365 (3)	6991 (3)	3447 (4)	4.7 (1)
C4	2184 (3)	6289 (3)	3393 (4)	4.2 (1)
C5	1794 (3)	4128 (3)	1541 (4)	4.5 (1)
C6	763 (4)	3809 (4)	1696 (4)	5.5 (2)
C7	138 (4)	2807 (4)	829 (4)	5.6 (2)
C8	549 (4)	2045 (4)	-178 (4)	5.3 (2)
C9	1577 (4)	2373 (4)	-317 (4)	5.6 (2)
C10	2216 (4)	3389 (4)	508 (4)	5.5 (2)
C11	-157 (4)	938 (4)	-985 (4)	5.9 (2)
C12	101 (4)	25 (4)	-1787 (5)	6.0 (2)
C13	-607 (4)	-1093 (4)	-2561 (4)	5.0 (2)
C14	-1667 (4)	-1386 (4)	-2433 (4)	5.4 (2)
C15	-2272 (4)	-2452 (4)	-3225 (4)	5.5 (2)
N16	-1881 (3)	-3247 (3)	-4131 (4)	5.4 (1)
C17	-892 (4)	-2961 (4)	-4229 (5)	5.9 (2)
C18	-239 (4)	-1917 (4)	-3491 (5)	5.8 (2)
C19	3872 (3)	7337 (3)	4686 (4)	4.7 (1)
C20	4569 (4)	8467 (4)	5140 (4)	5.1 (2)
C21	5065 (4)	8849 (4)	6275 (4)	5.9 (2)
C22	4896 (3)	8096 (4)	7010 (4)	5.1 (2)
C23	4198 (4)	6973 (4)	6524 (5)	5.3 (2)
C24	3720 (4)	6581 (4)	5407 (4)	5.2 (2)
C25	5344 (5)	8454 (5)	8233 (5)	6.2 (2)
C26	5969 (4)	9486 (4)	8895 (5)	6.0 (2)
C27	6355 (4)	9779 (4)	10162 (5)	6.1 (2)
C28	7027 (4)	10883 (5)	10752 (5)	6.9 (2)
C29	7380 (4)	11155 (6)	11954 (5)	7.2 (2)
N30	7172 (4)	10393 (5)	12594 (4)	7.2 (2)
C31	6536 (5)	9336 (7)	12031 (6)	7.2 (3)
C32	6130 (5)	8984 (5)	10849 (5)	7.3 (2)
C33	1629 (4)	6676 (4)	2608 (5)	5.7 (2)
O34	2066 (3)	7102 (4)	1783 (4)	7.6 (2)
O35	666 (3)	6427 (3)	2926 (3)	6.8 (1)
C36	35 (7)	6614 (8)	2146 (8)	9.2 (4)
C37	-943 (8)	5743 (10)	2002 (12)	12.6 (5)
C38	1656 (3)	6245 (3)	4616 (4)	4.6 (1)
N39	1242 (3)	6192 (3)	5589 (4)	6.3 (2)
C40	4385 (4)	5504 (4)	2463 (4)	5.2 (2)
O41	4266 (3)	4575 (3)	2612 (4)	7.0 (1)
O42	5284 (3)	6309 (3)	2424 (3)	6.5 (1)

Table 2.6. (continued)

Atom	x	y	z	B or B(eq)
C43	6153(4)	6082(5)	2531(6)	7.6(2)
C44	6266(6)	6317(7)	4003(7)	9.2(3)
C45	3719(4)	6115(4)	1032(5)	6.2(2)
N46	3907(4)	6280(4)	65(4)	9.0(2)
O47	2366(4)	8945(4)	4727(4)	8.9(2)
C48	2072(10)	9725(8)	4442(8)	11.4(5)
C49	1633(11)	10495(10)	5250(9)	15.7(8)
H1	260(3)	486(4)	313(4)	4.8(10)
H3	369(3)	761(4)	315(4)	5.8(10)
H6	39(4)	425(4)	233(5)	6.2(12)
H7	-62(4)	257(4)	88(4)	7.1(13)
H9	200(4)	193(5)	-94(5)	7.8(14)
H10	293(4)	359(4)	52(4)	5.8(11)
H11	-105(6)	106(6)	-78(7)	13.1(22)
H12	82(6)	20(6)	-153(7)	11.7(21)
H14	-210(4)	-84(4)	-175(5)	6.6(11)
H15	-307(5)	-269(5)	-309(5)	9.2(15)
H17	-55(4)	-362(5)	-487(5)	7.4(12)
H18	32(3)	-179(3)	-352(3)	2.7(8)
H20	481(3)	893(4)	464(4)	5.6(11)
H21	563(3)	963(4)	652(4)	4.7(9)
H23	389(4)	667(4)	702(5)	6.4(14)
H24	316(4)	585(4)	524(4)	6.2(11)
H25	554(4)	822(5)	855(5)	6.2
H26	644(0)	1011(0)	840(0)	5.0
H28	726(3)	1138(4)	1014(4)	11.8(9)
H29	777(5)	1193(6)	1221(7)	6.5(22)
H31	636(4)	887(5)	1234(5)	5.1(12)
H32	567(4)	832(4)	1057(5)	5.1(14)
H361	7(3)	729(4)	263(4)	7.9(10)
H362	47(5)	680(5)	162(6)	7.9
H371	-67(0)	561(0)	99(0)	11.0
H372	-90(5)	523(6)	222(6)	11.0
H373	-139(0)	594(0)	172(0)	11.0
H431	606(6)	530(6)	190(7)	8.6
H432	685(0)	683(0)	215(0)	8.6
H441	621(6)	730(7)	437(8)	9.5
H442	563(0)	590(0)	445(0)	9.5
H443	694(5)	705(6)	339(7)	9.5
H47	267(0)	936(0)	554(0)	10.8
H481	143(4)	937(5)	395(6)	9.9
H482	265(0)	1009(0)	391(0)	9.9
H491	155(4)	1105(5)	485(6)	11.6
H492	220(0)	1093(0)	586(0)	11.6
H493	99(5)	1019(6)	573(6)	11.6

Table 2.7. Final Atomic Coordinates ( $\times 10^4$  for C, N, and O;  $\times 10^3$  for H) with Equivalent Isotropic Thermal Parameters,  $B_{eq}$  ( $\text{\AA}^2$ ), for Non-Hydrogen Atoms and Isotropic Thermal Parameters,  $B$  ( $\text{\AA}^2$ ), for Hydrogen Atoms for **2c•PrOH**

$$B_{eq} = (1/3) \sum_i \sum_j B_{ij} a_i^* a_j^* a_i a_j$$

Atom	x	y	z	B or $B_{eq}$
C 1	7705 (4)	4047 (4)	2536 (6)	4.7 (2)
C 2	7415 (4)	5154 (5)	2857 (6)	4.7 (3)
C 3	6253 (4)	4431 (4)	1880 (6)	4.9 (3)
C 4	6466 (5)	3315 (5)	1878 (7)	4.8 (3)
C 5	5926 (4)	2793 (5)	2601 (6)	4.7 (3)
C 6	5316 (5)	1611 (5)	1996 (7)	5.3 (3)
C 7	4843 (5)	1110 (5)	2635 (8)	5.8 (3)
C 8	4933 (5)	1693 (5)	3848 (8)	5.5 (3)
C 9	5506 (5)	2859 (5)	4444 (7)	5.8 (3)
C 10	5999 (5)	3377 (5)	3795 (7)	5.0 (3)
C 11	4416 (4)	1113 (5)	4542 (8)	5.3 (3)
C 12	4469 (5)	1559 (6)	5700 (8)	5.8 (3)
C 13	3961 (5)	938 (6)	6327 (8)	5.2 (3)
C 14	3239 (5)	-193 (6)	5730 (8)	6.0 (3)
C 15	2816 (6)	-715 (7)	6389 (10)	6.4 (4)
N 16	3037 (5)	-200 (6)	7598 (9)	7.1 (3)
C 17	3740 (7)	913 (8)	8214 (9)	7.4 (4)
C 18	4202 (5)	1470 (6)	7575 (9)	6.3 (4)
C 19	8112 (4)	6241 (5)	2903 (6)	4.8 (3)
C 20	7693 (5)	6949 (5)	2600 (7)	6.1 (3)
C 21	8348 (5)	8028 (5)	2796 (7)	5.8 (3)
C 22	9467 (5)	8379 (4)	3288 (6)	5.0 (3)
C 23	9870 (5)	7649 (5)	3563 (7)	6.0 (3)
C 24	9213 (5)	6562 (5)	3395 (7)	5.7 (3)
C 25	10191 (5)	9492 (5)	3494 (7)	5.8 (3)
C 26	9950 (5)	10297 (5)	3302 (7)	6.1 (3)
C 27	10709 (5)	11406 (5)	3543 (6)	5.2 (3)
C 28	11812 (5)	11697 (5)	3952 (7)	6.1 (3)
C 29	12479 (5)	12764 (5)	4162 (6)	6.0 (3)
N 30	12129 (5)	13557 (4)	4029 (5)	6.2 (3)
C 31	11082 (6)	13281 (5)	3645 (6)	5.8 (3)
C 32	10361 (5)	12229 (5)	3401 (7)	6.1 (3)
C 33	8361 (6)	3958 (4)	1661 (7)	5.2 (3)
O 34	9295 (4)	4055 (4)	2015 (5)	7.9 (2)
O 35	7830 (4)	3818 (4)	551 (5)	6.4 (2)
C 36	8405 (8)	3909 (8)	-271 (10)	9.5 (5)
C 37	7612 (11)	-3469 (14)	-1603 (14)	14.8 (10)
C 38	8134 (13)	3589 (15)	-2502 (13)	18.6 (11)
C 39	8253 (5)	3917 (5)	3612 (7)	5.3 (3)
N 40	8635 (5)	3769 (4)	4465 (6)	6.8 (3)
C 41	5333 (5)	4662 (6)	2293 (7)	4.8 (3)
O 42	5463 (3)	5481 (4)	3204 (5)	6.5 (2)
O 43	4411 (3)	3809 (4)	1551 (4)	6.1 (2)
C 44	3436 (6)	3905 (7)	1799 (9)	7.9 (4)

Table 2.7. (continued)

Atom	x	y	z	B or B(eq)
C 45	2519( 7)	3093(12)	736(14)	13.7( 8)
C 46	1430(11)	2976(16)	605(15)	18.8(10)
C 47	6072( 4)	4422( 5)	641( 7)	4.8( 3)
N 48	5832( 4)	4381( 4)	-347( 7)	6.5( 3)
O 49	7472( 7)	1448( 8)	1057(12)	12.3( 6)
C 50	7824(25)	957(15)	46(17)	22.0(19)
C 51	8379(26)	613(31)	-816(33)	51.3(34)
C 52	9193(26)	175(39)	-436(28)	33.9(34)
H 2	752( 4)	543( 4)	363( 5)	3.9
H 4	627( 0)	276( 0)	98( 1)	6.1(15)
H 6	524( 0)	126( 0)	109( 1)	5.1(14)
H 7	436( 1)	34( 1)	195( 1)	10.0(21)
H 9	559( 1)	338( 1)	531( 1)	5.2(14)
H 10	633( 0)	418( 1)	448( 1)	4.8(12)
H 11	404( 0)	30( 1)	390( 1)	4.5
H 12	484( 1)	241( 1)	617( 1)	7.5(17)
H 14	301( 1)	-67( 1)	480( 1)	2.9(11)
H 15	224( 1)	-149( 1)	603( 1)	3.7(11)
H 17	387( 1)	122( 1)	914( 1)	13.1(32)
H 18	471( 1)	225( 1)	821( 1)	15.7(38)
H 20	690( 1)	668( 1)	216( 1)	11.7(24)
H 21	801( 0)	843( 0)	237( 1)	5.3(13)
H 23	1065( 0)	788( 1)	403( 1)	7.9(17)
H 24	955( 0)	607( 0)	365( 1)	2.5( 9)
H 25	1099( 0)	973( 1)	384( 1)	7.5(16)
H 26	918( 0)	1016( 1)	288( 1)	3.7(10)
H 28	1212( 1)	1111( 1)	402( 1)	6.9(15)
H 29	1325( 1)	1286( 1)	431( 1)	2.1( 8)
H 31	1081( 1)	1385( 0)	347( 1)	2.9( 9)
H 32	958( 1)	1211( 1)	322( 1)	2.5( 9)
H361	876( 1)	476( 1)	13( 1)	6.4
H362	897( 1)	357( 1)	-27( 1)	6.4
H371	706( 1)	383( 1)	-165( 1)	5.2
H372	726( 1)	262( 1)	-212( 1)	5.2
H381	763( 1)	327( 2)	-339( 1)	15.7
H382	851( 1)	306( 2)	-243( 1)	15.7
H383	868( 1)	435( 2)	-227( 1)	15.7
H441	329( 1)	461( 1)	189( 1)	4.6
H442	339( 1)	375( 1)	254( 1)	4.6
H451	259( 1)	313( 1)	-5( 1)	11.8
H452	238( 1)	230( 1)	64( 1)	11.8
H461	90( 1)	252( 2)	-27( 2)	18.2
H462	157( 1)	380( 2)	86( 2)	18.2
H463	113( 1)	274( 2)	120( 2)	18.2

## 2. 5. References

- 1) (a) Hasegawa, M. *Chem. Rev.* **1983**, 83, 507. (b) Nakanishi, H.; Hasegawa, M.; Sasada, Y. *J. Polym. Sci., Polym. Phys. Ed.* **1977**, 15, 173.
- 2) (a) Hasegawa, M.; Kato, S.; Yonezawa N.; Saigo, K. *J. Polym. Sci., Polym. Lett. Ed.* **1986**, 24, 153. (b) Hasegawa, M.; Harashina, H.; Kato, S.; Saigo, K. *Macromolecules* **1986**, 19, 1276. (c) Hasegawa, M.; Kato, S.; Saigo, K.; Wilson, S. R.; Stern, C. L.; Paul, I. C. *J. Photochem. Photobiolog., A Chem.* **1988**, 41, 385. (d) Hasegawa, M.; Katsumata, T.; Ito, Y.; Saigo, K. *Macromolecules* **1988**, 21, 3134. (e) Hasegawa, M.; Aoyama, M.; Maekawa, Y.; Ohashi, Y. *Macromolecules* **1989**, 22, 1568.
- 3) **1b** shows polymorphic modifications. Upon irradiation another modification gave amorphous oligomers.
- 4) Nakanishi H.; Sasada, Y. *Acta Cryst.* **1978**, B34, 332.
- 5) Hasegawa, M.; Endo, Y.; Maekawa, Y.; Hirano, T. to be published.
- 6) Tamaki, T.; Suzuki, Y.; Hasegawa, M. *Bull. Soc. Chem. Jpn.* **1972**, 45, 1988.
- 7) Kato, S. Master Thesis, The University of Tokyo, **1986**.
- 8) Molecular structure of **2b•EtOH**: The cyclobutane ring is puckered with a dihedral angle of  $22.9^\circ$  between planes C(1)-C(2)-C(4) and C(2)-C(3)-C(4), and the two phenylene groups, attached to the cyclobutane ring, are nearly perpendicular to each other with a dihedral angle of  $86.0^\circ$ . Molecular structure of **2c•PrOH**: The cyclobutane ring is puckered with a dihedral angle of  $22.4^\circ$  between planes C(1)-C(2)-C(4) and C(2)-C(3)-C(4), and the two phenylene groups, attached to the cyclobutane ring, are nearly perpendicular to each other with a dihedral angle of  $88.2^\circ$ .
- 9) Ichimura K.; Watanabe, S. *J. Polym. Chem. Ed.* **1982**, 20, 1420.

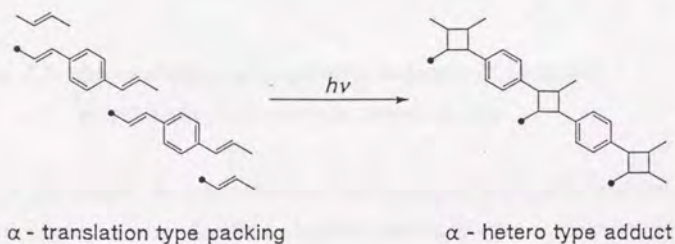
## CHAPTER 3

### A Design for Photopolymerizable Molecular Arrangement of Diolefin Crystals

#### 3.1. Introduction

For the recent years, topochemical [2+2] photoreaction has increasingly been attracting attention in viewpoints of organic and polymer syntheses due to its regio- and/or stereo-selectivity arising from the constraining environment of the crystal lattice.<sup>1)</sup> The structure of most of photoproducts has been reasonably interpreted on the basis of X-ray crystal structure analysis of the starting diolefin compounds. However, only a few papers dealt with crystal engineering, in which crystal structure was successfully designed for the purpose of preparing desirable photoproducts. For example, Schmidt and Green<sup>2)</sup> prepared a  $\beta$ -type dimer and a tricyclic dimer through [2+2] photocycloaddition by taking into account of Cl...Cl interaction; a chlorine atom that attached to an aromatic ring tends to interact with chlorine atom in the neighboring molecule and to make a crystal structure being the  $\beta$ -type packing.<sup>3)</sup> Lahav and his co-workers<sup>4)</sup> substantiated the first clear-cut example of an absolute asymmetric synthesis in the crystalline state by using isomorphous displacement method and exploited [2+2] photocycloaddition of unsymmetrically substituted diolefin compound, which formed chiral crystals, to give chiral dimer, trimer, and oligomers with quantitative enantiomeric purities.

Scheme 3.1



However, these methods can be applied only to a restricted compound. Moreover, as described in chapter 2, the photochemical behavior of unsymmetrically substituted diolefin compounds was highly diversified and was dependent even on a slight modification of the molecular structure and on the solvent used for recrystallization. These results mean that it is very difficult to predict the possibility of the reaction and the structure of the photoproduct. Namely, complete regulation of molecular arrangement has not realized yet.

Nakanishi and his co-workers,<sup>5)</sup> however, suggested that symmetric diolefin compounds with ester groups had a close contact between the ether oxygen of the ester group and the phenylene ring to make intermolecular double bonds in a crystal suitable for [2+2] photoreaction and for forming a crystalline polymer.<sup>6)</sup> The same close contact between the ether oxygen of an ester group and a phenylene ring was also observed in unsymmetric diolefin crystals of an  $\alpha$ -translation type packing;<sup>7)</sup> for example, Figure 3.1 shows an overlapping of neighboring molecules of ethyl 4-[2-(2-pyrazyl)ethenyl]cinnamate (**1a**) viewed perpendicular to the average phenylene ring. Recently, the author found that among diolefin derivatives analogous to **1a** such as amide (-CONHEt), ketones (-COMe and -COCH<sub>2</sub>CH<sub>2</sub>OH), and thioester (-COSEt) only the thioester analogue was photopolymerizable to afford a crystalline polymer.<sup>8)</sup>

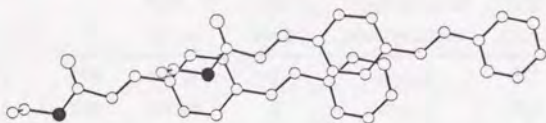


**Figure 3.1.** An overlapping of neighboring molecules of **1a** viewed perpendicular to the average phenylene ring.

In this chapter, the author describes the photopolymerizability and the crystal structure of unsymmetric diolefin compounds having an ester or thioester group in

order to elucidate the role of the ether oxygen of an ester group and the sulfur atom of a thioester for taking an  $\alpha$ -translation type packing.

### 3. 2. Results and Discussion

#### 3. 2. 1. Photoreaction of Monomers Having Pyrazyl Group

Irradiation of **2a** for 24 h at room temperature with a 500-W super-high-pressure mercury lamp gave a crystalline polymer ( $\eta_{inh} = 1.6$  dL/g). The  $^1\text{H}$  NMR spectrum of poly-**2a** was identical with that of the poly-**1a** except for the signals arising from the alkyl protons in the ester group.<sup>7a)</sup> The X-ray powder diffraction pattern of **2a** was identical with that of **1a**. These results clearly demonstrate that irradiation of **2a**, which is isomorphous to **1a**, gives a crystalline linear polymer having the alternating structure of an  $\alpha$ -homo-type cyclobutane ring and a 1,4-phenylene skeleton in the main chain as is in poly-**1a**.

Scheme 3.2

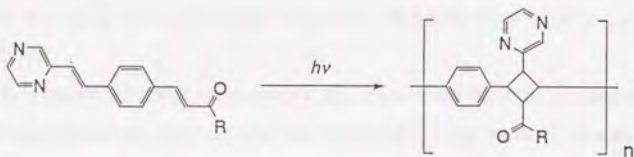


Table 3.1. Photoreaction of the Monomers Having Pyrazyl Group

compound	R	light <sup>a)</sup> source	reaction time [h]	morphology of photoproducts	$\eta_{inh}$ [dL/g]	ref.
<b>1a</b>	-OEt	500W	5	crystal	8.2	(7a)
<b>1b</b>	-OPr	100W	5	crystal	0.5	this work
<b>2a</b>	-SEt	500W	24	crystal	1.6	this work
<b>2b</b>	-SPr	500W	24	crystal	0.5	this work

a) A 100 W lamp set inside of the flask; a 500 W lamp set outside of the flask.

Photopolymerization was also carried out for monomers **1b** and **2b**, of which the ester moiety was replaced by larger propyl group.

Irradiation of **1b** for 24 h at  $-30$  °C with a 500-W super-high-pressure mercury lamp gave a crystalline polymer ( $\eta_{inh} = 0.5$  dL/g).<sup>9)</sup> The  $^1\text{H}$  NMR

spectrum was identical with that of poly-**1a** except for the signals arising from the alkyl protons in the ester group. Moreover, when **1b** was irradiated at wavelengths longer than 410 nm by using a cut-off filter in order to excite only the monomers, the dimer of **1b** was isolated from trimer and oligomers by preparative TLC. The dimer was determined to be an  $\alpha$ -hetero type adduct by its  $^1\text{H}$  NMR and mass spectra. The X-ray powder diffraction pattern of **1b** was different from that of **1a**. However, the formation of a crystalline polymer with  $\alpha$ -hetero type cyclobutane ring indicates that **1b** takes an  $\alpha$ -translation type packing in a similar manner to **1a**.

Irradiation of thioester derivative **2b** for 24 h at room temperature with a 500-W super-high-pressure mercury lamp gave a crystalline polymer ( $\eta_{\text{inh}} = 0.5$  dL/g). The  $^1\text{H}$  NMR spectrum was identical with that of poly-**2a** except for the signals arising from the alkyl protons in the ester group. The X-ray powder diffraction pattern of **2b** was identical with those of **1a** and **2a**. Thus, irradiation of **2b**, which was isomorphous to them, would also give a crystalline linear polymer having the same structure in the main chain as those of poly-**1a**, poly-**1b**, and poly-**2a**.

It is noteworthy that unsymmetrically substituted diolefin compounds having thioester group has tendency to take an  $\alpha$ -translation type packing in a similar manner to the corresponding ester compounds, resulting in the formation of a crystalline polymer.

### 3. 2. 2. Photoreaction of Monomers Having Methylpyrazyl Group

Since it is known that molecular symmetry influences molecular arrangement in a crystal,<sup>10)</sup> photopolymerization was carried out for monomers **1c**, **1d**, **2c**, and **2d** having a methylpyrazyl group, which decrease the molecular symmetry, in order to estimate the tendency of ester and thioester groups for taking an  $\alpha$ -translation type packing. The results are listed in Table 3.2.

Irradiation of **1c** for 2 h at room temperature gave amorphous oligomers. **1d** showed lower photoreactivity than the other monomers; irradiation for 24 h gave amorphous oligomers in below 50 % yield. The dimers obtained from **1c** and **1d** were confirmed on the basis of the spectral results to be  $\beta$ -hetero and  $\beta$ -homo

type adducts, respectively. These photochemical results strongly suggest that unsymmetric diolefins with lower molecular symmetry have a tendency not to take an  $\alpha$ - but  $\beta$ -type packing.

**Scheme 3.3**

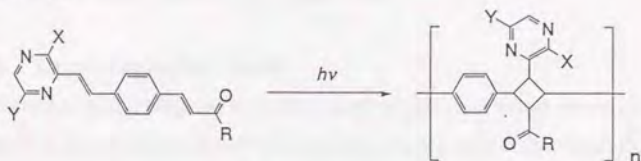


**Table 3.2.** Photoreaction of the Monomers Having Methylpyrazyl Group

compound	X	Y	R	light <sup>a)</sup> source	reaction time [h]	morphology of photoproducts	$\eta_{inh}$ [dL/g]
<b>1c</b>	Me	H	-OMe	500W	2	amorphous	— <sup>b)</sup>
<b>1d</b>	H	Me	-OMe	500W	24	amorphous	— <sup>b)</sup>
<b>2c</b>	Me	H	-SEt	100W	4	crystal	1.9
<b>2d</b>	H	Me	-SEt	100W	4	crystal	1.1

a) A 100 W lamp set inside of the flask; a 500 W lamp set outside of the flask.

b) The photoproducts of **1b**, **1c**, and **1d** comprised oligomers (degrees of polymerization were below 10), which were confirmed by GPC (DMF solution).

In contrast to **1c** and **1d**, irradiation of thioester derivatives having a 2- or 6-methylpyrazyl group, **2c** and **2d**, gave crystalline polymers ( $\eta_{inh} = 1.9$  and  $1.1$  dL/g, respectively). In the  $^1\text{H}$  NMR spectra, the cyclobutane proton signals were different from each other and also from those of poly-**2b**. The mass spectra, however, showed that these polymers were  $\alpha$ -hetero type adducts. Consequently, in spite of the lower molecular symmetry, unsymmetric diolefins having thioester group, can take an  $\alpha$ -translation type packing to give crystalline polymers.

It is well-known that a molecule having a bulky substituent barely crystallizes into a translationally related arrangement of neighboring molecules because of the repulsion between the substituents of the neighboring molecules.<sup>10)</sup> The same tendency concerning the bulkiness of a substituent is observed in diolefin compounds.<sup>11)</sup> In contrast, even though thioester derivatives (**2c** and **2d**) have a

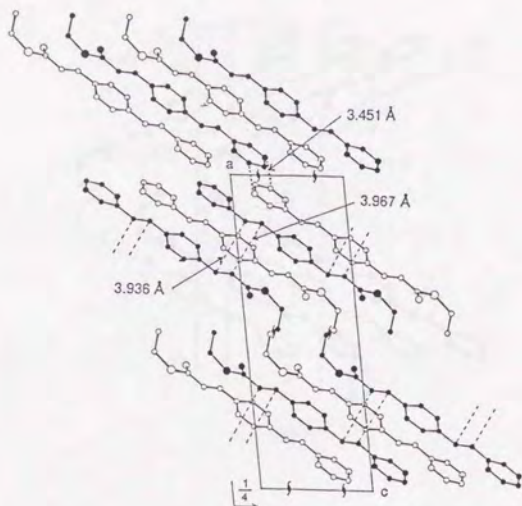
larger alkyl chain (-SEt) than that (-OMe) of ester derivatives (**1c** and **1d**), the thioester derivatives took an  $\alpha$ -translation type packing. Consequently, it is concluded that the contribution of sulfur atom to taking an  $\alpha$ -translation type packing is much larger than that of oxygen atom.

### 3. 2. 3. Crystallographic Study

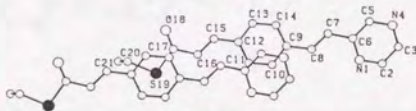
In order to elucidate the contribution of oxygen and sulfur atoms in taking an  $\alpha$ -translation type packing as well as the larger tendency of sulfur atom for taking an  $\alpha$ -translation type packing rather than that of oxygen atom, the author carried out the crystal structure analyses of **1b**, **1d**, **2a**, and **2d**.

Figures 3.2 show the crystal structure of **2a** (a) and the reacting molecules viewed perpendicular to the average plane of the phenylene rings with the numbering atoms of **2a** (b). The molecules are stacked along c-axis, in which molecules are related to each other by translation symmetry and are displaced in the direction of long molecular axis by half a molecule (an  $\alpha$ -translation type packing). The shortest double bonds are related by c-translation and are separated by distances of 3.936 Å (C(7)=C(15)) and 3.967 Å (C(8)=C(16)). There is no other contact of the double bonds, which are parallel and are within the photoreactive range. This molecular arrangement reasonably demonstrates that the double bonds related by c-translation react with each other to form a linear polymer with hetero-type cyclobutane rings. The molecular arrangement and the double bond contact of **2a** are almost the same as those of **1a**.<sup>7a)</sup> As shown in Figure 3.2 (b), the sulfur atom of the thioester group in **2a** approaches to the phenylene ring in the same manner as the ether oxygen of the ester group of **1a** (Figure 3.1).

**1b** takes a different crystal structure (Pbca) from **1a** and **2a** (P2<sub>1</sub>/c). However, the crystal structure of **1b** has the same  $\alpha$ -translation type packing (a-translation) as **1a** and **2a**, as shown in Figures 3.3 (a). The shortest double bonds are related by a-translation and are separated by distances of 3.878 Å (C(7)=C(15)) and 3.907 Å (C(8)=C(16)). There is no other contact of the double bonds, which are parallel and are within the photoreactive range. This molecular arrangement demonstrates that the double bonds related by a-translation react with each other to



(a)



(b)

**Figure 3.2.** (a) A crystal structure of **2a**. (b) An overlapping of neighboring molecules of **2a** viewed perpendicular to the average plane of the phenylene rings with the numbering atoms.

form a linear polymer with hetero-type cyclobutane rings. As shown in Figure 3.3 (b), the ether oxygen atom of the propylester group in **1b** approaches to the phenylene ring in the same manner as that of the ester group of **1a** and the sulfur atom of the thioester group of **2a**.

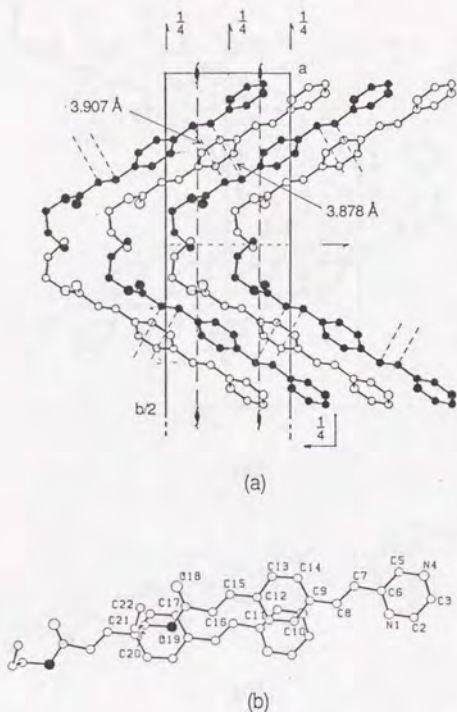


**Figure 3.3.** (a) A crystal structure of **1b**. (b) An overlapping of neighboring molecules of **1b** viewed perpendicular to the average plane of the phenylene rings with the numbering atoms.

Figures 3.4 show the crystal structure of **2d** (a) and the reacting molecules viewed perpendicular to the average plane of the phenylene rings with the numbering atoms of **2d** (b). The molecules are stacked in the same manner as **1a** and **2a** (an  $\alpha$ -translation type packing). The shortest double bonds are related by *c*-translation and are separated by a distances of 3.974 Å (C(8)=C(16)) and 3.973 Å (C(9)=C(17)). There is no other contact of the double bonds, which are parallel and within the photoreactive range. This molecular arrangement demonstrates that the double bonds related by *c*-translation react to form a linear polymer with



centrosymmetry. On the other hand, since **2d** has a methyl group in the pyrazyl ring, the pyrazyl groups of the interstack molecules can not take hydrogen bonding with each other. As a result, in contrast to **2a**, the interstack molecules are related by another two-fold axis parallel to the glide plane. Consequently, the interstack molecules are related by only 2-fold axis, and there is no centrosymmetry in crystal **2d**. In the same manner as **1a** and **2a**, the sulfur atom of the thioester group approaches to the phenylene ring, as shown in Figure 3.4 (b).

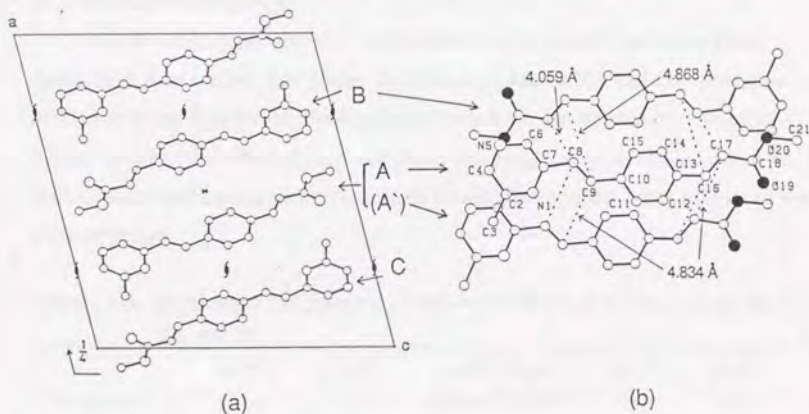


**Figure 3.5.** (a) A crystal structure of **1d**. (b) An overlapping of neighboring molecules of **1d** viewed perpendicular to the average plane of the phenylene rings with the numbering atoms.

Figures 3.5 show the crystal structure of **1d** (a) and the neighboring molecules viewed perpendicular to the average plane of the phenylene rings with the numbering atoms of **1d** (b). The molecular structure of **1d** is quite different from those of **1a**, **1b**, **2a**, and **2d**; two intramolecular double bonds are related by a cisoid conformation on the basis of the central phenylene ring. The molecule (A) is related to the neighboring molecules (A, B, and A') by centrosymmetry, two-fold axis, and b-translation (completely overlapping), respectively. Thus there is no stack structure such as observed in **1a**, **1b**, **2a**, and **2d**. As shown in Figure 3.5

(b), no intermolecular double bonds are parallel and shorter than 4.5 Å.

Considering the formation of a  $\beta$ -homo type dimer from **1d** upon irradiation, the transitionally related double bonds having the methylpyrazyl group, which are separated by a distance of 4.834 Å, should react with each other although this distance (4.834 Å) is quite longer than the photoreactive range accepted for the topochemical reaction. The longer distance coincides with the fact that the photoreactivity of **1d** is quite lower than those of the other diolefin crystals having an ester or thioester group.

As shown in figure 3.5 (b), molecules A' and B exist in the same plane; molecule A exists above this plane. In contrast to **1a**, **1b**, **2a**, and **2d**, there is no overlap with the neighboring molecules (A' and B) in **1d**; necessarily, no close contact between the ether-oxygen and phenylene ring was observed in crystal **1d**. It is unusual that the intrastack molecules do not overlap each other in spite of the stack structure.

**Table 3.3.** Parameters for Stability of Molecular Packing in the Crystals **1a**, **1b**, **2a**, and **2d**

compound	d <sub>1</sub> <sup>a)</sup> (Å)	d <sub>2</sub> <sup>b)</sup> (Å)	van der Waals contact (W, Å) <sup>c)</sup>	d <sub>1</sub> -W (Å)	d <sub>2</sub> -W (Å)
<b>1a</b>	3.505	3.421	3.32	0.19	0.10
<b>1b</b>	3.520	3.436	(C··O)	0.20	0.12
<b>2a</b>	3.499	3.643	3.65	-0.15	0.01
<b>2d</b>	3.581	3.632	(C··S)	-0.07	0.02

a) d<sub>1</sub>: A distance between least square planes of a conjugated system (two aromatic rings and two double bonds) in intrastacked molecules.

b) d<sub>2</sub>: A distance between least square planes of a phenylene ring and oxygen or sulfur atom.

c) van der Waals radii: C: 1.80 Å, O: 1.52 Å, S: 1.85 Å.<sup>10,12)</sup>

Figures 3.6 (a), (b), (c), and (d) show the neighboring molecules viewed along the average plane of the phenylene rings in **1a**, **1b**, **2a**, and **2d**, respectively. The environments around the ether-oxygen or sulfur atom in **1a**, **1b**, **2a**, and **2d** are almost the same each other. Since these diolefin compounds, which have a conjugated plane comprising two aromatic rings and two olefin groups, take a

plane-to-plane stack structure in the crystals, a contact of these planes in the stack may play an important role for the stabilization of the molecular packing. As shown in Table 3.3, the distance of the least square plane of the conjugated system between neighboring intrastacked molecules ( $d_1$ ) of **1a**, **1b**, **2a**, and **2d** ranges from 3.5 to 3.6 Å. On the other hand, van der Waals contact between sulfur atom and  $sp^2$  carbon and that between oxygen atom and  $sp^2$  carbon are 3.65 Å (1.85 + 1.80 Å) and 3.32 Å (1.52 + 1.80 Å), respectively.<sup>10,12</sup> Taking into account of the van der Waals contacts, the sizes of sulfur and oxygen atoms may be suitable for the stack structure of the molecules having a conjugated aromatic system. Thus, the contact between phenylene ring and oxygen or sulfur atom makes the molecular packing suitable for an  $\alpha$ -translation type packing of many diolefin compounds having ester or thioester group.

Moreover, it is well-known that the closest-packing of molecules is the most favorable in a crystal; namely, the van der Waals contact of neighboring molecules results in the most stable crystal structure.<sup>10</sup> The distances ( $d_2$  in Table 3.3) between the least square plane of phenylene ring and sulfur atom (**2a** : 3.643 Å and **2d** : 3.632 Å) are larger than those between the plane and oxygen atom (**1a** : 3.421 Å and **1b** : 3.436 Å). However, the difference ( $d_2 - W$ ) between the sulfur-phenylene distance ( $d_2$ ) and the van der Waals contact of sulfur- $sp^2$  carbon (**2a** : 0.01 Å and **2d** : 0.02 Å) is smaller than that between the oxygen-phenylene distance ( $d_2$ ) and the van der Waals contact of oxygen- $sp^2$  carbon (**1a** : 0.10 Å and **1b** : 0.12 Å). From the viewpoint of the closest-packing of molecules in a crystal, the contact of the sulfur-phenylene may be energetically more profitable than that of the oxygen-phenylene. The difference in stability for packing reasonably elucidates that the sulfur atom has larger tendency for taking an  $\alpha$ -translation (photopolymerizable) packing than that of the oxygen atom; as a result, the thioester derivatives having even a bulky group can take an  $\alpha$ -translation type packing, whereas ester derivatives having a bulky group take a  $\beta$ -type packing.

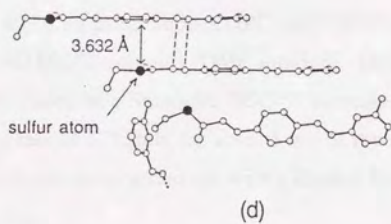
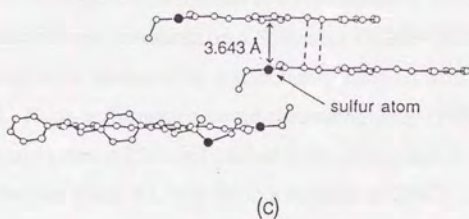
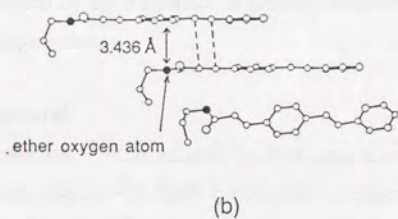
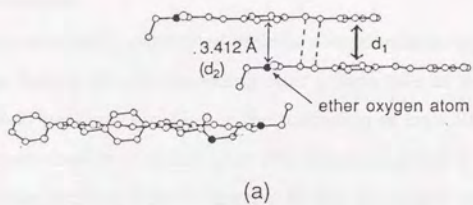


**Figure 3.5.** The neighboring molecules viewed along the average plane of the phenylene rings; (a) **1a**, (b) **1b**, (c) **2a**, and (d) **2d**.

### 3. 3. Conclusion

Unsymmetrically substituted diolefin compounds having thioester groups as well as those having the corresponding ester groups take an  $\alpha$ -translation type (photoreactive) packing, resulting in the formation of crystalline polymers.

The contribution of sulfur atom of a thioester group in taking an  $\alpha$ -translation type packing is much larger than that of oxygen atom of an ester group.

The larger tendency of the sulfur atom for taking an  $\alpha$ -translation type packing is elucidated by the difference of stability between sulfur-phenylene and oxygen-phenylene contacts.

### 3. 4. Experimental

**Measurements.** The infrared spectra were measured on a Jasco IR-810 spectrophotometer, and the  $^1\text{H}$  NMR spectra were measured by a Jeol PMX-60SI or a Jeol GX-400 instrument. The ultraviolet absorption spectra were measured on a Shimadzu UV-260 spectrophotometer at a concentration of 10.0 mg/l in  $\text{CH}_2\text{Cl}_2$ . The mass spectra were measured on a Shimadzu GCMS-QP2000 instrument. The melting points were measured by a Laboratory Devices MEL-TEMP and are uncorrected. High-performance liquid chromatography (HPLC) was performed on a steel column (4 mm x 250 mm) packed with LiChrosorb Si 60 (5  $\mu\text{m}$ , Merck and Co.) at a flow rate of 0.5 mL/min using a mixture of  $\text{CHCl}_3$  and  $\text{CH}_3\text{OH}$  (100:0.5) as an eluent, and the absorbance at 254 nm was monitored on a Shimadzu SPD-2A spectrophotometric detector. Gel permeation chromatography (GPC) was performed at 40  $^\circ\text{C}$  by using Shodex GPC (AD 800/P + AD 805/S + AD 803/S + AD 802/S + AD 802/S) columns (DMF solution). Differential scanning calorimetry (DSC) was measured on a Shimadzu DSC-50 instrument under a nitrogen stream with a heating rate of 5  $^\circ\text{C}/\text{min}$  for about 5 mg of the sample. X-ray powder diffraction analyses were carried out with a Rigaku Rotaflex RU-200 spectrometer ( $\lambda = 1.54184 \text{ \AA}$ ).

**Preparation of the Monomers.** Propyl 4-[2-(2-pyrazyl)ethenyl]cinnamate (**1b**): 4-[2-(2-Pyrazyl)ethenyl]cinnamic acid (**6**) was prepared according to the method in a literature.<sup>7a)</sup> Esterification of **6** with 1-

propanol gave **1b**. A pure crystal of **1b** was obtained by recrystallization from 1-propanol. Yield: 65 %; mp: 110-110.5 °C; IR (KBr) 1710, 1640, 1400, 990  $\text{cm}^{-1}$ ;  $^1\text{H NMR}$  ( $\text{CDCl}_3$ )  $\delta$  1.01 (t, 3H,  $J = 7$  Hz), 1.5-2.1 (m, 2H), 4.22 (t, 2H,  $J = 7$  Hz), 6.50 (d, 1H,  $J = 16$  Hz), 7.19 (d, 1H,  $J = 16$  Hz), 7.60 (s, 4H), 7.62 (d, 1H,  $J = 16$  Hz), 7.80 (d, 1H,  $J = 16$  Hz), 8.45 (d, 1H,  $J = 2$  Hz), 8.58 (bs, 1H), 8.68 (bs, 1H)

S-Ethyl 4-[2-(2-pyrazyl)ethenyl]thiocinnamate (**2a**): To a suspension of **6** (1.5 g, 5.94 mmol) in benzene (120 ml) was added a mixture of  $\text{SOCl}_2$  (10 ml, 137 mmol) and DMF (3 ml), and the mixture was refluxed for 3 hours to give a homogeneous solution. After concentration of the mixture under reduced pressure, residual  $\text{SOCl}_2$  was removed as benzene azeotrope (two times) under argon to give crude 4-[2-(2-pyrazyl)ethenyl]cinnamoyl chloride. To a solution of the resulting chloride in  $\text{CH}_2\text{Cl}_2$  (79 ml) at 0 °C under argon was added a solution of ethanethiol (1.7 ml, 23.6 mmol) and pyridine (1 ml) in  $\text{CH}_2\text{Cl}_2$  (30 ml) over a period of 30 min, and the reaction mixture was stirred for additional 30 min. After evaporation of the solvent, water was added and extracted with  $\text{CH}_2\text{Cl}_2$  (150 ml). After evaporation of the solvent, the residue was purified by column chromatography (Merck Kiesel gel 60,  $\text{CHCl}_3$ ). A pure crystal of **2a** was obtained by recrystallization from methanol (0.80 g, 62 %); mp: 165-166 °C; IR (KBr) 1660, 1620, 1060, 1030, 980, 760  $\text{cm}^{-1}$ ;  $^1\text{H NMR}$  ( $\text{CDCl}_3$ )  $\delta$  1.32 (t, 3H,  $J = 7$  Hz), 3.02 (d, 2H,  $J = 7$  Hz), 6.73 (d, 1H,  $J = 16$  Hz), 7.20 (d, 1H,  $J = 16$  Hz), 7.56 (d, 2H,  $J = 8$  Hz), 7.59 (d, 1H,  $J = 16$  Hz), 7.60 (d, 2H,  $J = 8$  Hz), 7.74 (d, 1H,  $J = 16$  Hz), 8.42 (bs, 1H), 8.55 (bs, 1H), 8.64 (s, 1H).

S-Propyl 4-[2-(2-pyrazyl)ethenyl]thiocinnamate (**2b**): **6** was esterified with propanethiol to give **2b** in the same manner as **2a**. A pure crystal of **2b** was obtained by recrystallization from methanol. Yield: 64 %; mp: 151-152 °C; IR (KBr) 1660, 1610, 1030, 980, 760  $\text{cm}^{-1}$ ;  $^1\text{H NMR}$  ( $\text{CDCl}_3$ )  $\delta$  1.02 (t, 3H,  $J = 7$  Hz), 1.6-1.7 (m, 2H), 3.01 (t, 2H,  $J = 7$  Hz), 6.74 (d, 1H,  $J = 16$  Hz), 7.21 (d, 1H,  $J = 16$  Hz), 7.5-7.6 (m, 5H), 7.75 (d, 1H,  $J = 16$  Hz), 8.43 (d, 1H,  $J = 1$  Hz), 8.56 (bs, 1H), 8.65 (bs, 1H).

Methyl 4-[2-(3-methyl-2-pyrazyl)ethenyl]cinnamate (**1c**): A solution of 2, 3-dimethylpyrazine (2.4 mg, 22 mmol) in THF (15 ml) at -78 °C was added to a

solution of lithium diisopropylamide (24 mmol), prepared from 15 ml of 1.62 M BuLi solution in hexane (24 mmol) and diisopropylamine (3.6 ml, 26 mmol), and the mixture was stirred for 20 min at 0 °C. To the mixture at -78 °C was added trimethylsilyl chloride (3.4 ml, 26 mmol). The mixture was stirred at -78 °C for 3 hours. To the reaction mixture was added water and the mixture was extracted with AcOEt (200 ml). After evaporation of the solvent, 2-methyl-3-(trimethylsilylmethyl)pyrazine was purified by column chromatography (Merck Kiesel gel 60, AcOEt-hexane, 1:5) (2.5 g, 63 % yield). To the resulting pyrazine derivative (0.99 g, 5.5 mmol) in THF (20 ml) was added 10.4 ml of 1.62 M BuLi solution in hexane (5.5 mmol). After stirring for 15 min at 0 °C, the reaction mixture was added to a solution of methyl 4-formylcinnamate (1.6 g, 8.5 mmol), prepared according to the procedure in a literature, in THF (40 ml) at -78 °C. The mixture was stirred for 2 hours. Water was added to the reaction mixture, and the resulting mixture was extracted with CH<sub>2</sub>Cl<sub>2</sub> (500 ml). After evaporation of the solvent, the residue was purified by column chromatography (Merck Kiesel gel 60, AcOEt-hexane, 1:3). A pure crystal of **1c** was obtained by recrystallization from methanol (0.61 g, 40 % yield); mp: 138-139 °C; IR (KBr) 1710, 1640, 1200, 1180, 980, 820 cm<sup>-1</sup>; <sup>1</sup>H NMR (CDCl<sub>3</sub>) δ 2.71 (s, 3H), 3.82 (s, 3H), 6.47 (d, 1H, J = 16 Hz), 7.34 (d, 1H, J = 16 Hz), 7.56 (d, 2H, J = 8 Hz), 7.63 (d, 2H, J = 8 Hz), 7.70 (d, 1H, J = 16 Hz), 7.83 (d, 1H, J = 16 Hz), 8.34 (d, 1H, J = 2 Hz), 8.41 (d, 1H, J = 2 Hz).

Methyl 4-[2-(6-methyl-2-pyrazyl)ethenyl]cinnamate (**1d**): 2-Methyl-6-(trimethylsilylmethyl)pyrazine was prepared from 2,6-dimethylpyrazine in the same manner as 2-methyl-3-trimethylsilylmethylpyrazine and purified by distillation (11-13 mmHg, 78-80 °C, 56 % yield). **1d** was prepared from 2-methyl-6-trimethylsilylmethylpyrazine and methyl 4-formylcinnamate in the same manner as **1c**. A pure crystal of **1d** was obtained by recrystallization from methanol. Yield: 31 %; mp: 133-134.5 °C; IR (KBr) 1720, 1640, 1210, 1170, 970, 820 cm<sup>-1</sup>; <sup>1</sup>H NMR (CDCl<sub>3</sub>) δ 2.60 (s, 3H), 3.82 (s, 3H), 6.47 (d, 1H, J = 16 Hz), 7.18 (d, 1H, J = 16 Hz), 7.55 (d, 2H, J = 9 Hz), 7.61 (d, 2H, J = 9 Hz), 7.69 (d, 1H, J = 16 Hz), 7.74 (d, 1H, J = 16 Hz), 8.31 (s, 1H), 8.46 (s, 1H).

S-Ethyl 4-[2-(3-methyl-2-pyrazyl)ethenyl]thiocinnamate (**2c**): A mixture of **1c** (0.84 g, 3.0 mmol) and 85 % KOH in ethanol (3.0 ml) and water (0.7 ml) was refluxed for 20 hours. After the mixture was neutralized with 1N HCl, the precipitated acid was filtrated and dried under vacuum (0.68 g, 86 % yield). To the resulting acid in benzene (110 ml) were successively added DMF (1.5 ml) and SOCl<sub>2</sub> (14 ml), and the mixture was refluxed for 3 hours to give a homogeneous solution. After concentration of the solution under reduced pressure, residual SOCl<sub>2</sub> was removed as benzene azeotrope (two times) under argon to give crude 4-[2-(3-methyl-2-pyrazyl)ethenyl]cinnamoyl chloride. To a solution of the resulting chloride in CH<sub>2</sub>Cl<sub>2</sub> (70 ml) at 0 °C under argon were added a solution of ethanethiol (1.2 ml, 17 mmol) and pyridine (1.2 ml) in CH<sub>2</sub>Cl<sub>2</sub> (45 ml) over a period of 30 min, and the reaction mixture was stirred for additional 30 min. After evaporation of the solvent, water was added and extracted with CH<sub>2</sub>Cl<sub>2</sub> (150 ml). After evaporation of the solvent the residue was purified by column chromatography (Merck Kiesel gel 60, CH<sub>2</sub>Cl<sub>2</sub>). A pure crystal of **2c** was obtained by recrystallization from methanol (0.42 g, 53 % yield); mp: 131-132.5 °C; IR (KBr) 1660, 1610, 1420, 1030, 980, 750 cm<sup>-1</sup>; <sup>1</sup>H NMR (TFA-d) δ 1.41 (t, 3H, J = 7 Hz), 3.09 (s, 3H), 3.16 (q, 2H, J = 7 Hz), 7.00 (d, 1H, J = 16 Hz), 7.54 (d, 1H, J = 16 Hz), 7.7-7.8 (m, 5H), 8.17 (d, 1H, J = 16 Hz), 8.68 (s, 1H), 9.14 (s, 1H).

S-Ethyl 4-[2-(6-methyl-2-pyrazyl)ethenyl]thiocinnamate (**2d**): **2d** was prepared by the hydrolysis of **1d** and esterification with ethanethiol in the same manner as **2c**. A pure crystal of **2d** was obtained by recrystallization from methanol. Yield: 32 %; mp: 125-126 °C; IR (KBr) 1660, 1610, 1420, 1030, 980, 820 cm<sup>-1</sup>; <sup>1</sup>H NMR (TFA-d) δ 1.41 (t, 3H, J = 7 Hz), 2.98 (s, 3H), 3.16 (q, 2H, J = 7 Hz), 7.00 (d, 1H, J = 16 Hz), 7.50 (d, 1H, J = 16 Hz), 7.7-7.8 (m, 5H), 8.20 (d, 1H, J = 16 Hz), 8.85 (s, 1H), 9.38 (s, 1H).

**Preparation of the Dimers.** Finely powdered crystals of **1b**, **1c**, or **1d** (100 mg) were dispersed in water (90 ml) and was irradiated with a 500-W high-pressure mercury lamp (Ushio USH-500D), set outside of the flask, through a Kenko L42 filter (cut off < 410 nm) at room temperature with vigorous stirring.

Dimers were separated from oligomers by preparative TLC (silica gel, CH<sub>2</sub>Cl<sub>2</sub>-CH<sub>3</sub>OH, 100:0.5).

Dimer of **1b**: 19 %; <sup>1</sup>H NMR (CDCl<sub>3</sub>) δ 0.71 (t, 3H, J = 7 Hz), 1.00 (t, 3H, J = 7 Hz), 1.2-1.4 (m, 2H), 1.6-1.8 (m, 2H), 3.6-3.9 (m, 2H), 4.1-4.2 (m, 3H), 4.6-4.7 (m, 2H), 4.8-4.9 (m, 1H), 6.44 (d, 1H, J = 16 Hz), 7.05 (d, 1H, J = 16 Hz), 7.09 (d, 2H, J = 8 Hz), 7.36 (d, 2H, J = 8 Hz), 7.41 (d, 2H, J = 8 Hz), 7.51 (d, 2H, J = 8 Hz), 7.61 (d, 1H, J = 16 Hz), 7.67 (d, 1H, J = 16 Hz), 8.2-8.8 (bs, 6H); MS m/e 588 (M<sup>+</sup>) 286 (unsym. cleav.) 243 (unsym. cleav. -OPr).

Dimer of **1c**: 20 %; <sup>1</sup>H NMR (CDCl<sub>3</sub>) δ 2.63 (s, 3H), 2.66 (s, 3H), 3.41 (s, 3H), 3.75 (s, 3H), 4.05 (dd, 1H, J = 10 Hz, J' = 7 Hz), 4.52 (dd, 1H, J = 10 Hz, J' = 7 Hz), 4.66 (dd, 1H, J = 10 Hz, J' = 7 Hz), 4.80 (dd, 1H, J = 10 Hz, J' = 7 Hz), 6.31 (d, 1H, J = 16 Hz), 7.02 (d, 2H, J = 8 Hz), 7.07 (d, 2H, J = 8 Hz), 7.19 (d, 1H, J = 16 Hz), 7.29 (d, 2H, J = 8 Hz), 7.41 (d, 2H, J = 8 Hz), 7.55 (d, 1H, J = 16 Hz), 7.72 (d, 1H, J = 16 Hz), 8.29 (d, 1H, J = 2 Hz), 8.35 (d, 1H, J = 3 Hz), 8.37 (d, 1H, J = 2 Hz), 8.42 (d, 1H, J = 2 Hz); MS m/e 560 (M<sup>+</sup>) 382 178 (unsym. cleav.) 147 (unsym. cleav. -OCH<sub>3</sub>).

Dimer of **1d**: 27 %; <sup>1</sup>H NMR (CDCl<sub>3</sub>) δ 2.42 (s, 6H), 3.78 (s, 6H), 4.7-4.8 (m, 2H), 4.9-5.0 (m, 2H), 6.33 (d, 2H, J = 16 Hz), 7.17 (d, 4H, J = 8 Hz), 7.30 (d, 4H, J = 8 Hz), 7.56 (d, 2H, J = 16 Hz), 8.09 (s, 2H), 8.11 (s, 2H); MS m/e 560 (M<sup>+</sup>).

**Photoirradiation.** Photopolymerization was carried out as follows:

Method 1) Finely powdered crystals (100 mg) were dispersed in 300 ml of water containing a few drops of a surfactant (Nikkol TL-10FF) and irradiated with a 100-W high-pressure mercury lamp (Eikousha EHB WF-100), set inside of the flask, through a Pyrex glass filter with vigorous stirring under a nitrogen atmosphere.

Method 2) Finely powdered crystals (100 mg) were dispersed in 90 ml of water containing a few drops of a surfactant (Nikkol TL-10FF) and irradiated with a 500-W super-high-pressure mercury lamp (Eikousha EHB WF-500), set outside of the flask, through a Kenko UV30 filter (cut off < 280 nm) with vigorous stirring under a nitrogen atmosphere.

poly-2a:  $^1\text{H}$  NMR (TFA-d)  $\delta$  0.9-1.1 (bs, 3H), 2.7-2.9 (m, 2H), 4.59 (bs, 1H), 4.85 (bs, 1H), 5.00 (bs, 2H), 7.1-7.3 (bs, 2H), 7.3-7.5 (bs, 2H), 8.61 (bs, 1H), 8.66 (bs, 1H), 9.38 (bs, 1H).

poly-2b:  $^1\text{H}$  NMR (TFA-d)  $\delta$  0.84 (t, 3H,  $J = 7$  Hz), 1.3-1.5 (m, 2H), 2.7-2.9 (m, 2H), 4.58 (bs, 1H), 4.86 (bs, 1H), 4.99 (bs, 2H), 7.20 (bs, 2H), 7.35 (bs, 2H), 8.60 (s, 1H), 8.65 (d, 1H,  $J = 2$  Hz), 9.37 (d, 1H,  $J = 2$  Hz).

poly-2c:  $^1\text{H}$  NMR (TFA-d)  $\delta$  1.09 (bs, 3H), 2.84 (bs, 3H), 2.92 (bs, 2H), 4.39 (bs, 1H), 4.92 (bs, 1H), 5.10 (bs, 1H), 5.33 (bs, 1H), 7.24 (bs, 2H), 7.38 (bs, 2H), 8.52 (bs, 1H), 9.32 (bs, 1H); MS  $m/e$  314 (unsym. cleav.) 245 (unsym. cleav.-COSEt) 184 (unsym. cleav.-(COSEt)<sub>2</sub>).

poly-2d:  $^1\text{H}$  NMR (TFA-d)  $\delta$  1.01 (s, 3H), 2.7-2.8 (m, 2H), 2.90 (s, 3H), 4.64 (bs, 1H), 4.75 (bs, 1H), 4.88 (bs, 1H), 4.98 (bs, 1H), 7.22 (bs, 2H), 7.36 (bs, 2H), 8.3-8.7 (bs, 2H); MS  $m/e$  314 (unsym. cleav.) 245 (unsym. cleav.-COSEt) 184 (unsym. cleav.-(COSEt)<sub>2</sub>).

**X-ray Structure Determinations.** Intensity data were measured on a Mac-Science four-circle diffractometer (MXC-18) with graphite monochromated Cu-K $\alpha$  radiation. Accurate cell dimensions were obtained by a least-squares refinement of 20 reflections in the range  $40^\circ < 2\theta < 60^\circ$ . Data were collected with three check reflections. The observed reflections with  $|F_0| > 3\sigma(|F_0|)$  were used in the solutions and refinements; no absorption correction was made. The structures were solved by a direct method with the MULTAN 78 program and refined by a full-matrix least-squares method with the SHELXS 76 program. The positions of hydrogen atoms were obtained from a difference map. Final refinements were performed with the anisotropic thermal parameters for the non-hydrogen atoms and with isotropic ones for the hydrogen atoms. Isotropic thermal parameters of all hydrogen atoms in **1b**, **1d**, and **2a** and the methyl and olefinic hydrogen atoms in **2d** are constructed to the Beq of the parent carbons.

The intensity data collection, refinement details, and crystal data are summarized in Table 3.4. The final molecular coordinates and thermal parameters are listed in Tables 3.5, 3.6, 3.7, and 3.8.

**Table 3.4.** Summary of Crystal Data, Intensity Collection Parameters, and Refinement Details

compounds	1b	1d	2a	2d
formula	C <sub>18</sub> H <sub>18</sub> N <sub>2</sub> O <sub>2</sub>	C <sub>17</sub> H <sub>16</sub> N <sub>2</sub> O <sub>2</sub>	C <sub>17</sub> H <sub>16</sub> N <sub>2</sub> OS	C <sub>18</sub> H <sub>18</sub> N <sub>2</sub> OS
crystal system	orthorhombic	monoclinic	monoclinic	orthorhombic
space group	Pbca	P2 <sub>1</sub> /a	P2 <sub>1</sub> /c	Pna2 <sub>1</sub>
a, Å	7.619(2)	18.539(8)	21.279(6)	9.568(2)
b, Å	40.60(1)	4.834(2)	9.489(4)	21.922(7)
c, Å	9.691(5)	17.197(12)	7.500(2)	7.788(3)
β, deg		104.40(3)	97.65(6)	
V, Å <sup>3</sup>	3071.7(4)	1493(1)	1500.9(3)	1636(1)
Z	8	4	4	4
cryst. solv.	propanol	methanol	methanol	methanol
crystal size, mm <sup>3</sup>	0.6x0.3x0.15	0.6x0.4x0.15	0.8x0.15x0.05	0.4x0.3x0.1
Dcal	1.21	1.25	1.31	1.26
μ, cm <sup>-1</sup>	5.91	5.87	17.98	16.69
scan mode	2θ-ω	2θ-ω	2θ-ω	2θ-ω
2θmax, deg	120	120	130	120
unique reflcns	2288	2506	2244	1409
obsd reflcns	1982	1853	2019	1135
( F <sub>0</sub>   > 3σ( F <sub>0</sub>  ))				
R factor	0.066	0.100	0.061	0.058
Rw factor	0.089	0.120	0.097	0.061
largest shift/esd	0.33	0.034	0.67	0.20
largest peak, e/Å <sup>3</sup>	0.62	0.63	0.50	0.23

Table 3.5. Final Atomic Coordinates ( $\times 10^4$  for C, N, and O;  $\times 10^3$  for H).with Equivalent Isotropic Thermal Parameters,  $B_{eq}$  ( $\text{\AA}^2$ ), for Non-Hydrogen Atoms and Isotropic Thermal Parameters,  $B$  ( $\text{\AA}^2$ ), for Hydrogen Atoms for **1b**

$$B_{eq} = (1/3) \sum_i \sum_j B_{ij} a_i^* a_j^* a_{ij}$$

Atom	x	y	z	B or $B_{eq}$
N 1	1148 (2)	4612 (1)	15108 (3)	4.4 (1)
C 2	1413 (3)	4795 (1)	16487 (4)	4.9 (1)
C 3	486 (3)	4843 (1)	17815 (4)	5.3 (1)
N 4	-764 (3)	4708 (1)	17803 (3)	5.6 (1)
C 5	-1035 (3)	4526 (1)	16409 (4)	5.0 (1)
C 6	-110 (2)	4474 (1)	5059 (3)	3.8 (1)
C 7	-437 (2)	4271 (1)	13556 (3)	4.2 (1)
C 8	364 (2)	4237 (1)	12155 (3)	4.0 (1)
C 9	136 (2)	4034 (1)	10620 (3)	3.8 (1)
C 10	1131 (2)	4030 (1)	9292 (3)	4.1 (1)
C 11	988 (2)	3846 (1)	7827 (3)	4.2 (1)
C 12	-187 (2)	3653 (1)	7584 (3)	3.8 (1)
C 13	-1175 (2)	3655 (1)	8910 (3)	4.3 (1)
C 14	-1023 (2)	3840 (1)	10393 (3)	4.1 (1)
C 15	-411 (2)	3456 (1)	6031 (3)	4.1 (1)
C 16	419 (3)	3419 (1)	4670 (4)	4.7 (1)
C 17	27 (3)	3221 (1)	3154 (3)	4.7 (1)
O 18	-1095 (2)	3107 (1)	2920 (3)	6.0 (1)
O 19	1100 (2)	3183 (1)	2065 (3)	5.7 (1)
C 20	908 (4)	2996 (1)	493 (4)	6.0 (1)
C 21	1649 (4)	2681 (1)	673 (4)	6.4 (1)
C 22	1020 (5)	2452 (1)	1958 (6)	7.7 (1)
H 2	234 (4)	490 (1)	1651 (4)	4.9 (0)
H 3	70 (4)	497 (1)	1883 (5)	5.3 (0)
H 5	-203 (3)	443 (1)	1636 (4)	3.9 (0)
H 7	-136 (3)	417 (1)	1360 (4)	4.3 (0)
H 8	122 (3)	435 (1)	1218 (4)	3.9 (0)
H 10	192 (3)	416 (1)	948 (4)	4.1 (0)
H 11	168 (3)	385 (1)	698 (4)	3.9 (0)
H 13	-201 (3)	354 (1)	875 (4)	4.3 (0)
H 14	-177 (3)	384 (1)	1130 (4)	3.9 (0)
H 15	-133 (3)	334 (1)	601 (4)	3.9 (0)
H 16	132 (3)	354 (1)	457 (4)	3.9 (0)
H201	-12 (4)	293 (1)	44 (5)	6.0 (0)
H202	135 (4)	311 (1)	-54 (5)	6.0 (0)
H211	168 (4)	257 (1)	-47 (5)	6.4 (0)
H212	264 (5)	274 (1)	96 (5)	6.4 (0)
H221	98 (5)	256 (1)	320 (6)	7.7 (0)
H222	13 (5)	239 (1)	152 (6)	7.7 (0)
H223	152 (5)	225 (1)	208 (6)	7.7 (0)

Table 3.6. Final Atomic Coordinates ( $\times 10^4$  for C, N, and O;  $\times 10^3$  for H) with Equivalent Isotropic Thermal Parameters,  $B_{eq}$  ( $\text{\AA}^2$ ), for Non-Hydrogen Atoms and Isotropic Thermal Parameters,  $B$  ( $\text{\AA}^2$ ), for Hydrogen Atoms for **1d**

$$B_{eq} = (1/3) \sum_i \sum_j B_{ij} a_i^* a_j^* a_{ij}$$

Atom	x	y	z	B or $B_{eq}$
N 1	-2451(2)	-9237(8)	2295(2)	5.7(1)
C 2	-2718(2)	-10080(9)	1548(2)	5.2(1)
C 3	-3330(3)	-12164(12)	1393(4)	7.6(2)
C 4	-2444(3)	-8978(11)	925(2)	5.9(1)
N 5	-1914(2)	-7074(9)	1040(2)	6.5(1)
C 6	-1659(3)	-6271(12)	1788(3)	6.3(1)
C 7	-1911(3)	-7293(10)	2418(2)	5.8(1)
C 8	-1591(3)	-6128(13)	3231(3)	7.7(2)
C 9	-1757(3)	-6876(13)	3861(3)	7.4(2)
C 10	-1465(3)	-5791(12)	4699(3)	7.1(2)
C 11	-1714(3)	-6878(14)	5293(3)	8.1(2)
C 12	-1461(3)	-6003(13)	6059(3)	7.6(2)
C 13	-928(3)	-3910(10)	6275(2)	5.9(1)
C 14	-656(4)	-2755(14)	5676(3)	8.3(2)
C 15	-922(4)	-3694(16)	4871(3)	8.9(2)
C 16	-689(3)	-3076(10)	7113(3)	6.0(1)
C 17	-231(3)	-1138(11)	7447(3)	5.9(1)
C 18	-63(2)	-655(9)	8317(2)	5.3(1)
O 19	-310(2)	-1931(7)	8780(2)	6.9(1)
O 20	403(2)	1468(7)	8531(2)	6.6(1)
C 21	605(.4)	2105(13)	9382(3)	7.0(2)
H 31	-332(0)	-1315(1)	88(0)	7.3(0)
H 32	-381(0)	-1116(1)	132(0)	7.3(0)
H 33	-327(0)	-1354(1)	184(0)	7.3(0)
H 4	-269(2)	-973(9)	42(3)	5.8(0)
H 6	-134(2)	-489(11)	187(3)	6.1(0)
H 8	-117(2)	-482(9)	323(1)	7.6(0)
H 9	-210(2)	-848(7)	388(1)	7.2(0)
H 11	-205(0)	-852(1)	519(0)	8.0(0)
H 12	-165(0)	-717(1)	644(0)	7.5(0)
H 14	-35(3)	-115(13)	574(3)	8.0(0)
H 15	-63(0)	-258(2)	457(0)	8.4(0)
H 16	-92(0)	-403(1)	751(0)	5.8(0)
H 17	0(2)	-3(10)	718(3)	5.8(0)
H211	73(3)	57(11)	974(3)	6.9(0)
H212	11(3)	272(11)	954(3)	6.9(0)
H213	88(3)	354(10)	944(3)	6.9(0)

Table 3.7. Final Atomic Coordinates ( $\times 10^4$  for C, N, O, and S;  $\times 10^3$  for H) with Equivalent Isotropic Thermal Parameters,  $B_{eq}$  ( $\text{\AA}^2$ ), for Non-Hydrogen Atoms and Isotropic Thermal Parameters,  $B$  ( $\text{\AA}^2$ ), for Hydrogen Atoms for  $2a$

$$B_{eq} = (1/3) \sum_i \sum_j B_{ij} a_i^* a_j^*$$

Atom	x	y	z	B or $B_{eq}$
N 1	9214 (1)	1156 (2)	-10328 (2)	3.8 (1)
C 2	9590 (1)	1419 (3)	-11565 (3)	4.3 (1)
C 3	9687 (1)	474 (3)	-12874 (3)	4.8 (1)
N 4	9406 (1)	-780 (3)	-13010 (3)	5.1 (1)
C 5	9033 (1)	-1060 (3)	-11762 (3)	4.4 (1)
C 6	8927 (1)	-111 (2)	-10422 (3)	3.3 (1)
C 7	8509 (1)	-444 (2)	-9090 (3)	3.6 (1)
C 8	8454 (1)	348 (2)	-7664 (3)	3.4 (1)
C 9	8041 (1)	117 (2)	-6285 (3)	3.2 (1)
C 10	8040 (1)	1112 (2)	-4902 (3)	3.3 (1)
C 11	7658 (1)	962 (2)	-3582 (3)	3.5 (1)
C 12	7247 (1)	-200 (2)	-3574 (3)	3.2 (1)
C 13	7248 (1)	-1179 (2)	-4950 (3)	3.7 (1)
C 14	7633 (1)	-1033 (2)	-6278 (3)	3.6 (1)
C 15	6844 (1)	-437 (2)	-2186 (3)	3.6 (1)
C 16	6804 (1)	347 (3)	-740 (3)	3.8 (1)
C 17	6378 (1)	-21 (2)	573 (3)	3.7 (1)
O 18	6130 (1)	-1157 (2)	669 (2)	4.9 (1)
S 19	6284 (0)	1396 (1)	2047 (1)	5.2 (0)
C 20	5714 (2)	690 (4)	3394 (4)	6.1 (1)
C 21	5078 (2)	1250 (10)	2862 (8)	14.4 (3)
H 2	978 (1)	230 (4)	-1154 (4)	4.3 (0)
H 3	992 (2)	78 (4)	-1370 (4)	4.8 (0)
H 5	882 (1)	-211 (4)	-1192 (4)	4.4 (0)
H 7	830 (1)	-126 (3)	-934 (4)	3.6 (0)
H 8	874 (1)	114 (3)	-739 (4)	3.4 (0)
H 10	832 (1)	188 (3)	-487 (4)	3.3 (0)
H 11	766 (1)	171 (3)	-272 (4)	3.5 (0)
H 13	698 (1)	-199 (3)	-493 (4)	3.7 (0)
H 14	759 (1)	-168 (3)	-723 (4)	3.6 (0)
H 15	655 (2)	-124 (3)	-232 (4)	3.6 (0)
H 16	700 (1)	120 (4)	-51 (4)	3.8 (0)
H201	580 (2)	-35 (4)	328 (5)	6.1 (0)
H202	592 (2)	90 (4)	494 (5)	6.1 (0)
H211	508 (4)	52 (9)	210 (10)	14.4 (0)
H212	506 (4)	202 (9)	240 (10)	14.4 (0)
H213	484 (4)	114 (8)	370 (10)	14.4 (0)

Table 3.8. Final Atomic Coordinates ( $\times 10^4$  for C, N, O, and S;  $\times 10^3$  for H) with Equivalent Isotropic Thermal Parameters,  $B_{eq}$  ( $\text{\AA}^2$ ), for Non-Hydrogen Atoms and Isotropic Thermal Parameters,  $B$  ( $\text{\AA}^2$ ), for Hydrogen Atoms for 2d

$$B_{eq} = (1/3) \sum_i \sum_j B_{ij} a_i^* a_j^* a_{ij}$$

Atom	x	y	z	B or $B_{eq}$
N 1	13697 (7)	4102 (5)	3020 (4)	4.5 (2)
C 2	15033 (9)	4004 (8)	3396 (4)	4.9 (2)
C 3	15163 (10)	2741 (9)	3783 (5)	6.6 (2)
C 4	16254 (11)	5027 (10)	3419 (5)	6.5 (3)
N 5	16169 (11)	6183 (7)	3090 (5)	7.8 (3)
C 6	14807 (11)	6302 (10)	2736 (6)	6.0 (2)
C 7	13578 (9)	5280 (7)	2687 (4)	4.4 (2)
C 8	12083 (8)	5487 (7)	2290 (4)	4.4 (2)
C 9	10736 (9)	4652 (7)	2256 (4)	4.5 (2)
C 10	9206 (9)	4851 (7)	1869 (4)	4.1 (2)
C 11	7851 (9)	3900 (7)	1895 (4)	4.3 (2)
C 12	6418 (10)	4046 (7)	1543 (5)	4.9 (2)
C 13	6248 (9)	5172 (7)	1136 (4)	4.4 (2)
C 14	7628 (9)	6130 (7)	1107 (4)	4.5 (2)
C 15	9021 (11)	5984 (8)	1470 (4)	4.7 (2)
C 16	4765 (9)	5391 (7)	751 (4)	4.3 (2)
C 17	3394 (10)	4623 (7)	711 (5)	5.1 (2)
C 18	1962 (8)	4938 (8)	282 (5)	5.1 (2)
O 19	1871 (7)	6033 (6)	0 (0)	7.1 (2)
S 20	452 (3)	3607 (2)	248 (3)	7.1 (1)
C 21	-1144 (16)	4339 (14)	-259 (6)	8.8 (4)
C 22	-1041 (17)	3692 (15)	-840 (7)	11.2 (5)
H 31	1588 (1)	277 (1)	416 (1)	8.1 (0)
H 32	1573 (0)	213 (0)	347 (0)	8.1 (0)
H 33	1400 (1)	236 (1)	388 (1)	8.1 (0)
H 4	1741 (0)	500 (0)	361 (0)	10.0 (0)
H 6	1480 (1)	698 (1)	247 (1)	5.1 (0)
H 8	1208 (0)	629 (0)	197 (0)	4.3 (0)
H 9	1092 (1)	382 (1)	253 (1)	3.9 (26)
H 11	803 (8)	324 (8)	224 (3)	4.3 (17)
H 12	530 (7)	340 (6)	158 (3)	4.5 (0)
H 14	760 (0)	694 (0)	82 (0)	5.5 (0)
H 15	970 (1)	660 (1)	141 (0)	4.5 (0)
H 16	481 (0)	613 (0)	47 (0)	3.6 (0)
H 17	309 (1)	370 (1)	90 (0)	4.3 (13)
H211	-238 (8)	426 (6)	-35 (3)	3.7 (14)
H212	-141 (8)	544 (7)	-42 (3)	9.9 (17)
H221	18 (9)	366 (7)	-98 (3)	9.5 (19)
H222	-174 (7)	425 (6)	-113 (2)	9.5 (0)
H223	-151 (0)	272 (0)	-81 (0)	9.5 (0)

### 3. 5. References

- 1) (a) Cohen, M. D.; Schmidt, G. M. J. *J. Chem. Soc.* **1964**, 1996. (b) Schmidt, G. M. J. *Pure Appl. Chem.* **1971**, 27, 647. (c) Ramamurthy, V.; Venkatesan, K. *Chem. Rev.* **1987**, 87, 433. (d) Hasegawa, M. *Chem. Rev.* **1983**, 83, 507.
- 2) Green, B. S.; Lahav, M.; Schmidt, G. M. J. *J. Chem. Soc. B* **1971**, 1552.
- 3) Thomas, J. M. *Nature (London)* **1981**, 289, 633.
- 4) Addadi, L.; van Mil, J.; Lahav, M. *J. Am. Chem. Soc.* **1982**, 104, 3422.
- 5) (a) Ueno, K.; Nakanishi, H.; Hasegawa, M.; Sasada, Y. *Acta Cryst.* **1978**, B34, 2034. (b) Nakanishi, H.; Ueno, K.; Sasada, Y. *Acta Cryst.* **1978**, B34, 2036. (c) Nakanishi, H.; Ueno, K.; Sasada, Y. *Acta Cryst.* **1978**, B34, 2209.
- 6) In contrast to the diolefin compounds which do not have a cyano group, diolefin compounds with a cyano group have a close contact between the carbonyl oxygen and the phenylene ring; (a) Nakanishi, H.; Ueno, K.; Sasada, Y. *Acta Cryst.* **1978**, B34, 2036. (b) Nakanishi, H.; Suzuki, M.; Nakanishi, F. *J. Polym. Sci., Polym. Lett. Ed.* **1982**, 20, 653.
- 7) (a) Hasegawa, M.; Aoyama, M.; Maekawa, Y.; Ohashi, Y. *Macromolecules* **1989**, 22, 1568. (b) Hasegawa, M.; Harashina, H.; Kato, S.; Saigo, K. *Macromolecules* **1986**, 19, 1276.
- 8) Unpublished result.
- 9) At room temperature polymerization of 1b proceed along with morphological change from crystalline to amorphous phase. In  $\alpha$ -type packing of diolefin crystals, this type of temperature dependence was often observed; see reference (1d) and chapter 2 in this thesis.
- 10) Kitaigorodsky, A. I. *Organic Crystals and Molecules*, Academic Press; New York, **1973**.
- 11) (a) Hasegawa, M.; Chung, C. I.; Muro, N.; Maekawa, Y. *J. Am. Chem. Soc.* **1990**, 112, 5676. (b) Chapter 2 in this thesis.
- 12) Desiraju, G. R. *Crystal Engineering: The Design of Organic Solids*, Elsevier, Amsterdam, 1989.

## CHAPTER 4

### Quantitative Formation of a Highly Strained Tricyclic [2.2]Paracyclophane Derivative from a Mixed Crystal of Ethyl and Propyl $\alpha$ -Cyano-4-[2-(4-pyridyl)ethenyl]cinnamates through a Topochemical Reaction

#### 4. 1. Introduction

There have been several reports concerning the topochemical [2+2] photodimerization of mixed crystals of olefin compounds to give mixed dimers.<sup>1</sup> By contrast, there is no obvious example of topochemical photo-copolymerization of a mixed crystal of diolefin compounds, although the topochemical photodimerization of olefin compounds can be extended to the topochemical photo-polymerization of diolefin compounds.<sup>2</sup>

Though an isolated report on the formation of a mixed crystal of 2,5-distyrylpyrazine and 1,4-bis[2-(2-pyridyl)ethenyl]benzene has appeared, the topochemical behavior of this mixed crystal was not mentioned in detail.<sup>3</sup> In our laboratory, the preparation of mixed crystals of diolefin compounds has been investigated from the viewpoint of topochemical photo-copolymerization. However, most couples of the diolefin compounds did not form a mixed crystal but, rather, separated into pure crystals.

In several series of photoreactive diolefin crystals, it has been observed that a few  $\alpha$ -type photoreactive crystals having a similar chemical structure have very similar molecular arrangements in these crystals.<sup>2,4b,c,5</sup> The results suggested the author that photoreactive mixed crystal would be obtained from two similar diolefin compounds and, subsequently, the mixed crystal would give a copolymer through topochemical copolymerization.<sup>4d</sup>

The crystal structures of ethyl and propyl  $\alpha$ -cyano-4-[2-(4-pyridyl)ethenyl]cinnamate crystals (**1a** and **1b**) are very similar to each other, as described in Chapter 2. However, contrary to the expectation of obtaining an  $\alpha$ -homo-type linear copolymer, the mixed crystal of **1a** and **1b** (**1a•1b**) did not

afford a linear copolymer but, rather, afforded a highly strained tricyclic [2.2]paracyclophane derivative crystal quantitatively by "double" photocycloaddition between two molecules. In this chapter the author describes the topochemical behavior of mixed crystal **1a**•**1b**, and the structure and properties of the resulting cyclophane **3**.

## 4. 2. Results and Discussion

The author has already described the crystal structures and topochemical behavior of pure crystals **1a** and **1b** in Chapter 2. In both crystals, one molecule is related to its neighboring molecules by two different inversion centers to make a plane-to-plane stack, although irradiation of **1a** and **1b** crystals afforded an  $\alpha$ -homo-type polymer (see scheme I) and the same type of photostable dimer, respectively.<sup>5</sup> On the basis of similarity in molecular arrangements between **1a** and **1b** crystals, it was expected that **1a** and **1b** would form a mixed crystal which would give a copolymer.

### 4. 2. 1. Preparation of the Mixed Crystals

Mixed crystals of **1a** and **1b** (**1a**•**1b**) in various molar ratios were obtained by the co-crystallization of **1a** and **1b** from an ethanol solution. X-ray powder diffraction analysis of the mixed crystals and characterization of the photoproducts indicated the presence of three crystal phases (denoted A, B, and C). Phase A, which has the same crystal structure as the **1a** crystal, was observed in the proportion of **1b**, ranging from 0 to 20 mol% in the mixed crystal. Phase B is a new crystal phase which is different from both pure **1a** nor **1b** crystals; it was achieved in the proportion of **1b** ranging approximately from 30 to 95 mol%. Phase C, which has the same structure as crystal **1b**, was observed in the proportion of **1b**, ranging from 90 to 100 mol%.

However, accurate boundaries between phases A and B as well as between phases B and C could not be clearly defined. This was because reproducibility of experimental runs regarding the boundaries was not satisfactory: in the proportion of **1b** ranging from 20 to 30 mol%, the photoproduct comprised cyclophane, an  $\alpha$ -

homo-type polymer, or a mixture of them; in the proportion of **1b** ranging from 90 to 100 mol%, the photoproduct comprised the cyclophane, an  $\alpha$ -homo-type dimer, or a mixture of them.

In contrast to the successful formation of mixed crystals from **1a** and **1b**, methyl  $\alpha$ -cyano-4-[2-(4-pyridyl)ethenyl]cinnamate, of which the crystal structure is quite different from **1a** and **1b**, did not co-crystallize into a mixed crystal with either **1a** or **1b** from an ethanol solution under several conditions.

#### 4. 2. 2. Topochemical Photoreaction of the Mixed Crystals

Mixed crystal **1a**•**1b** (1:1) (phase B) showed an extremely high photoreactivity and, upon irradiation for 2h at room temperature with a 500-W super-high-pressure mercury lamp, gave a highly crystalline product quantitatively. In the  $^1\text{H}$  NMR spectrum of the product, no olefinic proton signal was observed and there existed three signals assigned to the protons of a cyclobutane ring at  $\delta$  4.64, 5.36, and 5.51 ppm: doublet (2 H,  $J = 9$  Hz), double doublet (2 H,  $J_1 = 11$  Hz,  $J_2 =$

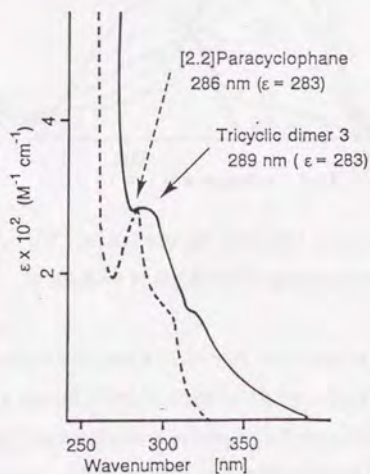


Figure 4.1. UV spectrum of tricyclic dimer **3** (solid line) and [2.2]paracyclophane (dashed line).

9 Hz), and doublet (2 H,  $J = 11$  Hz), respectively. The ABC pattern and the proton ratio indicate that there are two cyclobutane rings having the same configuration of a hetero-type structure in one molecule (see scheme I). The UV spectrum of the product (Figure 4.1) shows a shoulder peak at 289 nm ( $\epsilon = 283$ ) which is not observed in the absorption of the usual 1,4-disubstituted benzene. Such a shoulder peak is also observed in tricyclo[8.2.2.2<sup>4,7</sup>]hexadeca-4,6,10,12,13,15-hexaene ([2.2]paracyclophane) at 286 nm ( $\epsilon = 283$ ) and has been well-established as being characteristic of the close contact of two aromatic rings in a molecule at a distance shorter than the van der Waals contact.<sup>6</sup> On the basis of spectroscopic results, it is concluded that the product is a triecyclic dimer (3), having a [2.2]paracyclophane skeleton.

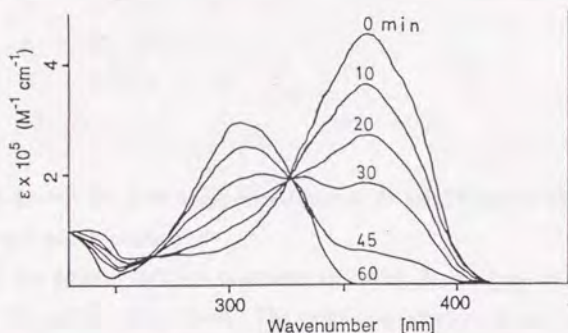
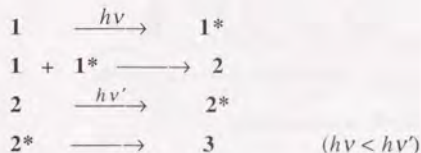


Figure 4.2. UV spectral change of mixed crystal **1a•1b** during the irradiation at the wavelengths longer than 410 nm.

When mixed crystal **1a•1b** (1:1) was irradiated at wavelengths longer than 410 nm by using a cut-off filter in order to excite only the starting monomers, the UV spectral change during the irradiation, which was measured in  $\text{CH}_2\text{Cl}_2$ , shows clear isosbestic points. After irradiation for 60 min the reaction leveled off while retaining a highly crystalline phase; in the product the absorption ( $\lambda_{\text{max}} = 369$  nm) due to **1a** and **1b** completely disappeared (Figure 4.2). Since these UV spectra showed that the starting monomers are completely converted into a sole product,

spectroscopic measurements were carried out for the photoproduct without purification. In the  $^1\text{H}$  NMR spectrum of the product, the olefinic proton signals still remained one-half in the integration, and proton signals, which corresponded to one cyclobutane ring, newly appeared. Upon further irradiation without a filter, the product was quantitatively converted into **3** in the crystalline state. From all these results the photoproduct is concluded to be a monocyclic dimer (**2**) having a hetero-type cyclobutane ring.

The isolation of monocyclic dimer **2** reveals that the photochemical process from mixed crystal **1a•1b** (1:1) to **3** occurs through step-growth photocycloaddition via **2**, as shown below:



where **1** denotes **1a** or **1b** in the mixed crystal; **1\*** and **2\*** denote the photoexcited species of **1** and **2**, respectively.

X-ray powder diffraction patterns of **1a•1b**, **2**, and **3** are shown in Figures 4.3 (a), (b), and (c), respectively. The continuous changes in the X-ray powder diffraction pattern from **1a•1b** to **2** and from **2** to **3** indicate that extremely high crystallinity is maintained during the entire course of the photoreaction; namely, these reactions proceed through a crystal-to-crystal transformation.

In order to determine the molecular arrangement of **1a** and **1b** in mixed crystal **1a•1b** (1:1), high-performance liquid chromatography (HPLC) of **2** was undertaken. Since four peaks with equal peak-areas were observed in the chromatogram (Figure 4.4), these peaks doubtlessly correspond to **2a-d** in Scheme 4.1; it is concluded that the molecular arrangement is a disordered sequence (a solid solution crystal). Though HPLC of **3** could not be measured because of the insolubility in common solvents, HPLC result of **2** indicates that the final

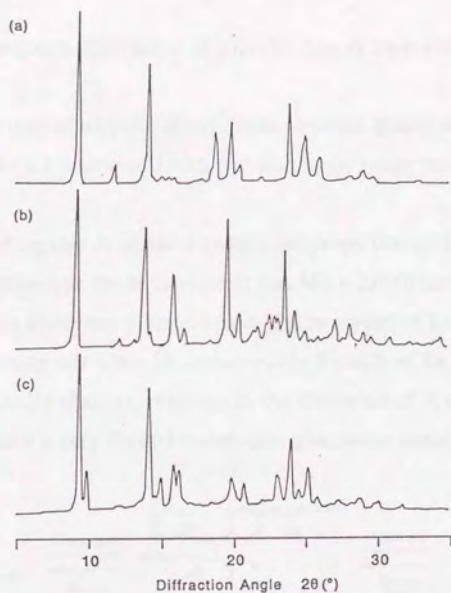


Figure 4.3. X-ray powder diffraction patterns of (a) mixed crystal **1a·1b** (1:1), (b) monocyclic dimer **2**, and (c) tricyclic dimer **3**.

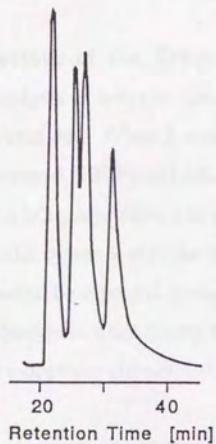


Figure 4.4. High-performance liquid chromatogram of **2**.

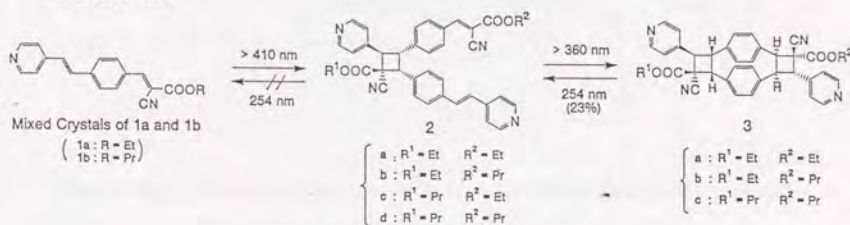
photoproduct comprises three kinds of tricyclic dimers **3a-c** with a ratio of 1:2:1 (Scheme 4.1).

The same type of tricyclic dimer **3** was obtained quantitatively from a mixed crystal not only in a 1:1 ratio of **1a**:**1b**, but also in the range from 70:30 to 5:95 (phase B).

The mixed crystals in phase A (where the proportion of **1a** was above 80 mol%) gave a homo-type linear copolymer (ca.  $\overline{M}_n = 2,600$ ) having the same skeleton as that in a polymer prepared from a pure crystal of **1a**.<sup>5b</sup>

It is surprising that when **1b** contains only 5 mol% of **1a**, the crystal structure dramatically changes, resulting in the formation of **3**, and that only mixed crystals within such a very limited molar ratio give linear copolymers.

Scheme 4.1



#### 4. 2. 3. Molecular Structure of the Tricyclic Dimer

A crystal structure analysis of tricyclic dimer **3**, comprising **1a** and **1b** in a molar ratio of 5:95, was carried out. When **3** was recrystallized from a mixture of 1,1,1,3,3,3-hexafluoro-2-propanol (HFIP) and ethanol, a single crystal of the complex of **3** with HFIP in a 1:2 molar ratio was obtained. Figure 4.5(a) shows the molecular structure of tricyclic dimer **3** with the numbering of atoms; both of the ester alkyl moieties are depicted by a propyl group. Since there is a pseudo-center of symmetry between the phenylene rings facing to each other, four carbon atoms in one cyclobutane ring have opposite chirality to the corresponding carbon atoms in the other.

Figure 4.5(b) shows the molecular structure viewed along the phenylene planes. The intramolecular nonbonded distance (c) between the para-carbon atoms,

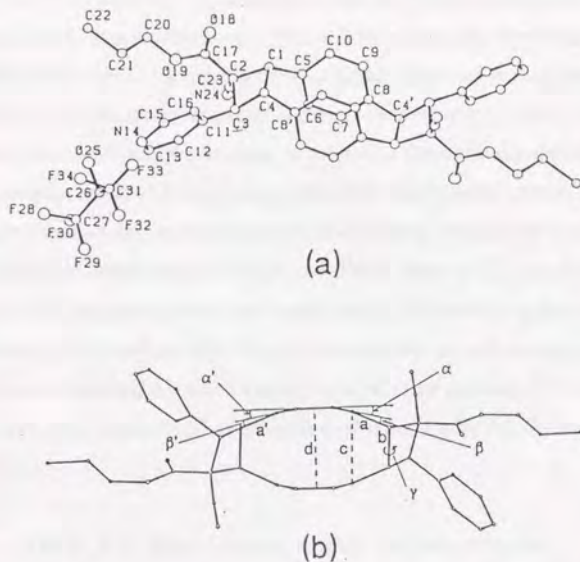


**Figure 4.5.** Molecular structures of **3**; (a) with the numbering of atoms and (b) viewed along the phenylene planes.

C(5) and C(8'), is 2.85 Å. The distance (d) between the least-square planes formed by four carbon atoms in each of the facing benzene rings, C(6)-C(7)-C(9)-C(10) and C(6')-C(7')-C(9')-C(10'), is 3.13 Å. These distances are considerably shorter than the van der Waals contact (3.4 Å). The para-carbon atoms, C(5) and C(8), bend 12.8° and 13.5°, respectively, out of the other four atoms of the aromatic ring.

The short nonbonded distances and deformation of the benzene rings are similar to those of [2.2]paracyclophane, as previously reported.<sup>7</sup> The bond lengths and angles, as well as the intramolecular non-bonded distances between the facing benzene rings of both **3** and [2.2]paracyclophane, are listed in Table 4.1.

The bond length (b) of the methylene moiety (C(1) and C(4)) in **3** is slightly longer than that in [2.2]paracyclophane (b = 1.61 Å for **3**; b = 1.59 Å for [2.2]paracyclophane). Moreover, the torsion angle about the bridged methylene

carbons, C(5)-C(1)-C(4)-C(8'), is larger than that of [2.2]paracyclophane ( $\gamma = 13.9^\circ$  for **3**;  $\gamma = 6^\circ$  for [2.2]paracyclophane). These differences may stem from the nature of the cyclobutane rings condensed to the [2.2]paracyclophane moiety, because the  $\sigma$  bond length of cyclobutane is longer than that of cyclohexane (0.02 Å); the ring in a cyclobutane compound puckers in order to minimize the steric repulsions between the substituents on the cyclobutane ring. Thus, the [2.2]paracyclophane skeleton has a twist shape about an axis perpendicular to and passing through the benzene rings, resulting in slightly larger values of  $\alpha$ ,  $\beta$ , and  $d$  than those in [2.2]paracyclophane.<sup>8</sup> Compared to [2.2]paracyclophane, the longer length of  $b$  and the greater average angles of  $\alpha$  and  $\beta$  in **3** indicate that tricyclic dimer **3** has a strain energy caused by two cyclobutane rings and a torsion about two methylene carbons (C(1)-C(4)) which bond the phenylene rings, in addition to that caused by the deformation of the benzene rings.

**Table 4.1.** Bond Lengths, Angles, and Intramolecular Non-bonded Distances of **3** and [2.2]Paracyclophane

compounds	<b>3</b>	[2.2]paracyclophane
a, (Å)	1.52	1.51
a', (Å)	1.50	
b, (Å)	1.61	1.59
c, (Å)	2.85	2.78
d, (Å)	3.13	3.09
$\alpha$ , deg	12.8	12.6
$\alpha'$ , deg	13.5	
$\beta$ , deg	10.6	11.2
$\beta'$ , deg	12.9	
$\gamma$ , deg	13.9	6
ref.	this work	(7)

Of a great interest is that the topochemical driving force is sufficient to give such a highly strained molecule **3** quantitatively, even though a great amount of internal energy should be exhausted in twisting two phenylene rings during the reaction from **2** to **3**.

#### 4. 2. 4. Photochemical Properties of the Tricyclic Dimer

The strained structure of **3** is remarkably reflected in the photochemical behavior in solution and in the crystalline state.

In poly(2,5-distyrylpyrazine) and its derivative polymers, which have cyclobutane rings in the main chain, no appreciable photocleavage was observed when these topochemically produced as-prepared crystals were irradiated.<sup>10</sup>

On the other hand, when an as-prepared crystal of **3** was irradiated with a low-pressure mercury lamp (254 nm) for 2 h, monocyclic dimer **2** was produced as a major product (23 % conversion). However, further irradiation did not give detectable amount of the monomer (**1a** and **1b**), but resulted in the formation of indefinable materials, being soluble neither in HFIP nor in trifluoroacetic acid. The enhanced tendency for a cycloreversion of **3** in the crystalline state, in comparison with poly-DSP and some other crystals, would be explained by the higher strain of **3**.

When tricyclic dimer **3** in a HFIP solution was irradiated at wavelengths of  $254 \pm 10$  nm for 10 h, the photocleavage of one cyclobutane ring in **3** occurred, while giving **2** (69 %) and the starting monomers, **1a** and **1b** (16 %). The difference between the photocleavage behavior in solution and in the crystalline state indicates that the crystal lattice suppresses any cycloreversion of the cyclobutane ring to a certain extent. This type of matrix effect is very commonly observed in the thermal and photochemical behavior of the products obtained through a topochemical [2+2] photoreaction.<sup>10</sup>

#### 4. 2. 5. Crystallographic Interpretation of the Photoreaction of the Mixed Crystal

Figure 4.6(a) shows the crystal structure of **1a•1b** viewed along the *c*-axis with the numbering of atoms; the ester alkyl moiety is depicted by an ethyl group. The molecular arrangement of **1a•1b** (P2<sub>1</sub>/c) is entirely different from those of pure **1a** and **1b** (P1).<sup>5,11</sup>

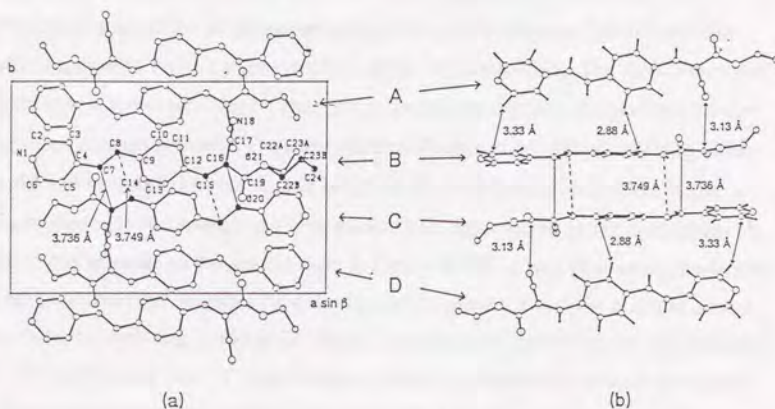


**Figure 4.6.** (a) A crystal structure of mixed crystal **1a•1b** (1:1) viewed along *c*-axis. The shaded atoms in molecule B correspond to propyl group; the ester moiety of the other molecules are depicted by an ethyl group. (b) Two molecules making a pair (B and C) and two neighboring molecules in the other pairs (A and D) viewed along the phenylene groups in molecules B and C.

The reactive molecules, which are related by a pseudo-center of symmetry, make a pair and are superimposed along the [011] direction without any displacement of the molecular long axis. The double bond at the pyridyl side in one molecule (B) is separated from the double bond at the ester side in the other molecule (C) by 3.736 Å (C(7)-C(16')) and 3.749 Å (C(8)-C(15')), which are within the distance topochemically allowed for [2+2] photocycloaddition.<sup>1a</sup> Figure

4.6(b) shows the molecular arrangement of the reacting paired molecules (B and C) as well as the molecules in neighboring pairs (A and D). As is obvious in Figures 4.6 (a) and (b), the irradiation of **1a•1b** should give a  $\beta$ -type dimer having a hetero-type cyclobutane ring.

Figures 4.7 (a) and (b) show two typical molecular arrangements in a  $\beta$ -type packing crystal viewed along the direction of the molecular long axis. Each line in Figure 4.7 depicts the average plane of a diolefin compound. In the cases of photoreactive diolefin compounds in the  $\beta$ -type packing reported so far, the aromatic planes of the neighboring molecules in both sides are parallel and are superimposed to make a plane-to-plane stack (Figure 4.7(a)). The direction of the molecular plane should not be changed so greatly by the first cycloaddition under the topochemical process. Thus, the residual double bonds in the resulting dimer could still be parallel to the double bonds in the neighboring monomer; as the result, those olefins could react with each other. In contrast, in the case of **1a•1b**, which corresponds to the crystal type in Figure 4.7(b), a pair of reacting molecules is isolated from the neighboring pairs by a glide plane. Thus, the residual double bonds in the resulting monocyclic dimer **2** could not be parallel to the double bonds in any neighboring pair. Consequently, a second cycloaddition should occur only between intramolecular olefins to give **3**, not between intermolecular olefins.

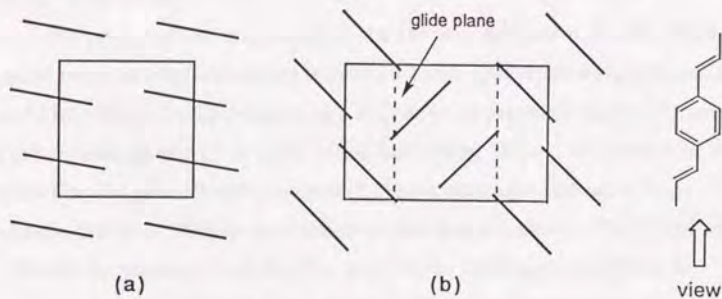


**Figure 4.7.** Schematic molecular arrangements of (a) a photoreactive  $\beta$ -type crystal and (b) **1a•1b** viewed along the molecular long axis.

In Figure 4.6(b) molecules A and B (also C and D) come into contact with each other at the van der Waals distances (C19...N18': 3.13 Å, C12...H10': 2.88 Å, and C2...H2': 3.33 Å). Thus, after the first cycloaddition between two molecules in one pair, the residual olefins in monocyclic dimer **2** would be forced to stay within the reactive distance by virtue of a repulsion with the neighboring molecules.

The quantitative formation of highly strained compound **3** is reasonably interpreted in terms of the crystal structure of **1a•1b**, which was formed by an unexpected shuffle of the molecular arrangement from **1a** or **1b** to **1a•1b**.<sup>12</sup>

There is no evidence whether the crystal lattice and symmetry of **1a•1b** are the same as those of **2**, since the author has not yet succeeded in a crystal structure analysis of an as-prepared crystal of **2**. However, the molecular structure of **3** coincides with that expected from the molecular arrangement of **1a•1b**; namely, the two reactive molecules in the starting crystal **1a•1b** and the tricyclic dimer molecule **3** are related by a pseudo-center of symmetry, as shown in Figures 4.5(a) and 4.6(a). This coincidence of the crystal symmetry strongly suggests that photoreaction proceeded with a retention of the crystal lattice and symmetry of **1a•1b**.

#### 4. 3. Conclusion

A photoreactive mixed crystal (**1a•1b**) was obtained over a wide range of molar ratios of ethyl and propyl  $\alpha$ -cyano-4-[2-(4-pyridyl)ethenyl]cinnamates (**1a** and **1b**). The resulting crystal had a molecular arrangement quite different from pure crystals **1a** and **1b** in molar ratios from 70:30 to 5:95. Photoreaction of the mixed crystal gave a highly strained [2.2]paracyclophane derivative **3** in quantitative yield through a crystal-to-crystal transformation. The mixed crystal afforded the monocyclic dimer **2** in quantitative yield upon irradiation at wavelengths longer than 410 nm, indicating that the photoreaction of mixed crystal **1a•1b** into tricyclic dimer **3** proceeded through a step-growth mechanism.

The intramolecular aromatic rings in tricyclic dimer **3** are placed within the van der Waals distance and bend in a way similar to those of [2.2]paracyclophane.

An enhanced photocycloreversion of the cyclobutane ring in the crystalline state was interpreted by such a highly strained structure of **3**.

#### 4. 4. Experimental

**Measurements.** Infrared spectra were measured on a Jasco IR-810 spectrophotometer, and  $^1\text{H-NMR}$  spectra were measured on a Jeol GX-400 instrument. Ultraviolet absorption spectra were measured on a Shimadzu UV-260 spectrophotometer at a concentration of 10.0 mg/L in  $\text{CH}_2\text{Cl}_2$  or HFIP. HPLC was performed on a steel column (4 mm x 250 mm) packed with LiChrosorb Si 60 (5  $\mu\text{m}$ , Merck and Co.) at a flow rate of 0.5 mL/min using ethyl acetate as an eluent, and the absorbance at 330 nm was monitored on a Shimadzu SPD-2A spectrophotometric detector. Differential scanning calorimetry (DSC) was measured on a Shimadzu DSC-50 instrument or a Rigaku Thermoflex TG-DSC under a 50 mL/min nitrogen stream at a heating rate of 5  $^\circ\text{C}/\text{min}$  for about 5 mg of the sample. X-Ray powder diffraction analyses were carried out with a Rigaku Rotaflex RU-200 spectrometer ( $\lambda = 1.54184 \text{ \AA}$ ).

**Preparation of the Mixed Crystals of **1a** and **1b** in Various Ratios.** Monomers **1a** and **1b** were prepared as previously described.<sup>13</sup> Mixed crystals of **1a** and **1b** in various ratios were obtained by the co-crystallization of a mixture of **1a** and **1b** in the corresponding ratio from ethanol. The ratios of **1a** and **1b** in the mixed crystals were determined by 400 MHz  $^1\text{H NMR}$ . Melting points of **1a**•**1b** were measured by DSC (**1a**:**1b**): Phase A, 90:10 = 163-173  $^\circ\text{C}$ , 82:18 = 158.5-168.5  $^\circ\text{C}$ ; Phase B: 70:30 = 153.5-165  $^\circ\text{C}$ , 60:40 = 144.5-151  $^\circ\text{C}$ , 50:50 = 145.5-151.5  $^\circ\text{C}$ , 31:69 = 143.5-148.5  $^\circ\text{C}$ , 19:81 = 142-150  $^\circ\text{C}$ , 5:95 = 146.5-151  $^\circ\text{C}$ .

**Photocycloaddition.** Fine powder of mixed crystals **1a**•**1b** were dispersed in 90 ml of a mixture of water/methanol (90/10 v/v) containing a few drops of a surfactant (NIKKOL TL-10FF) and were irradiated with a 500-W super-high-pressure mercury lamp (EIKOUSA EHB WF-500) set outside of the flask with vigorous stirring under a nitrogen atmosphere at room temperature.

(1RS,2RS,3RS,4RS)-1-Cyano-3-[4-(2-alkoxycarbonyl-2-cyanoethenyl)phenyl]-2-(4-pyridyl)-4-[4-[2-(4-

pyridyl)ethenyl]phenyl]cyclobutanecarboxylic Acid Ester **2**. (a mixture of ethyl ethyl, ethyl propyl, propyl ethyl, and propyl propyl for alkyl groups of alkoxy carbonyl and ester): Mixed crystal **1a·1b** was quantitatively converted into dimer **2** upon irradiation through a cut-off filter (Kenko L42).

**2**: IR (KBr) 2230, 1720, 1600, 980, 840  $\text{cm}^{-1}$ ;  $^1\text{H NMR}$  ( $\text{CDCl}_3$ )  $\delta$  0.98 (t, 1.5 H,  $J = 8$  Hz), 1.08 (t, 1.5 H,  $J = 8$  Hz), 1.28 (t, 1.5 H,  $J = 7$  Hz), 1.48 (t, 1.5 H,  $J = 7$  Hz), 1.69 (q, 1 H,  $J = 7$  Hz), 1.88 (q, 1 H,  $J = 7$  Hz), 4.0-4.4 (m, 2 H), 4.43 (t, 2 H,  $J = 6$  Hz), 4.53 (q, 1 H,  $J = 7$  Hz), 4.90 (d, 1 H,  $J = 10$  Hz), 5.45 (t, 1 H,  $J = 11$  Hz), 5.63 (d, 1 H,  $J = 11$  Hz), 7.2-7.3 (m, 3 H), 7.40 (d, 2 H,  $J = 8$  Hz), 7.63 (d, 2 H,  $J = 8$  Hz), 7.74 (d, 1 H,  $J = 16$  Hz), 7.96 (d, 2 H,  $J = 8$  Hz), 8.09 (d, 2 H,  $J = 6$  Hz), 8.23 (d, 2 H,  $J = 6$  Hz), 8.47 (s, 1 H), 8.63 (d, 2 H,  $J = 6$  Hz), 8.98 (d, 2 H,  $J = 6$  Hz); UV  $\lambda_{\text{max}}$  ( $\epsilon$  in  $\text{CH}_2\text{Cl}_2$ ) 304.8 nm (59,700). The melting range (101-145  $^\circ\text{C}$ ) and decomposition (191  $^\circ\text{C}$ ) were detected by TG-DSC.

(**2RS,3RS,4RS,5RS,10SR,11SR,12SR,13SR**)-**3,11-Dicyano-4,12-di(4-pyridyl)pentacyclo[12.2.2.2<sup>6,9</sup>.0<sup>2,5</sup>.0<sup>10,13</sup>]**icosane-**6,8,14,16,17,19-hexaene-3,11-dicarboxylic Acid Diester 3**. (a mixture of ethyl ethyl, ethyl propyl, propyl ethyl, and propyl propyl diesters): Mixed crystal **1a·1b** was quantitatively converted into dimer **3** upon irradiation without any cut-off filter. **3**: IR (KBr) 2220, 1740, 1420, 1220, 830  $\text{cm}^{-1}$ ;  $^1\text{H NMR}$  (TFA- $d$ )  $\delta$  1.02 (t, 3 H,  $J = 7$  Hz), 1.34 (t, 3 H,  $J = 7$  Hz), 1.75 (q, 2 H,  $J = 7$  Hz), 4.2-4.5 (m, 4 H), 4.44 (d, 2 H,  $J = 9$  Hz), 5.36 (dd, 2 H,  $J_1 = 11$  Hz,  $J_2 = 9$  Hz), 5.51 (d, 2 H,  $J = 11$  Hz), 6.77 (d, 2 H,  $J = 8$  Hz), 7.01 (s, 4 H), 7.26 (d, 2 H,  $J = 9$  Hz), 8.25 (d, 4 H,  $J = 6$  Hz), 8.95 (d, 4 H,  $J = 6$  Hz); UV ( $\epsilon$  in HFIP) 247.4 nm (696), 285.6 nm (283).

**Photochemical Reactions of 3.** 1) Photoreaction in solution: A solution of **3** (30 mg) in HFIP (4 ml) was irradiated at wavelengths of  $254 \pm 10$  nm, generated from a spectroirradiator equipped with a 2000-W xenon lamp and a grating monochromator (Jasco CRM-FM). 2) Photoreaction in the crystalline state: As-prepared crystal **3**, consisting of **1a** and **1b** (1:1), was dispersed in 300 ml of water containing a few drops of a surfactant (Nikkol TL-10FF) and was irradiated with a 20-W low-pressure mercury lamp (Eikousha EL J-20) set inside of the flask with vigorous stirring under a nitrogen atmosphere.

**X-ray Structure Determinations.** **1a•1b:** Intensity data were measured on a Mac-Science four-circle diffractometer (MXC-18) with graphite monochromated Cu-K $\alpha$  radiation. Accurate cell dimensions were obtained by a least-squares refinement of 20 reflections in the range  $40^\circ < 2\theta < 60^\circ$ . Data were collected with three check reflections. The observed reflections with  $|F_0| > 3\sigma(|F_0|)$  were used in the solutions and refinements; no absorption correction was made. The structures were solved by a direct method with the MULTAN 78 program and refined by a full-matrix least-squares method with the SHELXS 76 program. The positions of hydrogen atoms were obtained from a difference map. Final refinements were performed with the anisotropic thermal parameters for the non-hydrogen atoms and with isotropic ones for the hydrogen atoms. The hydrogen atoms of the ester alkyl groups could not be located in the difference map and were not included in the least-squares calculation. The occupancy factors of the ethyl and propyl groups in the disordered ester moiety were fixed with 0.5; the bond lengths in the alkyl groups were fixed with 1.50 Å for C-C bond and 1.46 Å for O-C bond.

**3:** Intensity data were measured on a Rigaku four-circle diffractometer (AFC-5) with graphite monochromated Cu-K $\alpha$  radiation. Accurate cell dimensions were obtained by a least-squares refinement of 20 reflections in the range  $40^\circ < 2\theta < 60^\circ$ . Data were collected with three check reflections. The observed reflections with  $|F_0| > 2.5\sigma(|F_0|)$  were used in the solutions and refinements; no absorption correction was made. The structures were solved by a direct method with the MULTAN 82 program and refined by a full-matrix least-squares method with the SHELXS 76 program. The positions of hydrogen atoms were obtained from a difference map. Final refinements were performed with the anisotropic thermal parameters for the non-hydrogen atoms and with isotropic ones for the hydrogen atoms. Isotropic thermal parameters of hydrogen atoms attached to sp<sup>3</sup> carbons are constructed to 1.2 times the B<sub>eq</sub> of parent carbons.

The intensity data collection, refinement details, and crystal data are summarized in Table 4.2. The final molecular coordinates and thermal parameters are listed in Tables 4.3, and 4.4.

**Table 4.2.** Summary of Crystal Data, Intensity Collection Parameters, and Refinement Details

compound	<b>1a•1b</b>	<b>3</b>
formula	C <sub>19</sub> H <sub>16</sub> N <sub>2</sub> O <sub>2</sub> •C <sub>20</sub> H <sub>18</sub> N <sub>2</sub> O <sub>2</sub>	C <sub>40</sub> H <sub>36</sub> N <sub>4</sub> O <sub>4</sub> •2[C <sub>3</sub> H <sub>2</sub> OF <sub>6</sub> ]
crystal system	monoclinic	monoclinic
space group	P2 <sub>1</sub> /c	P2 <sub>1</sub> /a
a, Å	18.604(6)	9.162(3)
b, Å	11.969(6)	35.296(15)
c, Å	7.521(4)	7.662(2)
β, deg	99.63(5)	109.80(2)
V, Å <sup>3</sup>	1651(1)	2331(1)
Z	4	2
cryst. solv.	ethanol	ethanol/HFIP
crystal size, mm <sup>3</sup>	0.6x0.4x0.2	0.8x0.3x0.1
Dcal, g/cm <sup>3</sup>	1.25	1.38
m, cm <sup>-1</sup>	5.79	9.87
scan mode	2θ-ω	2θ-ω
2θmax, deg	130	100
unique reflns	2741	2240
obsd reflns	2132	1520
	( F <sub>0</sub>   > 3σ( F <sub>0</sub>  ))	( F <sub>0</sub>   > 2.5σ( F <sub>0</sub>  ))
R factor	0.088	0.076
Rw factor	0.103	0.082
largest shift/esd	0.67	0.17
largest peak, e/Å <sup>3</sup>	0.38	0.26

Table 4.3. Final Atomic Coordinates ( $\times 10^4$  for C, N, and O;  $\times 10^3$  for H) with Equivalent Isotropic Thermal Parameters,  $B_{eq}$  ( $\text{\AA}^2$ ), for Non-Hydrogen Atoms and Isotropic Thermal Parameters,  $B$  ( $\text{\AA}^2$ ), for Hydrogen Atoms for **1a·1b**

$$B_{eq} = (1/3) \sum_i \sum_j B_{ij} a_i^* a_j^* a_{ij}$$

Atom	x	y	z	B or $B_{eq}$
N 1	9325(2)	1331(4)	-165(6)	8.6(1)
C 2	8849(3)	2178(4)	-414(7)	7.8(1)
C 3	8147(2)	2116(4)	-40(6)	6.7(1)
C 4	7902(2)	1117(3)	574(4)	5.6(1)
C 5	8394(2)	242(4)	806(6)	6.6(1)
C 6	9084(3)	366(4)	427(7)	7.9(1)
C 7	7176(2)	946(3)	1016(5)	5.7(1)
C 8	6619(2)	1659(3)	852(5)	5.7(1)
C 9	5914(2)	1397(3)	1330(4)	5.1(1)
C 10	5314(2)	2121(2)	876(4)	5.3(1)
C 11	4644(2)	1885(3)	1287(4)	5.4(1)
C 12	4516(2)	889(2)	2187(4)	5.1(1)
C 13	5113(2)	167(3)	2621(5)	5.9(1)
C 14	5785(2)	410(3)	2217(5)	6.2(1)
C 15	3843(2)	543(3)	2701(5)	5.5(1)
C 16	3210(2)	1080(3)	2803(4)	5.3(1)
C 17	3081(2)	2234(3)	2368(5)	5.5(1)
N 18	2992(2)	3150(3)	2052(5)	7.1(1)
C 19	2625(2)	450(3)	3486(5)	5.9(1)
O 20	2700(2)	-473(2)	4111(4)	7.7(1)
O 21	2018(1)	1050(2)	3385(4)	6.9(1)
C22A	1394(12)	718(10)	4213(41)	11.1(8)
C22B	1441(5)	485(8)	4139(24)	7.2(4)
C23A	989(8)	1699(12)	4796(25)	11.0(6)
C23B	834(6)	1325(13)	3857(25)	12.8(7)
C 24	396(19)	879(31)	5203(42)	49.4(24)
H 2	918(5)	291(7)	-93(10)	16.5(26)
H 3	787(3)	277(4)	-11(6)	8.7(12)
H 5	822(3)	-36(4)	134(6)	8.1(11)
H 6	943(2)	-35(4)	73(6)	23.6(10)
H 7	713(2)	27(4)	155(5)	7.3(10)
H 8	661(3)	232(4)	33(6)	7.3(10)
H 10	537(2)	285(3)	6(5)	6.7(8)
H 11	423(3)	242(4)	109(6)	8.8(12)
H 13	512(3)	-42(4)	330(6)	8.6(12)
H 14	619(2)	-13(4)	254(6)	7.3(10)
H 15	382(2)	-16(4)	308(6)	6.6(8)

Table 4.4. Final Atomic Coordinates ( $\times 10^4$  for C, N, O, and F;  $\times 10^3$  for H) with Equivalent Isotropic Thermal Parameters,  $B_{eq}$  ( $\text{\AA}^2$ ), for Non-Hydrogen Atoms and Isotropic Thermal Parameters,  $B$  ( $\text{\AA}^2$ ), for Hydrogen Atoms for 3

$$B_{eq} = (1/3) \sum_i \sum_j B_{ij} a_i^* a_j^* a_{ij}$$

Atom	x	y	z	B (eq)
C 1	6704 (7)	4832 (2)	8360 (9)	4.0 (2)
C 2	5883 (7)	4495 (2)	7106 (8)	4.0 (2)
C 3	7013 (7)	4215 (2)	8497 (9)	3.8 (2)
C 4	7474 (7)	4529 (2)	9976 (10)	4.1 (2)
C 5	7930 (7)	5076 (2)	7969 (9)	3.9 (2)
C 6	9040 (7)	4929 (2)	7268 (8)	3.9 (2)
C 7	10490 (8)	5098 (2)	7726 (9)	3.9 (2)
C 8	10858 (7)	5408 (2)	8896 (9)	3.7 (2)
C 9	9653 (8)	5598 (2)	9221 (9)	4.1 (2)
C 10	8185 (8)	5433 (2)	8730 (9)	3.9 (2)
C 11	6408 (7)	3840 (2)	8874 (10)	4.4 (2)
C 12	6232 (10)	3537 (2)	7694 (12)	6.7 (3)
C 13	5665 (13)	3195 (2)	8061 (18)	8.7 (4)
N 14	5281 (9)	3138 (2)	9561 (13)	8.1 (3)
C 15	5414 (12)	3422 (3)	10668 (15)	8.0 (4)
C 16	5960 (11)	3775 (2)	10405 (12)	6.9 (3)
C 17	4222 (8)	4444 (2)	7095 (11)	4.6 (2)
O 18	3768 (5)	4593 (2)	8232 (8)	6.6 (2)
O 19	3422 (5)	4208 (2)	5819 (7)	5.5 (2)
C 20	1829 (9)	4140 (3)	5713 (14)	7.3 (4)
C 21	1603 (14)	3792 (4)	6181 (36)	19.8 (12)
C 22	-266 (19)	3716 (6)	5675 (35)	23.5 (15)
C 23	5901 (7)	4480 (2)	5211 (11)	4.6 (2)
N 24	5999 (7)	4466 (2)	3764 (10)	6.6 (3)
O 25	4411 (10)	2484 (2)	10635 (13)	11.4 (4)
C 26	5781 (15)	2308 (3)	11534 (24)	10.2 (6)
C 27	5884 (27)	1935 (4)	10813 (41)	16.1 (11)
F 28	4750 (10)	1706 (2)	10967 (18)	20.2 (6)
F 29	7137 (14)	1744 (3)	11770 (29)	25.2 (10)
F 30	5625 (25)	1959 (5)	9044 (26)	27.1 (12)
C 31	6104 (33)	2326 (6)	13742 (34)	15.8 (12)
F 32	7298 (16)	2166 (4)	14632 (20)	23.8 (8)
F 33	6024 (19)	2686 (3)	14062 (16)	23.5 (8)
F 34	4897 (19)	2153 (4)	13937 (19)	22.4 (8)
H 1	598 (7)	502 (2)	851 (8)	5.1
H 3	1203 (7)	581 (2)	1197 (8)	4.9
H 4	690 (7)	451 (2)	1073 (9)	5.2
H 6	890 (7)	468 (2)	672 (9)	5.1
H 7	1130 (7)	494 (2)	765 (8)	5.1
H 9	986 (7)	587 (2)	963 (9)	5.3
H 10	735 (1)	559 (0)	894 (1)	5.0
H 12	682 (1)	350 (0)	682 (1)	8.2
H 13	553 (1)	299 (0)	713 (2)	11.7
H 15	513 (1)	330 (0)	1168 (2)	9.8
H 16	612 (1)	398 (0)	1137 (1)	8.8
H 25	1523 (14)	731 (4)	980 (18)	15.2
H 26	659 (13)	252 (3)	1156 (16)	13.1
H201	123 (1)	403 (0)	447 (1)	10.3
H202	139 (1)	439 (0)	584 (1)	10.3
H211	239 (1)	359 (0)	630 (4)	23.9
H212	190 (1)	394 (0)	736 (4)	23.9
H221	-125 (2)	361 (1)	480 (4)	28.6
H222	29 (2)	386 (1)	495 (4)	28.6
H223	-52 (2)	390 (1)	654 (4)	28.6

#### 4. 5. References

- 1) (a) Cohen, M. D.; Cohen, R.; Lahav, M.; Nie, P. L. *J. Chem. Soc., Perkin Trans. 2*, **1973**, 1095. (b) Elgavi, A.; Green, B. S.; Schmidt, G. M. J. *J. Am. Chem. Soc.* **1973**, *95*, 2058. (c) Theocharis, C. R.; Desiraju, G. R.; Jones, W. J. *J. Am. Chem. Soc.*, **1984**, *106*, 3606. (d) Sarma, J. A. R. P., Desiraju, G. R. *J. Chem. Soc., Perkin Trans. 2*, **1985**, 1905. (e) Sarma, J. A. R. P., Desiraju, G. R. *J. Chem. Soc., Perkin Trans. 2*, **1987**, 1187.
- 2) Hasegawa, M. *Chem. Rev.*, **1983**, *83*, 507.
- 3) Nakanishi, H.; Jones, W.; Parkinson, G. M. *Acta Cryst.* **1979**, *B 35*, 3103.
- 4) (a) Hasegawa, M. *Pure Appl. Chem.* **1986**, *58*, 1179. (b) Hasegawa, M.; Katsumata, T.; Ito, Y.; Saigo, K. *Macromolecules* **1988**, *21*, 3134. (c) Hasegawa, M.; Aoyama, M.; Maekawa, Y.; Ohashi, Y. *Macromolecules* **1989**, *22*, 1568. (d) Hasegawa, M.; Endo, Y.; Aoyama, M.; Saigo, K. *Bull. Chem. Soc. Jpn.* **1989**, *62*, 1556. (e) Hasegawa, M. *Comprehensive Polymer Science*, Vol. 5, Step Polymerization; Allen, G., Ed.; Pergamon Press: Oxford, **1989**; pp217-232.
- 5) (a) Hasegawa, M.; Kato, S.; Saigo, K.; Wilson, S. R.; Stern, C. L.; Paul, I. C. *J. Photochem. Photobiol., A Chem.* **1988**, *41*, 385. (b) Maekawa, Y.; Kato, S.; Saigo, K.; Hasegawa, M.; Ohashi, Y. submitted for publication in *Macromolecules*.
- 6) Cram D. J.; Steinberg, H. *J. Am. Chem. Soc.* **1951**, *73*, 5691.
- 7) Hope, H.; Bernstein, J.; Trueblood, K. N. *Acta Cryst.* **1972**, *B 28*, 1733.
- 8) Lonsdale, L.; Milledge, H. J.; Rao, K. V. K. *Proc. Roy. Soc., Ser. A* **1960**, *555*, 82.
- 9) Unpublished result.
- 10) Suzuki, Y.; Tamaki, T.; Hasegawa, M. *Bull. Chem. Soc. Jpn.* **1974**, *47*, 210.
- 11) There are some reports, in which the mixed crystal (a solid solution) has the different space group and molecular arrangement from the pure crystals though each pure crystal has the same space group: Kitaigorodsky, A. I. *Mixed Crystals*, Springer-Verlag: Berlin, **1984**; Addadi, L.; van Mil, J.; Lahav, M. *J. Am. Chem. Soc.* **1982**, *104*, 3422.

- 12) An alternating arrangement of paired molecules related by glide and twofold axis symmetries similar to **1a•1b** was reported for pyrene crystal:  
Kitaigorodsky, A. I. *Organic Crystals and Molecules*, Academic Press; New York, 1973.
- 13) Ichimura K.; Watanabe, S. *J. Polym. Chem. Ed.* **1982**, 20, 1420.

## CHAPTER 5

### Preparation of a Crystalline Linear High Copolymer by Topochemical Photo-Polymerization of Diolefin Mixed Crystals

#### 5. 1. Introduction

As mentioned in chapter 4, the author has also attempted to prepare mixed crystals from several couples of unsymmetric diolefin compounds. Ethyl and propyl  $\alpha$ -cyano-4-[2-(4-pyrimidyl)ethenyl]cinnamates arranged in the  $\beta$ -translation-type and  $\beta$ -centrosymmetry-type packings, respectively; upon irradiation they gave amorphous oligomers. A mixed crystal of these compounds arranged in a  $\beta$ -centrosymmetry-type packing, which was isomorphous to that of propyl ester; upon irradiation it also gave only amorphous oligomers.<sup>1</sup> Moreover, ethyl and propyl  $\alpha$ -cyano-4-[2-(4-pyridyl)ethenyl]cinnamates, which arranged in an  $\alpha$ -type packing, formed a mixed crystal. However, the molecular arrangement of the mixed crystal drastically changed into a  $\beta$ -type packing to give, upon irradiation, [2.2]paracyclophane derivatives in quantitative yield instead of the expected linear copolymer.<sup>2</sup>

It is well-known that some couples of two isomorphous compounds form a mixed crystal, of which the crystal structure is isomorphous to each pure crystal.<sup>3</sup> On the other hand, it has been reported that most  $\alpha$ -type unsymmetric diolefin crystals topochemically photopolymerize into crystalline linear polymers.<sup>4</sup> On the basis of these facts, it was considered that a couple of two diolefin compounds, which are isomorphous to each other in  $\alpha$ -type packing, should possibly form a mixed crystal and, subsequently, give a crystalline linear copolymer.

The author mentioned in Chapter 3 that ethyl 4-[2-(2-pyrazyl)ethenyl]cinnamate (**1a**)<sup>4b</sup> and S-ethyl 4-[2-(2-pyrazyl)ethenyl]thiocinnamate (**1b**)<sup>5</sup> crystallized in an  $\alpha$ -type packing and that these crystals, upon irradiation, gave crystalline linear polymers (Scheme 5.1). Moreover, the crystal structures of the two diolefin compounds were isomorphous to each other, suggesting the possibility of mixed-crystal formation.

In this chapter, the author describes the formation and topochemical behavior of a mixed crystal of **1a** and **1b**, which is the first example of clear-cut topochemical photo-copolymerization.

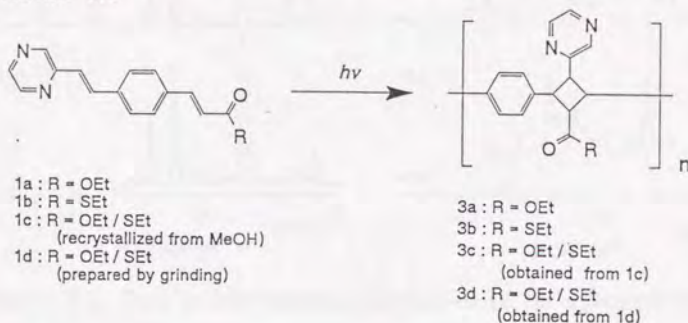
## 5. 2. Results and Discussion

A mixed crystal of **1a** and **1b** was formed not only by recrystallization from a methanol solution but also, surprisingly, by simple grinding of two monomers with an agate mortar and pestle, or an amalgamator.

### 5. 2. 1. Topochemical Behavior of a Mixed Crystal Prepared by Recrystallization from a Methanol Solution

When a mixture of equimolar amounts of **1a** and **1b** was recrystallized from a methanol solution, microcrystals (**1c**) comprising **1a** and **1b** in a molar ratio of 45:55 deposited.

Scheme 5.1



**1c** showed a lower photoreactivity than those of **1a** and **1b** in the crystalline state; irradiation of **1c** for 24 h at room temperature with a 500-W super-high-pressure mercury lamp gave a crystalline polymer (**3c**) ( $\eta_{inh} = 1.9$  dL/g). The  $^1\text{H}$  NMR spectrum of **3c** showed the same signals as those of **3a** and **3b**, except for signals arising from the alkyl protons in the ester groups. On the basis of the  $^1\text{H}$  NMR spectral evidence, it is concluded that polymer **3c** also has an alternating

structure of an  $\alpha$ -homo-type cyclobutane ring and a 1,4-phenylene skeleton in the main chain (Scheme 5.1).

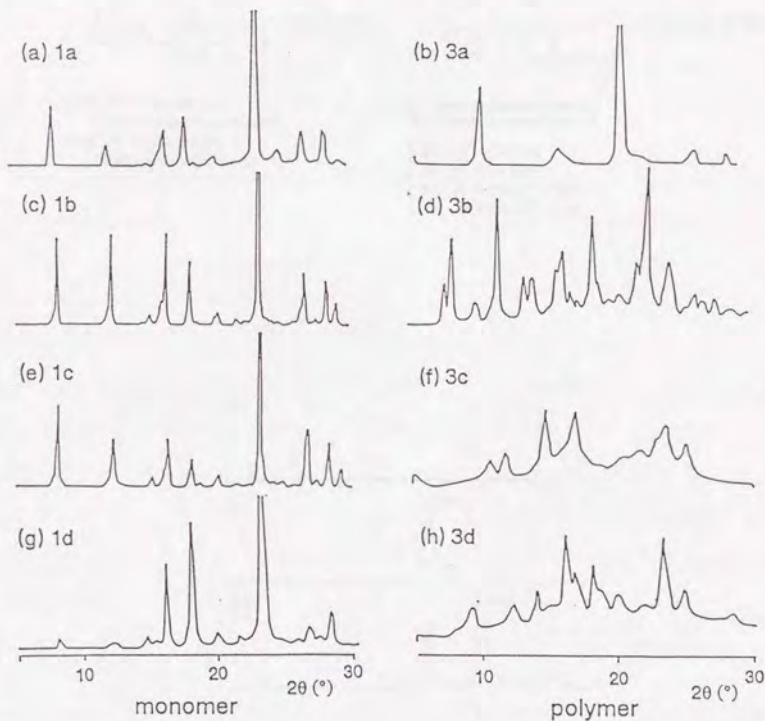


**Figure 5.1.** X-ray powder diffraction patterns; (a) **1a**, (b) a photoproduct of **1a** (**3a**), (c) **1b**, (d) a photoproduct of **1b** (**3b**), (e) a mixed crystal of **1a** and **1b** prepared by recrystallization from a methanol solution (**1c**), (f) a photoproduct of **1c** (**3c**), (g) a mixed crystal of **1a** and **1b** prepared by grinding (**1d**), and (h) a photoproduct of **1d** (**3d**).

As shown in Figure 5.1, the X-ray powder diffraction pattern of **1c** (e) is identical with those of pure crystals **1a** (a) and **1b** (c). The identical pattern implies that the crystal structure of **1c** is isomorphous to those of pure crystals **1a** and **1b**.

Scheme 5.2

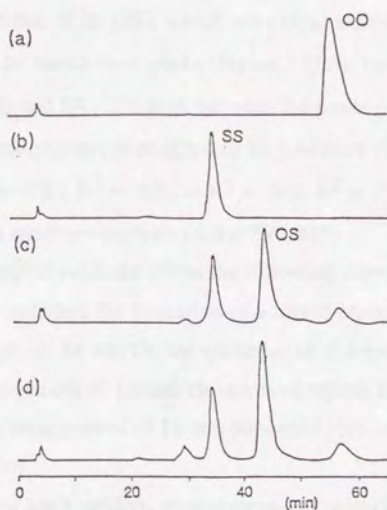
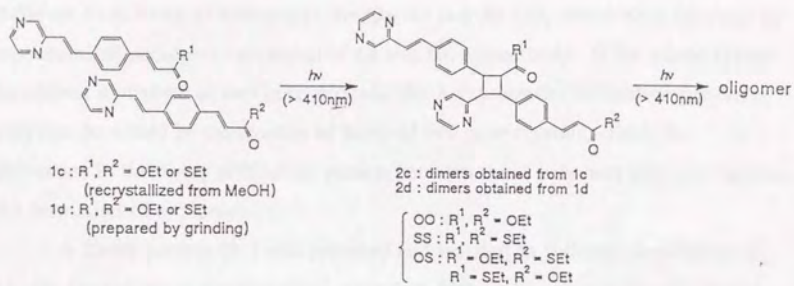


Figure 5.2. High performance liquid chromatogram of the dimers; (a) the dimer of **1a** (OO), (b) the dimer of **1b** (SS), (c) the dimer of **1c** (**2c**), and (d) the dimer of **1d** (**2d**).

On the other hand, the X-ray powder diffraction pattern of polymer **3c** (f) is quite different from those of homopolymers **3a** (b) and **3b** (d), which were obtained by topochemical photopolymerization of **1a** and **1b**, respectively. If the mixed system comprises a mixture of two pure crystals, the X-ray powder diffraction pattern of polymer **3c** would be the overlap of those of two pure crystals. Thus, the difference in the X-ray diffraction pattern between these polymers strongly suggests the formation of a copolymer.

A dimer portion (**2c**) was prepared and isolated as follows. Irradiation of **1c** was carried out at wavelengths longer than 410 nm by using a cut-off filter in order to excite only the monomers; then, dimer **2c** was separated from trimer and oligomers by preparative TLC (Scheme 5.2).

Figures 5.2 (a) and (b) show the high-performance liquid chromatograms of dimers of **1a** (OO) and that of **1b** (SS), which were obtained in a similar manner. The chromatogram of **2c** shows three peaks (Figure 5.2(c)); two of them are attributed to dimers OO and SS. The peak between the peaks of dimers OO and SS, in the order of retention time, is assigned to be a mixture of two mixed dimers of **1a** and **1b** (OS;  $R^1 = -OEt$ ,  $R^2 = -SEt$ , or  $R^1 = -SEt$ ,  $R^2 = -OEt$  in Scheme 5.2) on the basis of its mass spectrum analysis ( $m/e = 580$ ,  $M^+$ ).

The chromatographic evidence offers the following conclusion: The existence of dimer OS indicates the formation of a mixed crystal, resulting in the formation of a copolymer of **1a** and **1b**; the existence of dimers OO and SS means that the molecular arrangement of **1a** and **1b** in mixed crystal **1c** is not alternating, because the alternating arrangement of **1a** and **1b** would give only dimer OS without either OO or OS.

If a mixed crystal has a random arrangement and photodimerizes in a quantitative yield, the ratio of the resulting two homo dimers and mixed dimer would coincide with the statistical value (1:1:2).<sup>2</sup> In this reaction, however, since the resulting dimer reacts to give a trimer and oligomers, even by the photoexcitation of the monomer, the degree of mixing of **1a** and **1b** in mixed crystal **1c** could not be precisely determined only by the molar ratio of the resulting dimers. However, the non-stoichiometric ratio of **1a** and **1b** (45:55) in

mixed crystal **1c** and the proportions of **OO**, **OS**, and **SS** (1:4.9:2.9) strongly suggest that a mixed crystal of **1a** and **1b** should have a random arrangement (a solid solution); thus, the photoproduct should be a random copolymer comprising **1a** and **1b** monomer units. This is the first example of topochemical photocopolymerization, in which the copolymer formation was completely substantiated by the spectroscopic results.

**Table 5.1.** Photoreaction of the Mixed Crystals

compound	R	crystal prep.method	reaction time [h]	morphology of photoproducts	$\eta_{inh}$ [dL/g]
<b>1a</b>	-OEt	—	5	crystal	8.2
<b>1b</b>	-SEt	—	24	crystal	1.6
<b>1c</b>	-OEt / -SEt	recryst.(MeOH)	24	crystal	1.9
<b>1d</b>	-OEt / -SEt	grinding	7	crystal	0.6

### 5. 2. 2. Topochemical Behavior of a Mixed Crystal Prepared by Grinding of a Mixture of the Crystals

When an equimolar amount of pure crystals **1a** and **1b** was mixed by grinding for 10 min with an agate mortar and pestle or by agitation for 30 min with an amalgamator, the resulting crystal mixture (**1d**) showed a similar photoreactivity to that of **1c**, suggesting the formation of a mixed crystal of **1a** and **1b** through crystal-crystal contact. In the latter method slight increase in the temperature of the sample was observed (ca. 50 °C). However, since this temperature was much lower than the melting points of either crystal **1a** or **1b**, and since a fine powder shape of the crystal mixture was maintained, melting of the crystal mixture could be ruled out during agitation with the amalgamator.

Irradiation of **1d** for 7 h at room temperature with a 100-W high-pressure mercury lamp gave a crystalline polymer (**3d**) ( $\eta_{inh} = 0.6$  dL/g). Since the  $^1\text{H}$  NMR spectrum of **3d** is identical with that of **3c**, it is concluded that polymer **3d** has the alternating structure of an  $\alpha$ -homo-type cyclobutane ring and a 1,4-phenylene in the main chain (Scheme 5.1).

As shown in Figure 5.1, the X-ray powder diffraction pattern of **1d** (g) is very similar to that of **1c** (e) as well as those of **1a** (a) and **1b** (c), indicating that the crystal structure of **1d** is also isomorphous to that of **1c**, as well as those of **1a** and **1b**. Furthermore, the different diffraction pattern of polymer **3d** (h) from the overlap of those of **3a** (b) and **3b** (d) also indicates that **3d** is a copolymer comprising **1a** and **1b** monomer units.

As shown in Figure 5.2 (d), a high-performance liquid chromatogram of a dimer portion (**2d**), which was isolated from the photoproduct of **1d** in a similar manner to **2c**, shows three peaks of **OO**, **OS**, and **SS** in a ratio of 1.0:5.0:2.5. From these results it is concluded that only through crystal-crystal contact by grinding could the **1a** and **1b** crystals be transformed into a mixed crystal, resulting in a formation of a copolymer of **1a** and **1b**.

Although X-ray diffraction pattern of **1d** is similar to that of **1c** and HPLC of **2d** to that of **2c**, the X-ray diffraction pattern and inherent viscosity of **3d** were different from those of **3c**. These differences strongly suggest that **1c** and **1d** have any difference in degree of mixing of **1a** and **1b** and/or degree of crystallinity, which can not be detected by X-ray diffraction measurement, whereas, the difference may be amplified during the polymerization, resulting in a different morphology between **3c** and **3d**.

There have been some reports concerning the formation of mixed crystals by grinding of two compounds in the solid state. However, in these reports the combinations are limited to the compounds having strong intermolecular interactions such as host-guest<sup>6</sup> and CT complex systems.<sup>7</sup> In contrast, it is very unusual that **1a** and **1b**, in which no particular intermolecular interaction exists, except for the van der Waals force, readily form a mixed crystal through a crystal-crystal contact only by grinding the two crystals.

### 5. 3. Conclusion

A mixed crystal (**1c**) of ethyl 4-[2-(2-pyrazyl)ethenyl]cinnamate (**1a**) and S-ethyl 4-[2-(2-pyrazyl)ethenyl]thiocinnamate (**1b**) was obtained by co-crystallization

from a methanol solution. Mixed crystal **1c** had an isomorphous structure to those of pure crystals **1a** and **1b** and, upon irradiation, gave a crystalline linear copolymer having the same main chain as those of the homo-polymers. The copolymer formation was ascertained by the isolation of a mixed dimer comprising **1a** and **1b**.

A mixed crystal of **1a** and **1b** was also obtained through crystal-crystal contact by simple grinding of the monomers with an amalgamator. Irradiation of the resulting mixed crystal gave a crystalline linear copolymer having the same structure.

#### 5. 4. Experimental

**Measurements.** The infrared spectra were measured on a Jasco IR-810 spectrophotometer, and the  $^1\text{H}$  NMR spectra were measured by a Jeol PMX-60SI or a Jeol GX-400 instrument. The ultraviolet absorption spectra were measured on a Shimadzu UV-260 spectrophotometer at a concentration of 10.0 mg/L in  $\text{CH}_2\text{Cl}_2$ . The mass spectra were measured on a Shimadzu GCMS-QP2000 instrument. The melting points were measured by a Laboratory Devices MEL-TEMP and are uncorrected. High-performance liquid chromatography (HPLC) was performed on a steel column (4 mm x 250 mm) packed with LiChrosorb Si 60 (5  $\mu\text{m}$ , Merck and Co.) at a flow rate of 0.5 mL/min using a mixture of  $\text{CHCl}_3$  and  $\text{CH}_3\text{OH}$  (100:0.5) as an eluent, and the absorbance at 254 nm was monitored on a Shimadzu SPD-2A spectrophotometric detector. Gel permeation chromatography (GPC) was performed at 40  $^\circ\text{C}$  by using Shodex GPC (AD 800/P + AD 805/S + AD 803/S + AD 802/S + AD 802/S) columns (DMF solution). Differential scanning calorimetry (DSC) was measured on a Shimadzu DSC-50 instrument under a nitrogen stream with a heating rate of 5  $^\circ\text{C}/\text{min}$  for about 5 mg of the sample. X-ray powder diffraction analyses were carried out with a Rigaku Rotaflex RU-200 spectrometer ( $\lambda = 1.54184 \text{ \AA}$ ).

**Preparation of the Mixed Crystal of 1a and 1b (1c) by Recrystallization from Methanol.** Monomer **1a** was prepared as previously described.<sup>4</sup> Monomer **1b** was prepared from the corresponding acid chloride and

ethanethiol by standard procedures. A mixture of **1a** and **1b** in an equimolar amount (1.42 mmol) was recrystallized from methanol (200 ml), giving a mixed crystal of **1a** and **1b** (**1c**) in a molar ratio of 45:55. The stoichiometry was confirmed by its  $^1\text{H}$  NMR. Mp: 155-161 °C (DSC analysis); IR (KBr) 1700, 1630, 1610, 1180, 1030, 980, 840, 760  $\text{cm}^{-1}$ .

**Preparation of the Mixed Crystal of 1a and 1b (1d) by Grinding of a Mixture of 1a and 1b Crystals.** A mixture of the pure crystals **1a** and **1b** in an equimolar amount (0.20 mmol) was agitated for 30 minutes by using an amalgamator (GC-HMIX, G-C Dental Industrial Corp.) to give a mixed crystal of **1a** and **1b** (**1c**). Mp: 152-160 °C (DSC analysis); IR (KBr) 1700, 1630, 1610, 1180, 1030, 980, 840, 760  $\text{cm}^{-1}$ .

**Preparation of the Dimers.** A finely powdered crystal of **1a**, **1b**, **1c**, or **1d** (100 mg) was dispersed in water (90 ml) and was irradiated with a 500-W high-pressure mercury lamp (Ushio USH-500D), set outside of the flask, through a Kenko L42 filter (cut off < 410 nm) at room temperature with vigorous stirring until the monomer was completely consumed. Dimers were separated from oligomers by preparative TLC (silica gel,  $\text{CH}_2\text{Cl}_2/\text{CH}_3\text{OH}=100:0.5$ ).

**OO:** 4 %;  $^1\text{H}$  NMR ( $\text{CDCl}_3$ )  $\delta$  0.90 (t, 3H, J = 7 Hz), 1.34 (t, 3H, J = 7 Hz), 3.8-3.9 (m, 2H), 4.1-4.2 (m, 1H), 4.27 (q, 2H, J = 7 Hz), 4.63 (d, 2H, J = 6 Hz), 4.8-4.9 (m, 1H), 6.43 (d, 1H, J = 16 Hz), 7.04 (d, 1H, J = 16 Hz), 7.09 (d, 2H, J = 8 Hz), 7.36 (d, 2H, J = 8 Hz), 7.41 (d, 2H, J = 8 Hz), 7.51 (d, 2H, J = 8 Hz), 7.60 (d, 1H, J = 16 Hz), 7.67 (d, 1H, J = 16 Hz), 8.21 (s, 1H), 8.26 (s, 1H), 8.35 (s, 1H), 8.39 (s, 1H), 8.52 (s, 1H), 8.59 (s, 1H); MS m/e 560 ( $\text{M}^+$ ).

**SS:** 5 %; IR (KBr) 2230, 1720, 1600, 980, 840  $\text{cm}^{-1}$ ;  $^1\text{H}$  NMR ( $\text{CDCl}_3$ )  $\delta$  0.94 (t, 3H, J = 7 Hz), 1.32 (t, 3H, J = 7 Hz), 2.5-2.6 (m, 1H), 2.7-2.8 (m, 1H), 4.36 (dd, 1H, J = 10 Hz, J' = 6 Hz), 4.63 (dd, 1H, J = 10 Hz, J' = 7 Hz), 4.69 (dd, 1H, J = 10 Hz, J' = 6 Hz), 4.85 (dd, 1H, J = 10 Hz, J' = 7 Hz), 6.69 (d, 1H, J = 16 Hz), 7.09 (d, 2H, J = 8 Hz), 7.10 (d, 1H, J = 16 Hz), 7.38 (d, 2H, J = 8 Hz), 7.40 (d, 2H, J = 8 Hz), 7.51 (d, 2H, J = 8 Hz), 7.58 (d, 1H, J = 16 Hz), 7.70 (d, 1H, J = 16 Hz), 8.23 (s, 1H), 8.27 (s, 1H), 8.40 (s, 1H), 8.47 (s, 1H), 8.57 (s, 1H), 8.70 (s, 1H); MS m/e 592 ( $\text{M}^+$ ).

**2c** (5 %) and **2d** (7 %) were a mixture of the dimers **OO**, **SS**, and **OS**.

Their  $^1\text{H}$  NMR spectra were the same as those of **OO** and **SS**, except for a signal of the alkyl group in esters. The mass spectra of **2c** and **2d** showed  $m/e$  560 (**OO**  $\text{M}^+$ ), 576 (**OS**  $\text{M}^+$ ), and 592 (**SS**  $\text{M}^+$ ).

**Photoirradiation.** Photopolymerization was carried out as follows:

Method 1) Finely powdered crystals (100 mg) were dispersed in 300 ml of water containing a few drops of a surfactant (Nikkol TL-10FF) and irradiated with a 100-W high-pressure mercury lamp (Eikousha EHB WF-100), set inside of the flask, through a Pyrex glass filter with vigorous stirring under a nitrogen atmosphere.  
Method 2) Finely powdered crystals (100 mg) were dispersed in 90 ml of water containing a few drops of a surfactant (Nikkol TL-10FF) and irradiated with a 500-W super-high-pressure mercury lamp (Eikousha EHB WF-500), set outside of the flask, through a Kenko UV30 filter (cut off < 280 nm) with vigorous stirring under a nitrogen atmosphere.

**3c:** IR (KBr): 1720, 1660, 1400, 1180, 1020  $\text{cm}^{-1}$ .  $^1\text{H}$  NMR (TFA-d)  $\delta$  0.9-1.1 (m, 3H), 2.7-2.9 (m, 1H), 3.9-4.1 (m, 1H), 4.3-4.5 (m, 0.5H), 4.5-4.7 (m, 0.5H), 4.85 (bs, 1H), 5.00 (bs, 2H), 7.1-7.3 (bs, 2H), 7.3-7.5 (bs, 2H), 8.61 (s, 1H), 8.66 (bs, 1H), 9.38 (bs, 1H).

**3d:** IR (KBr) 1710, 1630, 1310, 1180, 1020  $\text{cm}^{-1}$ ;  $^1\text{H}$  NMR (TFA-d)  $\delta$  0.9-1.1 (m, 3H), 2.7-2.9 (m, 1H), 3.9-4.1 (m, 1H), 4.3-4.5 (m, 0.5H), 4.5-4.7 (m, 0.5H), 4.85 (bs, 1H), 5.00 (bs, 2H), 7.1-7.3 (bs, 2H), 7.3-7.5 (bs, 2H), 8.61 (s, 1H), 8.66 (bs, 1H), 9.38 (bs, 1H).

## 5. 5. References

- 1) Hasegawa, M.; Endo, Y.; Aoyama, M.; Saigo, K. *Bull. Chem. Soc. Jpn.* **1989**, 62, 1556.
- 2) Chapter 4 in this thesis.
- 3) Kitaigorodsky, A. I. *Mixed Crystals*, Springer-Verlag; Berlin, **1984**.
- 4) (a) Hasegawa, M.; Katsumata, T.; Ito, Y.; Saigo, K. *Macromolecules* **1988**, 21, 3134. (b) Hasegawa, M.; Aoyama, M.; Maekawa, Y.; Ohashi, Y. *Macromolecules* **1989**, 22, 1568.

- 5) A crystal structure and topochemical behavior of **1b** will be published elsewhere.
- 6) Toda, F.; Tanaka, K.; Sekikawa, A. *J. Chem. Soc., Chem. Commun.*, **1987**, 279.
- 7) (a) Patil, A. O.; Curtin, D. Y.; Paul, I. C. *J. Am. Chem. Soc.*, **1984**, 106, 348. (b) Pennington, W. T.; Patil, A. O.; Paul, I. C.; Curtin, D. Y. *J. Chem. Soc., Perkin Trans. 2*, **1986**, 557, and references cited therein.

LIST OF PUBLICATIONS

- 1) Quantitative Formation of a [2.2]paracyclophane Derivative via Topochemical Photoreaction of Crystal Complex of Ethyl and Propyl  $\alpha$ -Cyano-4-[2-(4-pyridyl)ethenyl]cinnamates  
Masaki Hasegawa, Yasunari Maekawa, Satoshi Kato, and  
Kazuhiko Saigo.  
*Chem. Lett.*, **1987**, 907.
- 2) Topochemical Photoreaction of Unsymmetrically Substituted Diolefins. 3. Photochemical Behavior of 4-[2-(2-Pyrazyl)ethenyl]styrene Derivative Crystals  
Masaki Hasegawa, Masato Aoyama, Yasunari Maekawa, and  
Yuji Ohashi  
*Macromolecules*, **1989**, 22, 1568.
- 3) Crystallographic Interpretation of the Topochemical Behavior of Alkyl  $\alpha$ -Cyano-4-[2-(4-pyridyl)ethenyl]cinnamates in the Crystalline State. Enhancement of Photopolymerizability by Complex Formation  
Yasunari Maekawa, Satoshi Kato, Kazuhiko Saigo, Masaki Hasegawa,  
and Yuji Ohashi  
*Macromolecules*, in press.
- 4) Quantitative Formation of a Highly Strained Tricyclic [2.2]Paracyclophane Derivative from a Mixed Crystal of Ethyl and Propyl  $\alpha$ -Cyano-4-[2-(4-pyridyl)ethenyl]cinnamates through a Topochemical Reaction  
Yasunari Maekawa, Satoshi Kato, and Masaki Hasegawa  
*J. Am. Chem. Soc.*, in press.

- 5) Preparation of a Crystalline Linear High Copolymer by Topochemical Photopolymerization of Diolefin Mixed Crystals

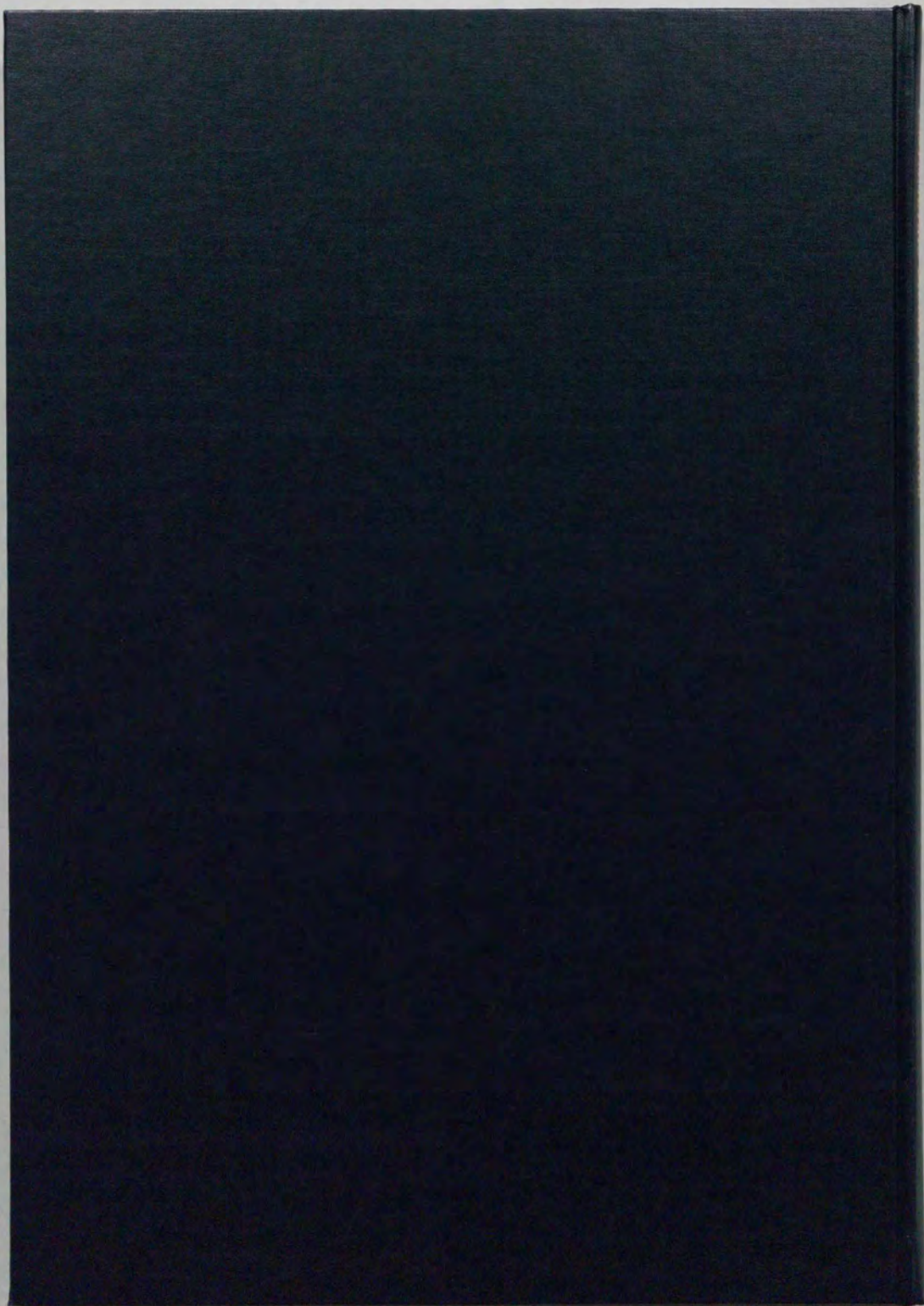
Yasunari Maekawa, Peng-Jin Lim, Kazuhiko Saigo, and  
Masaki Hasegawa

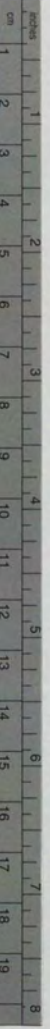
*Macromolecules*, submitted.

- 6) A Design for Photopolymerizable Molecular Arrangement of Diolefin Crystals

Yasunari Maekawa, Makoto Sukegawa, Peng-Jin Lim,  
Kazuhiko Saigo, and Masaki Hasegawa

in preparation.





# Kodak Color Control Patches

© Kodak, 2007 TM, Kodak



# Kodak Gray Scale



© Kodak, 2007 TM, Kodak

A 1 2 3 4 5 6 M 8 9 10 11 12 13 14 15 B 17 18 19

